Illinois U Library

Transactions

of the

ASME

Meter for Flowing Mixtures of Air and Pulverized Coal . . . . *H. M. Carlson, P. M. Frazier, and R. B. Engdahl* 65

Test Data on Gas-Side Sulphate-Type Deposits on Tubes Beyond Boiler Furnace . . . . *J. F. Barkley, L. R. Burdick, and A. A. Berk* 81

Progress Report No. 1 on Tool-Chip Interface Temperatures . . . *K. J. Trigger* 91

The Role of Meehanite Metal Castings in Engineering Production . . *C. R. Austin* 99

Nozzle Flow Characteristics in Pneumatic Force-Balance Circuits . . . *D. B. Kirk* 111

Some Properties and Mechanical Applications of Compar . . . . . . *J. J. Hitov* 117

Cross-Laminated Oak . . . . *E. G. Stern* 123

Stretch Notch Sensitivity With Eccentric Holes . . . *L. Schapiro and R. H. Esling* 135

Discussion . . . . *J. K. Salisbury* 139

FEBRUARY, 1948

VOL. 70, NO. 2

Transactions

of The American Society of Mechanical Engineers

Published on the tenth of every month, except March, June, September, and December

---

OFFICERS OF THE SOCIETY:

E. G. Bailey, *President*

K. W. Jappe, *Treasurer*

C. E. Davies, *Secretary*

COMMITTEE ON PUBLICATIONS:

H. L. Dryden, *Chairman*

J. M. Juran

John Haydock

Ronald B. Smith

C. B. Campbell

George A. Stetson, *Editor*

K. W. Clendinning, *Managing Editor*

ADVISORY MEMBERS OF THE COMMITTEE ON PUBLICATIONS:

Hunter R. Hughes, Jr., Atlanta, Ga.

JUNIOR MEMBERS

Louis Feld, Newark, N. J.

John H. Prentiss, New York, N. Y.

Published monthly by The American Society of Mechanical Engineers. Publication office at 20th and Northampton Streets, Easton, Pa. The editorial department is located at the headquarters of the Society, 29 West Thirty-Ninth Street, New York 18, N. Y. Cable address, "Dynamic," New York. Price $1.50 a copy, $12.00 a year; to members and affiliates, $1.00 a copy, $6.00 a year. Changes of address must be received at Society headquarters three weeks before they are to be effective on the mailing list. Please send old as well as new address. . . . By-Law: The Society shall not be responsible for statements or opinions advanced in papers or . . . printed in its publications (B13, Par. 4). . . . Entered as second-class matter March 2, 1928, at the Post Office at Easton, Pa., under the Act of August 24, 1912. . . . Copyrighted, 1948, by The American Society of Mechanical Engineers. Reprints from this publication may be made on condition that full credit be given the Transactions of the ASME and the author, and that date of publication be stated.

Illinois U Library

Meter for Flowing Mixtures of Air and Pulverized Coal

BY H. M. CARLSON,[1] P. M. FRAZIER,[1] AND R. B. ENGDAHL[2]

In the course of research by Battelle on the fundamentals of flow of mixtures of air and pulverized coal, for Bituminous Coal Research, Inc., a meter has been developed which measures the rate of flow of both constituents. The meter depends on a unique property of the mixture when passing through a sharp-edged rubber-faced orifice to which coal does not adhere. It was found that the presence of finely divided coal in the air stream has very little effect on the accuracy with which the orifice ndicates the flow of the air component, whereas a flow nozzle placed in series with the orifice measures the total of the air plus coal. Thus the simultaneous use of the two elements provides a means for determining the amount of coal flowing. This paper describes the development of the meter, presents data on its performance, and gives the details of practical application. The rate of coal flow is measured with an accuracy of plus or minus 5 per cent for coal-air ratios ranging from 0.5 to 1.4, and for coal sizes ranging from 75 to 92 per cent through 200 mesh, after allowance has been made for the small effects of these variables. The meter has been used successfully in the aboratory in vertical and horizontal pipe lines from /4 to 4 in. diam and it is believed to be applicable to larger ines.

DEVELOPMENT OF THE METER

IN the initial stages of the search for a meter for flowing mixtures of air and pulverized coal, several approaches were made. A swinging vane suspended in a horizontal pipe was tried. Such an instrument is reported (1)[3] to have been in use since 1923 to measure ventilating air flow in a number of Witwatersrand gold mines in South Africa. It has been proposed (2) that where flow in a single line is to be measured, the air flow an be measured by such a device ahead of the point of introducion of the coal, and the deflection of an identical device followng the addition of coal would, by comparison with the clean-air ndication, give an indication of the amount of coal flow.

However, in the brief investigation of a single vane in the coal-ir line, the effect of the coal was not distinct, and a thorough nvestigation of the principle was not made in view of the obious problem of maintaining a tight yet frictionless seal for a shaft transmitting the vane motion to an indicating mechanism, or, on the other hand, of developing a remote electrical indication of the motion.

The application of a Pitot tube was also tried, but, because of he difficulties with plugging of the impact opening within a very short time, it was abandoned as not practical. The conventional orifice was then tried, but it was found that even though coal was flowing in the air stream, the orifice differential was only slightly affected by the presence of the particles of solid. The discovery of this interesting property opened the way for further investigation and study. About this time, a photoelectric meter was being investigated which employed a nozzle to converge the stream of air and coal, across which a beam of light was directed, so that the coal in this stream could be measured by the light-extinction principle, while the air would be measured by the nozzle. However, it was discovered that the nozzle was affected by the presence of the coal in the line, and, further, it was found that if the density of the coal-air mixture was known, it was possible to calculate the total flow of coal and air in the line using conventional flowmeter formulas. This action of a nozzle or Venturi has been tacitly assumed in the technical and patent literature but, to the authors' knowledge, has never been demonstrated from published data (3, 4).

The authors have been unable to develop a completely satisfactory theory for the action of the meter, but possible explanations of the phenomena of flow of fine solids in suspension will now be described.

THEORIES OF METER PRINCIPLE

The simplest theory to explain the difference in action of the air-suspended solids when passing through an orifice or a nozzle is that the particles do not have time to accelerate in the abrupt contraction of the orifice; hence their passage is not indicated by the orifice pressure differential which measures acceleration alone. On the other hand, the fact that a flow nozzle has been shown to measure the flow of the coal-air mixture indicates that the particles do have time to accelerate in such a gradual constriction. As an indication of this effect, an attempt was made to calculate the distance traveled by a 200-mesh particle when decelerating in still air from an initial velocity of 30 fps. The empirical equations of Drinker and Hatch (5) for spherical particles in turbulent and laminar flow were used. That coal particles are not spherical means that their resistance to relative motion with air would be greater, hence the deceleration distance would be less. Fig. 1 shows the shape of coal particles pulverized in a jet mill and photographed through an electron microscope for the investigations being made for the Locomotive Development Committee of Bituminous Coal Research, Inc.

For laminar flow the equation is

$$v = v_0 - \left(\frac{kdy}{4.19}\right)\frac{s}{ma^2}$$

where

v = final particle velocity = 0 fps
v_0 = initial particle velocity = 21.5 fps (based on 125 lb per hr air flow in a 2-in. pipe)
k = constant (18.85 for laminar flow)
d = density of fluid (0.075 lb per cu ft for air)
y = kinematic viscosity, sq ft per sec
s = distance of travel, ft
m = density of the particle, (85 lb per cu ft)

---

[1] Research Engineer, Battelle Memorial Institute, Columbus, Ohio. un. ASME.

[2] Assistant Supervisor, Battelle Memorial Institute, Columbus, hio. Mem. ASME.

[3] Numbers in parentheses refer to the Bibliography at the end of he paper.

Contributed by the Fuels Division and presented at the Semi-nnual Meeting, Chicago, Ill., June 16–19, of THE AMERICAN SOCIETY F MECHANICAL ENGINEERS.

NOTE: Statements and opinions advanced in papers are to be nderstood as individual expressions of their authors and not those the Society.

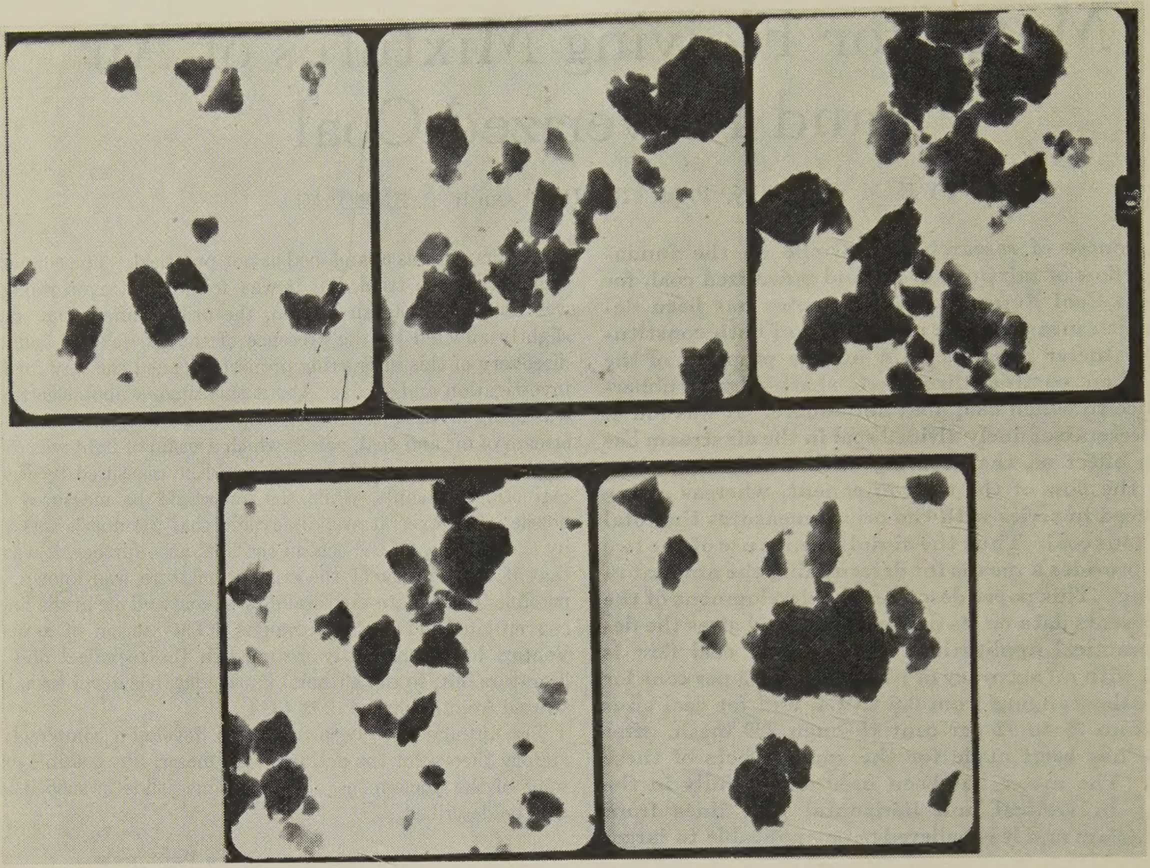

Fig. 1 Electronmicrograph of Coal Pulvérized in a Jet Mill to 90 Per Cent Through 325 Mesh; ×6000, Approximately

a = particle radius (3.1×10^{-5} ft avg size of particle through 200-mesh screen), determined by Lea-Nurse permeability method (6)

For turbulent flow, the equation is

$$v = v_0\, e^{\left(\frac{-kds}{4.19\, ma}\right)}$$

where in this case

v = final particle velocity = assumed 0.0001 fps for purpose of calculations
v_0 = initial velocity = 21.5 fps (as obtained for laminar flow)
k = constant (1.35 for turbulent flow)
d = density of fluid (0.075 lb per cu ft for air)
s = distance of travel, ft
m = density of particle (85 lb per cu ft)
a = radius of particle (3.1×10^{-5} ft avg size of particle through 200-mesh screen), determined by Lea-Nurse permeability method (6)

The results of these calculations for deceleration were 0.364 in. and 1.34 ft for laminar and turbulent flow, respectively. The values are so different that they are of value only to indicate that a measurable distance is probably required for a suspended particle to accelerate in an accelerating gas stream.

Another indication of the lag of suspended particles is given by the deduction of Stodola (7) and others that, in a nozzle passing wet steam, the particles of water which are formed at the throat lag behind the main stream because of their inertia. However, this well-known effect did not indicate the unique difference between the acceleration in a sharp-edged orifice and in a flow nozzle.

Further evidence of the lag of particles in an accelerating stream is given by Wood and Bailey (8) who conclude:

"Because of the appreciable time required for solid particles to accelerate from rest when dropped into a fluid current, the pressure gradient in a conveyer pipe is steepest at the inlet and diminishes until it reaches a steady value for both sand and grain. The distance to reach this value is approximately constant under all conditions."

A corollary of this last is that the distance required for a particle of a given material to accelerate to a given velocity is independent of the fluid velocity.

However, none of these cases indicates that the acceleration of the particles through a sharp-edged orifice is negligible, or at least that it is too small to be accurately measurable.

An additional effect of the lag of the particles in the accelerating stream may be the distortion of the flow pattern through the orifice. Instead of solid surfaces to guide the flow, this pattern is normally established by the orifice face and sharp edge and is maintained by the dynamic effect of the convergent flow. In the flow of a dust suspension there is probably a concentration of particles near the face of the orifice and around the edge, and perhaps also a slight expansion and shift in position of the normal *vena-contracta* as a result of the differential velocities of coal and air. These effects have not been demonstrated and can only be surmised. Their combined result could be either to increase or decrease the indicated flow rate when computed by means of the conventional orifice coefficient. Later, under the discussion of the effect of coal-particle size on meter performance, the existence of both positive and negative orifice errors, depending upon size, will be shown to lend credence to the possibility of some such interaction as just described.

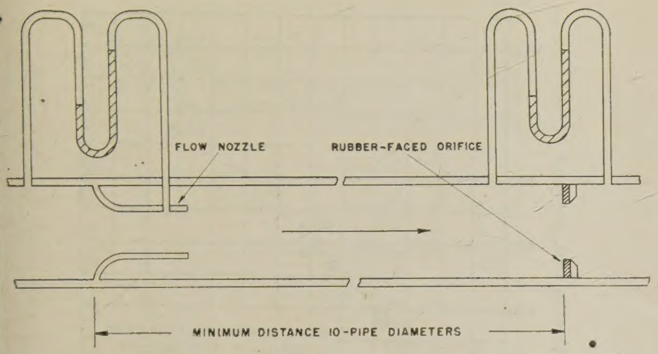

FIG. 2 COAL-AIR FLOWMETER

METER EQUATION

After it was observed that the orifice differential was not greatly affected by the presence of coal particles passing in the line, whereas the nozzle differential was affected, the two elements were placed in series to measure both the flow of air and coal at any point in a coal-air line, as shown in Fig. 2. This method of measuring solids in an air or gas stream was believed to be new, and a patent application has been filed. Further algebraical manipulations showed that by using the calculations of both of these elements, together with a minor simplifying assumption, it was possible to obtain a simple mathematical formula which enabled the direct calculation of the amount of coal flowing without knowing the density of the mixture flowing, as would be required if the nozzle alone were used. The derivation of this formula follows.

The equation for gravimetric flow through a constriction is

$$W = \rho C A f \sqrt{2g\Delta h} \ldots\ldots [1]$$

where

W = weight rate of flow of the fluid, lb per hr
ρ = fluid density, lb per cu ft
C = coefficient of discharge
A = area of constriction, sq ft
f = velocity of approach factor
g = acceleration of gravity, fps
Δh = differential head in feet of fluid

If we now assume the mixture of coal and air flowing through the constriction to be a homogeneous fluid, and assume that C, the coefficient of discharge, remains constant for fluids of different densities, only the factor ρ in the equation will change as coal is added, however

$$\Delta h = \frac{iw}{12\rho}$$

where

i = pressure drop across constriction in inches of manometer fluid
w = density of manometer fluid used in measuring pressure differential, lb per cu ft

The formula then becomes

$$W = \rho C A f \sqrt{\frac{2giw}{12\rho}} \ldots\ldots [2]$$

which equals

$$W = CAf \sqrt{\frac{2giw}{12}} \sqrt{\rho} \ldots\ldots [3]$$

Now for a coal-air mixture passing through the constriction

$$\rho = \frac{W_a + W_c}{W_a} \rho_a \ldots\ldots [4]$$

where

ρ = density of mixture, lb per cu ft
ρ_a = density of air, lb per cu ft
W_a = weight rate of air flow, lb per hr
W_c = weight rate of coal flow, lb per hr

If it is assumed for the density of the mixture herein considered that the coal occupies no space, an assumption that makes less than 0.25 per cent error in the calculations, Equations [3] and [4] can be combined to give

$$W_a + W_c = CAf \sqrt{\frac{2giw\,\rho_a}{12}} \sqrt{\frac{W_a + W_c}{W_a}} \ldots\ldots [5]$$

which in turn equals

$$W_a + W_c = \rho_a CAf \sqrt{\frac{2giw}{12\rho_a}} \sqrt{\frac{W_a + W_c}{W_a}} \ldots\ldots [6]$$

Squaring both sides, we have

$$(W_a + W_c)^2 = \left(\rho_a CAf \sqrt{\frac{2giw}{12\rho_a}}\right)^2 \frac{(W_a + W_c)}{W_a}$$

or

$$W_a(W_a + W_c) = \left(\rho_a CAf \sqrt{\frac{2giw}{12\rho_a}}\right)^2$$

Thus the coal rate is

$$W_c = \frac{\left(\rho_a CAf \sqrt{\frac{2giw}{12\rho_a}}\right)^2}{W_a} - W_a \ldots\ldots [7]$$

The expression in parentheses in Equation [7] is a fictitious "mixture flow," where i is the pressure drop for the nozzle passing air plus coal, but the density used in the expression is not that of the mixture, but of the air alone. It is computed from the measurements as though air alone were flowing. If this expression is replaced by W_{an}, Equation [7] becomes

$$W_c = \frac{W^2_{an}}{W_a} - W_a \ldots\ldots [8]$$

W_a is obtained very nearly by using an orifice with the usual flow formula in the mixed flow line. Thus the weight rate of coal flow may be calculated by using the flow equation for both orifice and nozzle as though air alone were flowing, and substituting these two calculated rates in Equation [8].

PERFORMANCE OF LABORATORY METERS

Laboratory work with this instrument has given satisfactory results in several installations. The discovery and development were in connection with the measurement of coal-feed rate in the pulverized-coal and air-circulating system for a radiant-tube furnace. This system was composed of a $2^1/_2$-in. horizontal line reducing to a 2-in. line after the first two burner take-off positions. The conveying air was measured by means of an orifice in the inlet pipe to the blower for the circulating system. The coal was fed to the blower inlet from a bin on a scale by means of a screw feeder so that, by means of weight and time readings, the feed rate could be determined. After the coal passed the furnace and meter, it was returned to the feed bin by means of a cyclone collector, and the nearly clean air was exhausted to the atmosphere. The results of this first work with the meter were encouraging.

In order to investigate the performance of a larger meter, a vertical line of standard 4-in. pipe was installed in connection with the same feeding and collecting equipment, but with a larger blower. The higher air capacity was desired not simply because of the larger system, but also because it had been found desirable to maintain the Reynolds number for the two meter elements high enough so that the coefficients remained practically constant over the desired range of flow rates. At Reynolds numbers under 100,000, the coefficients may vary enough to require determination of their value at each flow rate.

The size of the orifice and nozzle used in the 4-in. line was determined from standard flowmeter practice. The largest ratio of orifice-to-pipe diameter for which coefficients are available (10) is 0.7, and this was selected for the initial tests. Later an orifice with a diameter ratio of 0.75 was made in order to decrease the pressure drop through the element. The coefficient for this larger-diameter orifice was determined by extrapolation from the curve given in "Flow Measurement" and checked with another orifice whose coefficient was known. The ratio of nozzle to pipe diameter was chosen as 0.5 in order to keep the Reynolds number as high as possible without too great a pressure drop across this element. Addition of a diffuser following the nozzle aided greatly in regaining most of the pressure loss across the nozzle.

In all of the tests, except the last six of the 4-in. line series, the following procedure was used: A clean-air test was first run to check the operation of the orifice, nozzle, manometers, and gages. Then the coal feeder was started and gradually the coal-air ratio was increased in steps to the maximum permitted by the existing equipment and then decreased in steps to check the data taken when increasing the coal feed. Because the blower was handling the maximum amount of air possible before the coal feeder was started, the amount of air entering the system gradually decreased while the coal-feed rate was increased as the energy to convey the coal was taken from the air, which in turn received its energy from the fan. In the last six tests run on the 4-in. line, the air entering the system was kept constant and only the feed rate was changed. The performance of the meter under these conditions was as in the previous tests.

Effect of Pipe Size on Performance of Meter. Coal flowmeters have now been used in four different sizes of pipe, $^3/_4$, $1^1/_2$, 2, and 4-in. nominal pipe diameter. Within the range investigated, pipe size has no effect upon the performance of the meter.

It is possible that the ratio of the diameters of the metering elements to the pipe diameters could have some effect upon meter performance. This has not been fully investigated. The range of ratios for the orifices used in tests was 0.6 to 0.75. It appears that the error of the orifice when passing coal, changes slightly as the ratio becomes smaller. This change was observed to be about one per cent over the ranges studied.

No accurate study has been made on the effect of ratio of nozzle-to-pipe diameter on the flow indication of the nozzle.

Location of Pressure Taps in Nozzle. In the development of the meter, various positions of throat taps were used with different lengths of parallel throat sections on the nozzle. This was done to determine the tap location which gave the best indication of the total mixture flowing. It was found that the tap position as specified in standard flowmeter practice gave satisfactory flow indications. It is not known definitely whether pipe-wall taps can be used instead of throat taps. Preliminary tests indicate that this is possible.

Effect of Coal Fineness and Coal-Air Ratio

Owing to the assumption made that the meter operates on the principle of differential acceleration of the coal particles through the meter, it appeared likely that particle size would affect the coal-flow indication. Three groups of tests, with varying coal-air ratios, were made with three different average coal finenesses of 75, 85, and 92 per cent through 200-mesh screen. The results of these tests are shown in Fig. 3, indicating that for finenesses above 85 per cent, the meter registers less than actual coal flow, and greater than actual for finenesses below 85 per cent.

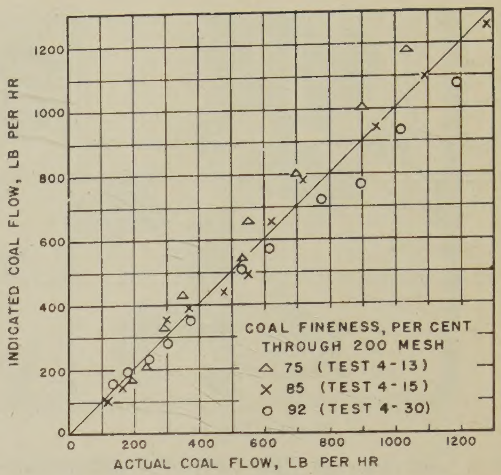

Fig. 3 Effect of Coal Fineness on Uncorrected Coal Flow

Further study showed that the flow indications of both the orifice and the nozzle were affected by changes in coal fineness and in coal-air ratio.

Figs. 4 and 5 show, respectively, the effect of fineness and of coal-air ratio on the flow indication of the orifice and the nozzle. The curves were obtained by calculating the errors of the orifice alone for the data shown in Fig. 3, and plotting the results against fineness for three different mixture densities. These curves can be used to correct conventional clean-air orifice and nozzle coefficients to give a corrected calculated coal and air flow. Because of the presence of coal, the existence of both positive and negative errors in the air-flow indication of the orifice seems to show that there is a small but definite influence of the coal on the orifice-flow pattern.

In operating the 4-in. circulating system over a period of time, it was noted that coal-size degradation was taking place probably by impact and attrition. As a result, the laboratory meter performance was probably affected to a small extent by the change in fineness. This would not be the case, however, in an installation where the coal passes through the system only once and little or no coal is recirculated.

Accuracy. In all of the testing of the meter, it was found to be very important that every precaution be taken to obtain correct readings on the gages used, particularly because the meter equation magnifies in the result any errors in the differential readings. This meant that every manometer line had to be checked for leaks and for plugging owing to coal accumulation. The tests of the instrument have given accurately the coal flow in an air-and-coal mixture within plus or minus 5 per cent over a range of coal-air ratios from 0.5 to 1.4 when correction factors, shown in Figs. 4 and 5, are used. This is considered accurate enough for purposes of measurement and control. It is reasonable to expect that the accuracy will improve as development and application are continued.

For coal-air ratios less than 0.5, increasing care is required to maintain accuracy. Very dense mixtures have not been tried, but above a solid-air ratio of unity there is probably some point where the thick mixture disrupts flow in the orifice.

Accumulation of Coal in Meter. Soon after the test work began on the meter in the 2-in. line, a change in material for the orifice plate was found to be necessary as the brass orifice plate which

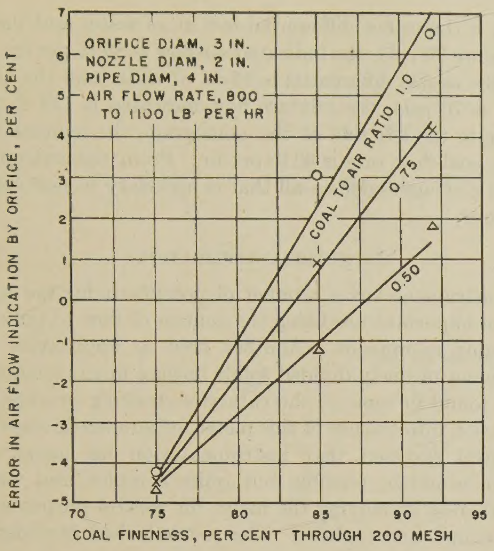

Fig. 4 Effect of Coal Size and Coal-Air Ratio on Air-Flow Indication of Orifice

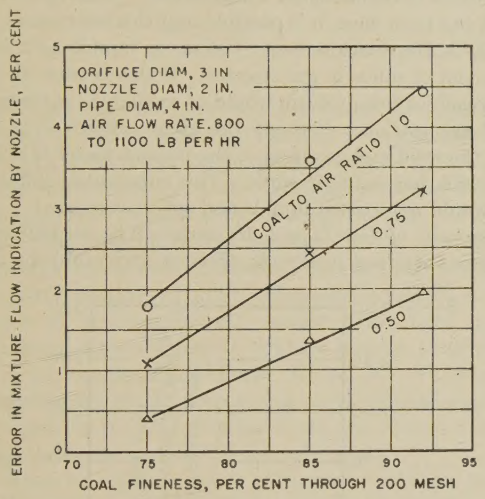

Fig. 5 Effect of Coal Size and Coal-Air Ratio on Mixture Flow Indication of Nozzle

was employed initially accumulated a hard crust of coal on the orifice edge, rounding the entrance to the orifice and thereby increasing its coefficient. Fig. 6 shows the accumulation. It was believed that this build-up on the face of the orifice was the result of the coal particles impinging on the hard brass surface, sticking and accumulating as the flow of the mixture continued. The problem was solved by the use of an orifice made up of a sheet of rubber bonded to metal. The turning of the rubber-faced orifice was not possible with standard lathe tools, but was accomplished very satisfactorily by the use of a coarse grinding wheel turning at high speed. This orifice gave good results in measuring the air and, of most importance, coal did not accumulate on the face of the orifice. It is believed that the particles of coal which impinge on the rubber surface rebound and are carried through the orifice by the oncoming stream. This usage was believed to be new and a patent application has been filed. No other difficulty was experienced with coal settling or accumulating at the orifice or nozzle.

Applications to High-Pressure Fuel-Supply Lines

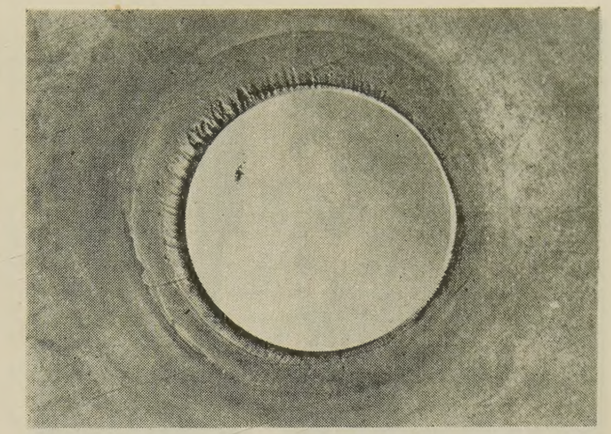

Fig. 6 Accumulation of Coal on Edge of Brass Orifice

Besides the application of the meter to the 4-in. line, two opportunities were found in the laboratory for trying the meter in a practical way. The first was in connection with a high-pressure combustion unit where pressures up to 100 psi are encountered. Considerable difficulty was experienced in keeping the manometer lines free of coal, even though filters were placed in the lines. It was a major problem to make these lines absolutely airtight at the high pressures. If the tube connections are perfectly tight, no air can escape from them to allow coal to flow into the line. However, if there is the slightest leak in the line, the air under the high pressures escapes, leaving the coal behind to fill up the filters and plug the line completely.

A solution in actual practice is to bleed a very small quantity of air directly into the manometer lines, so as to maintain flow toward the main coal-flow line in the manometer lines. The rate at which this air is allowed to flow in is made so small that the differential pressure is not affected, but high enough to eliminate the possibility of any coal getting into the manometer lines. The rate of flow of air bled into the two manometer lines on each element must be made nearly equal to avoid influencing the pressure-differential indication of the manometer. This is done by metering the air visually through transparent water-filled "bubblers" commercially available. By means of valves in the bleed lines, the rate of bubbling of air through the water can be regulated. Where large pressure fluctuations occur, the meter should be equipped with blowout connections for periodic cleaning. The application of the meter to this high-pressure system is still in the development stage and has not been entirely satisfactory, owing to plugged manometer taps caused by fluctuations in the coal-air ratio which take place very rapidly because of feeding difficulties.

The second installation was in a low-pressure, pulverized-coal and air line where the pressure did not exceed 15 psi. Manometer line leakage was experienced with this meter, but when this was eliminated it gave very satisfactory operation. This meter, shown in Fig. 7, indicates immediately any change in coal-air ratio produced by uneven coal feeding or air-pressure fluctuations.

A quick indication of the coal flow is provided by a chart shown in Fig. 8 which can be placed adjacent to the two manometers. This was prepared by H. R. Hazard for use with the meter shown in Fig. 7 for a particular application where the coal-air ratio is always maintained at 1.00. The meter was so constructed that when clean air was flowing the differential pressure across the orifice was twice that across the nozzle. When an equal amount of coal and air was flowing, the differential pressures across both elements were the same. In operation of the low-pressure furnace where it was desirable to maintain a coal-air ratio of 1 to 1, it was necessary only to maintain the two differentials at the same level.

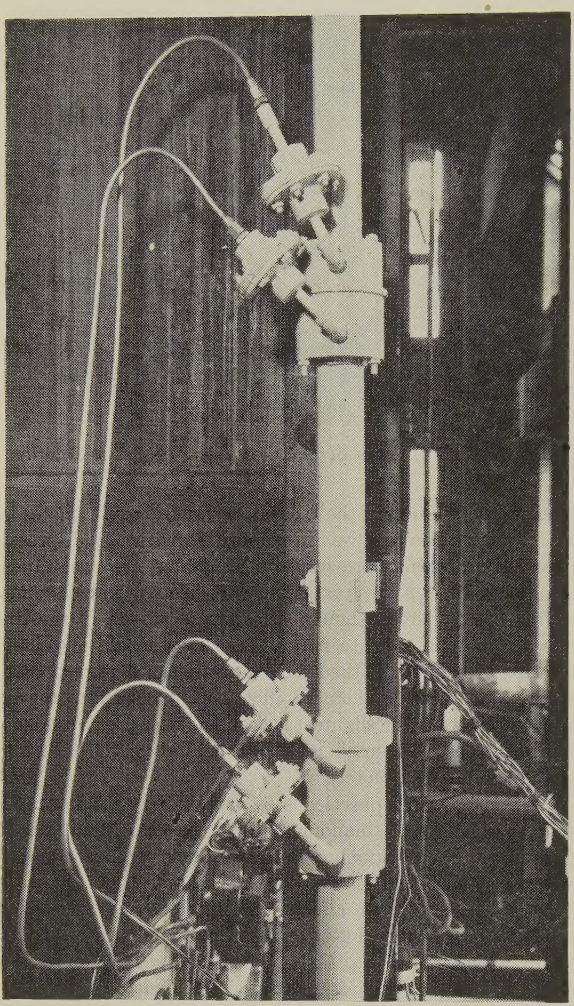

FIG. 7 FLOWMETER INSTALLED IN LOW-PRESSURE, COAL-AIR SUPPLY LINE

Any other desired coal-air ratio could be obtained by adjusting the amount of coal being fed to give an intermediate reading on the right scale between the 1 to 1 differential reading and the differential obtained when air alone was flowing.

For example, in Fig. 8, when air alone is flowing at a rate of 250 lb per hr, the orifice and nozzle differentials are 5.6 and 2.8 in. water, respectively. When coal is flowing in addition at the same rate, the nozzle differential rises from 2.8 to 5.6 in. Then, referring to the final meter Equation [8], if air flow is held constant, coal flow is proportional to nozzle differential. Thus the interval on the right scale between zero coal flow and a coal-air ratio of 1 can be subdivided uniformly into equal intervals representing equally spaced coal-air ratios between 0 and 1. For purposes of reading, these points are connected in Fig. 8 by dashed lines radiating from the point of constant air flow on the left scale, and each line is labeled with the coal flow corresponding to its intersection with the uniformly subdivided coal scale. Therefore for a coal-air ratio of 0.6, the nozzle manometer would read 4.6 in. water and the coal rate would be 150 lb per hr.

The nomogram shown in Fig. 9 provides a means for determining quickly the amount of coal and air flowing when using the coal-air flowmeter in a high-pressure line. The three parallel scales shown on the right side of the nomogram furnish the flow rates of the air and the mixture, and when transferred to the scales on the left side, give the amount of coal flowing directly. For example, if the orifice differential is 8 in. of water and the absolute pressure 70 psia, the indicated air flow is 86 lb per hr. Likewise, if the nozzle differential is 15 in. of water and the absolute pressure is 70 psia, the mixture flow indicated is 119 lb per hr. Referring to the left side of the nomogram, the indicated corresponding coal-flow rate is 80 lb per hr. From the example it is seen that a straightedge is all that is necessary to perform these calculations.

INDUSTRIAL APPLICATIONS

This instrument has a number of possible industrial applications, one important use being the control of flow to pulverized-coal-burning equipment. Another field of application is the measurement of finely divided solids flowing in gas streams such as those found in some of the catalytic cracking processes. An investigation into the use of this meter for automatic registration and control revealed that instrumentation for instantaneous indication would be possible but quite complex and therefore costly, whereas employing the meter for control purposes would be very simple and positive. The research field provides other applications for this instrument where it is necessary to know the amount of finely divided solids flowing in gas streams.

Application to Solid-Liquid Suspensions. Although no actual test work has been done, it is possible that this instrument may be applicable to the measurement of solids in liquids as it is in the measurement of solids in gas streams. If this is true, an entirely new approach to this problem would be available for research and practical application. Perhaps the great difference in density between the solid and gas used in the present meter is one of the factors which has made it work. This substantial difference in density would not exist if liquids and solids were used.

Measurement of Gas-Liquid Mixtures. The measurement of air or gases entrained in liquids offers similar problems to those

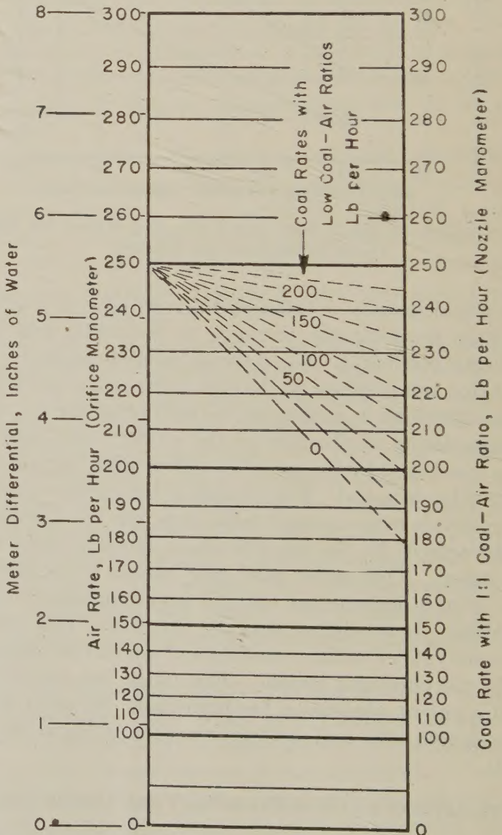

FIG. 8 COAL METER SCALE SHOWING EFFECT OF COAL-AIR RATIO

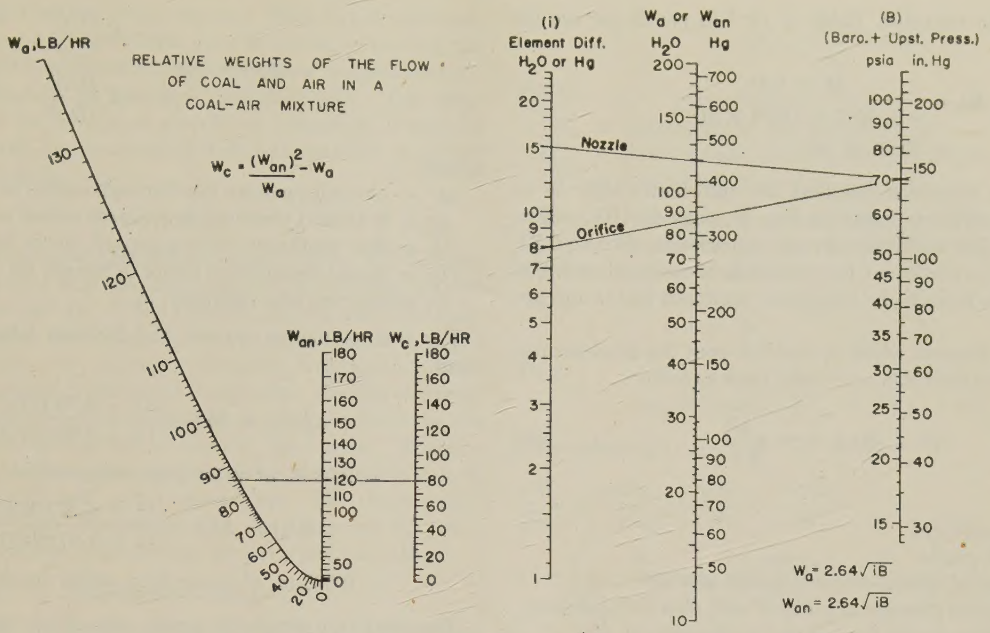
W_a, LB/HR
RELATIVE WEIGHTS OF THE FLOW OF COAL AND AIR IN A COAL-AIR MIXTURE
$W_c = \frac{(W_{an})^2}{W_a} - W_a$
W_an, LB/HR
W_c, LB/HR
(i) Element Diff. H₂O or Hg
Nozzle
Orifice
W_a or W_an H₂O Hg
(B) (Baro.+ Upst. Press.) psia in. Hg
$W_a = 2.64\sqrt{iB}$
$W_{an} = 2.64\sqrt{iB}$

FIG. 9 TYPICAL NOMOGRAM FOR COAL-FLOW CALCULATION

with other mixtures. An ingenious instrument for doing this has been devised by the Gulf Research and Development Company. It consists of a small motor-driven pump which samples a mixture of oil and air and forces the mixture through a small orifice where the air entrained is compressed to a small fraction of its former volume so that the differential pressure across the orifice accounts for only the oil and not the air. This fact makes it possible to obtain curve relations of orifice differential pressures, at known percentages of air entrainment against pump-inlet pressure. The instrument was installed in military aircraft to give an indication of the actual air entrained in the oil (9). The use of one element insensitive to the presence of air is quite similar to the principle used in the coal flowmeter but the means to achieve this insensitivity are necessarily quite different.

Orifice Alone as a Meter. Study of the meter principle indicated that with suitable remote location of the downstream tap for the orifice, the coal would have time to accelerate so that the orifice might be used to indicate both coal and air flow. This was tried in the 4-in. line with considerable success, although the error with the orifice alone was consistently very large, and the spread of the data was greater than for the nozzle-orifice combination. It appears that the rate of pressure regain following the orifice has an important influence on the indication of the pressure tap situated some distance downstream.

Photoelectric Meter. When the possibility of using the orifice and the nozzle in series was discovered, the work on the photoelectric meter was dropped to concentrate effort on this new principle. The work on the photoelectric meter had progressed to the point where satisfactory indication of the presence of the coal in the air stream was obtained. Some difficulty was experienced in keeping the lenses free of coal dust. It is the authors' opinion that a meter of this type does show promise, and that more work should be done on developing it further, although calibration, in some instances, may be difficult.

DESIGN CALCULATIONS

A typical calculation for the installation of the meter in a situation would take the following form:

Assume the following:

Boiler capacity, 500,000 lb steam per hr
Fuel, approximately 25 tons per hr
4 burners, 12,500 lb of coal per hr
Coal-air ratio in primary line, 0.5 lb of coal per lb of air
Primary air required, 25,000 lb per hr, or 6.94 lb per sec
Required pipe velocity, 100 fps

Volume = 6.94/.075 = 92.6 cfs

From this

$$\pi/4\, D^2 \times 100 = 92.6$$

$$D^2 = 1.17$$

$$D = 1.08 \text{ ft} = 13 \text{ in.}$$

where

D = diameter of coal- and primary-air line

For a minimum pressure drop, use orifice-to-pipe ratio of 0.70 giving an orifice 9.1 in. diam. Selecting the largest nozzle-to-pipe ratio results in a nozzle diameter 10.5 in. The orifice-to-pipe diameter ratio of 0.70 and the nozzle-to-pipe diameter ratio of 0.80 are the largest values for which coefficients are given in "Flow Measurement" (10).

Calculation of the Reynolds number for these conditions gives the following:

$$R_0 = \frac{48\,w}{\pi D_0 \mu}$$

where

w = flow, 6.94 lb per sec
D_0 = diameter of orifice, 9.1 in.
μ = absolute viscosity, 12.75×10^{-6} lb per ft per sec for 100 F[4]

$$R_0 = \frac{48 \times 6.94}{\pi \times 9.1 \times 12.75 \times 10^{-6}} = 912.0 \times 10^3$$

and

$$R_n = \frac{48\,w}{\pi D_n \mu}$$

where

w = flow, 6.94 lb per sec
D_n = diameter of nozzle, 10.5 in.

---

[4] Reference (10), Fig. 14, p. 25.

μ = absolute viscosity, 12.75×10^{-6} lb per ft per sec for 100 F[4].

$$R_n = \frac{48 \times 6.94}{\pi \times 10.5 \times 12.75 \times 10^{-6}}$$
$$= 792.0 \times 10^3$$

Both of these Reynolds numbers are sufficiently high as to give constant coefficients found in Fig. 31, page 44 (10), where on page 54, the flow coefficient for the orifice is found to be 0.70, and on page 44 the coefficient for the nozzle is obtained as 1.272. These coefficients include the velocity of approach factor and are referred to as K.

The practical formula which is derived from the fundamental flow formula gives fluid flow on weight basis as follows

$$W = 413.3\, KD^2 \sqrt{\frac{iB}{T}} \quad \ldots\ldots\ldots\ldots\ldots [9]$$

where

K = flow coefficient
W = flow, lb per hr
i = differential across element, inches of water
B = barometric pressure at point of test, plus the upstream pressure in the line before the element, in. Hg
T = temperature of fluid flowing through element, F abs

Substituting values

$$W_{\text{orifice}} = 413.3 \times 0.70 \times (9.1)^2 \sqrt{\frac{iB}{T}}$$
$$= 24{,}000 \sqrt{\frac{iB}{T}}$$
$$W_{\text{nozzle}} = 413.3 \times 1.272 \times (10.5)^2 \sqrt{\frac{iB}{T}}$$
$$= 58{,}000 \sqrt{\frac{iB}{T}}.$$

The differential pressures on the gages, when operating under design conditions are obtained as follows

For the orifice

$$25{,}000 = 24{,}000 \sqrt{\frac{i \times 29.90}{560}}$$

from which

$$i = 20.3 \text{ in. of water}$$

For the nozzle, it is necessary to use the formula for coal flow to obtain first W_{an}

$$12{,}500 = \frac{W^2_{an}}{25{,}000} - 25{,}000$$

or

$$W^2_{an} = 938 \times 10^6$$

and

$$W_{an} = 30{,}600$$

Therefore

$$30{,}600 = 58{,}000 \sqrt{\frac{i \times 29.90}{560}}$$

and

$$i = 5.23 \text{ in. of water}$$

An approximation of the total pressure drop across the orifice is obtained by the use of the formula[5]

$$\Delta p' = \Delta p \, \frac{1 - K \dfrac{(D_2)^2}{(D_1)^2}}{1 + K \dfrac{(D_2)^2}{(D_1)^2}}$$

where

$\Delta p'$ = over-all pressure loss through orifice or nozzle, psi
Δp = indicated pressure drop across orifice or nozzle, psi
K = flow coefficient with approach factor included
D_2 = throat diameter of orifice or nozzle, in.
D_1 = internal pipe diameter, in.

For this particular system, the formula takes the following form

$$\Delta(p'_o) = 20.3 \times \frac{[1 - 0.70(0.7)^2]}{[1 + 0.70(0.7)^2]}$$
$$= 9.93 \text{ in. of water drop across orifice}$$
$$\Delta(p'_n) = 5.23 \times \frac{[1 - 1.272(0.8)^2]}{[1 + 1.272(0.8)^2]}$$
$$= 0.533 \text{ in. of water drop across nozzle}$$

The total drop across the meter, then, is the sum of these pressure drops, or 10.46 in. of water. Thus the system would have to be designed for the desired pressure at the burner to include the drop through the meter, plus the customary pressure drops in the line, mill, or other equipment.

The largest drop is across the orifice, and this could be decreased appreciably by the use of a slightly larger orifice diameter. For example, if the orifice just chosen were increased 1 in. in diam, the difference in pressure drop would be as follows:

Evaluating the Reynolds number

$$R_0 = \frac{48 \times 6.94 \times 10^6}{\pi \times 10.1 \times 12.75} = 821.0 \times 10^3$$

which is satisfactory.[6] The differential pressure as obtained using this orifice would be obtained from the flow formula previously used, Equation [9]; K in this case must be extrapolated from the graph of reference (10),[7] and would be 0.735. The flow formula then becomes, changing D from 9.1 to 10.1 in.

$$W_0 = 31{,}000 \sqrt{\frac{iB}{T}}$$

The differential pressure in this case would be

$$i = \frac{560 \times 0.65}{29.90}$$
$$= 10.3 \text{ in. of water}$$

The pressure drop across the orifice would then be from the formula used previously

$$\Delta(p')_0 = 10.3 \, \frac{[1 - 0.735(0.78)^2]}{[1 + 0.735(0.78)^2]}$$
$$= 3.96 \text{ in.}$$

This would then make the pressure drop across the meter 4.5 in., a value far more acceptable than the 10.46 in. obtained with the 9.1-in. orifice.

The power requirements for carrying the coal and primary air for such a system would be approximately 60 hp on the basis of an over-all pressure drop of 24 in. In all probability, the system would be installed with a 75-hp motor. This would take care adequately of an additional meter drop of 4.5 in., providing the proper exhauster were chosen, since the power requirement increases approximately as the total head increases. For other situations where the system is already in operation, it may be necessary to install an exhauster of sufficient capacity to permit the use of the meter.

---

[5] Reference (10), p. 17, par. 56.

[6] In view of Fig. 366, p. 54, reference (10).

[7] Test Code on "Flow measurement," reference (10), p. 54.

CONCLUSIONS

It has been discovered that a sharp-edged orifice will indicate essentially the flow of only the air component of a flowing mixture of pulverized coal and air. It has also been shown that if the coal-air ratio is known, a flow nozzle or Venturi may be used to measure the rate of flow of the mixture. However, if the small volume occupied by the finely divided coal is neglected, the knowledge of the air rate provided by the orifice can be used to eliminate the necessity for knowing the coal-air ratio at the nozzle. Thus the combination of the two elements composes a meter which can be used to measure the coal- and air-flow rates. The performance of the meter has been demonstrated in the laboratory for practical ranges of pipe size, coal-particle size, and coal-air ratio.

ACKNOWLEDGMENTS

The authors are indebted to many persons for their contributions to the work, particularly F. E. Graves, formerly of Battelle, who proposed the work on fundamentals of flow after considerable experience with various systems in the laboratory which indicated the need for this information. The work has been aided materially with suggestions and in the analysis of the problem by R. J. Martin, formerly of Battelle. Other contributors of the Battelle staff were F. R. Beatty, who assisted in the construction of the instruments; J. C. Bell, who prepared the nomogram, Fig. 9; George Armour and Frank Stoffel, who assisted in the development program.

BIBLIOGRAPHY

1 "A New Form of Air Meter and the Measurement of Compressed Air," by E. J. Laschinger, Trans. of the South African Institution of Engineers, vol. 23, February, 1925, pp. 360–369.

2 John I. Yellott letter to R. A. Sherman at Battelle Memorial Institute, Columbus, Ohio, January 8, 1946.

3 "Billet Heating," by C. F. Herington, *Iron Age*, vol. 146, 1940, pp. 26–29.

4 "Means for Measuring a Substance Carried in Suspension by a Second Substance," by A. R. Smith, U. S. Patent 1,677,691, issued July 17, 1928.

5 "Industrial Dust," by Phillip Drinker and Theodore Hatch, McGraw-Hill Book Company, Inc., New York, N. Y., 1936, p. 179.

6 "Specific Surface of Fine Powders," by G. M. Lea and R. W. Nurse, Trans. of the Society of Chemical Industries, vol. 58, 1939, p. 277.

7 "Steam and Gas Turbine," by A. Stodola and L. C. Loewenstein, Peter Smith, New York, N. Y., 1945, p. 118.

8 "The Horizontal Carriage of Granular Material by an Injector-Driven Air Stream," by S. A. Wood and A. Bailey, Proceedings of The Institution of Mechanical Engineers, vol. 142, 1939, pp. 149–164; discussion, pp. 164–173.

9 "An Instrument for Indicating the Amount of Gas in Gas-Liquid Mixture," by B. R. Walsh and G. S. Peterson, Trans. ASME, vol. 67, 1945, pp. 399–404.

10 "Information on Instruments and Apparatus, Part 5, Measurement of Quantity of Materials, chapt. 4, Flow Measurement by Means of Standardized Nozzles and Orifice Plates," ASME, Power Test Codes, 1940.

Appendix

INFLUENCE OF ERRORS IN INSTRUMENT READING ON FINAL RESULTS USING COAL

The equation for the coal-flow rate as developed in the paper is

$$W_c = \frac{W^2_{an}}{W_a} - W_a \ldots\ldots\ldots\ldots\ldots\ldots [8]$$

where

W_c = weight rate of coal flow, lb per hr
W_{an} = flow through nozzle by air formula, lb per hr
W_a = weight rate of air flow, lb per hr

To show the effect of errors in W_{an} and W_a on W_c, Equation [8] may be differentiated. To simplify the differentiation, Equation [8] may be written

$$W_c = \frac{W^2_{an} - W^2_a}{W_a}$$

Then

$$\log W_c = \log (W^2_{an} - W^2_a) - \log W_a$$

Differentiating

$$\frac{\Delta W_c}{W_c} = \frac{\Delta W^2_{an} - \Delta W^2_a}{W^2_{an} - W^2_a} - \frac{\Delta W_a}{W_a}$$
$$= \left(\frac{W^2_{an}}{W^2_{an} - W^2_a}\right)\left(\frac{\Delta W^2_{an}}{W^2_{an}}\right) - \left(\frac{W^2_a}{W^2_{an} - W^2_a}\right)\left(\frac{\Delta W^2_a}{W^2_a}\right)$$
$$- \frac{\Delta W_a}{W_a} \ldots\ldots\ldots [10]$$

At this point it is necessary to determine what factors of W_{an} and W_a are subject to appreciable error.

From the equations

$$W_{an} = 413.3\, K_{an} D^2_{an} \sqrt{\frac{i_{an} B_{an}}{T_{an}}} \ldots\ldots\ldots\ldots [11]$$

and

$$W_a = 413.3\, K_a D^2_a \sqrt{\frac{i_a B_a}{T_a}} \ldots\ldots\ldots\ldots\ldots [12]$$

it can be seen that there are five possible variables.

(*a*) The factors D and K may be determined with a high degree of accuracy for any given flow condition.

(*b*) Possible errors in temperature and pressure measurements would have negligible effect in the range of temperatures and pressures used, considering that T and B are expressed in absolute units.

(*c*) The factor i is the only variable which changes appreciably during any test. Any error in its determination will affect the calculated flow rate.

In view of considerations (*a*), (*b*), and (*c*), Equation [11] will be expanded to show the effect on W_c of errors in measuring i_{an} and i_a.

Equations [11] and [12] may be written

$$W_{an} = Z_{an} \sqrt{i_{an}} \ldots\ldots\ldots\ldots\ldots\ldots [13]$$

and

$$W_a = Z_a \sqrt{i_a} \ldots\ldots\ldots\ldots\ldots\ldots [14]$$

where

$$Z_{an} = 413.3\, K_{an} D^2_{an} \sqrt{\frac{B_{an}}{T_{an}}}$$

and

$$Z_a = 413.3\, K_a D^2_a \sqrt{\frac{B_a}{T_a}}$$

Taking the logarithms and differentiating the squares of Equations [13] and [14] gives

$$\log W^2_{an} = \log i_{an} + 2 \log Z_{an}$$

$$\frac{\Delta W^2_{an}}{W^2_{an}} = \frac{\Delta i_{an}}{i_{an}} = Y$$

and

$$\log W^2_a = \log i_a + 2 \log Z_a$$

$$\frac{\Delta W^2_a}{W^2_a} = \frac{\Delta i_a}{i_a} = X$$

Also

$$\log W_a = {}^1/_2 \log i_a + \log Z_a$$

$$\frac{\Delta W_a}{W_a} = ({}^1/_2) \frac{\Delta i_a}{i_a} = {}^1/_2 X$$

From Equation [8]

$$W^2_{an} = W_a(W_c + W_a)$$

Substituting in Equation [10]

$$\frac{\Delta W_c}{W_c} = \left(\frac{W_a}{W_c} + 1\right) Y - \left(\frac{W_a}{W_c} + {}^1/_2\right) X \ldots\ldots [15]$$

From Equation [15] it is evident that for any values of Y and X, the error in W_c is directly proportional to the air/coal ratio.

For example, assume the numerical values of Y and X to be equal. From Equation [15] the error will be maximum for this special case when the signs of Y and X are opposite.

Let

$$Y = +0.01$$

and

$$X = -0.01$$

then

$$\frac{\Delta W_c}{W_c} = \left(\frac{W_a}{W_c} + 1\right) (+0.01) - \left(\frac{W_a}{W_c} + {}^1/_2\right) (-0.01)$$

$$= 0.02 \frac{W_a}{W_c} + 0.015$$

Assume

$$W_a = 1000 \text{ lb per hr}$$

$$W_c = 750 \text{ lb per hr}$$

Then for the foregoing conditions

$$\frac{\Delta W_c}{W_c} = 0.02 \left(\frac{1000}{750}\right) + 0.015 = 0.042 = 4.2 \text{ per cent}$$

Discussion

The mathematical analysis given in this discussion is based upon condensed material supplied by John Blizard.[8] The authors believe that this contribution gives further evidence of the difference in fluid-flow performance of nozzles and orifices and throws further light on possible causes for the velocity difference which exists between the particles and the conveying air stream passing through a nozzle.

Nusselt[9] has analyzed, by means of Pitot tubes, the behavior of a gas as it passes through a sharp-edged orifice and through a nozzle. Fig. 10 of this discussion is a plot of the results obtained by Nusselt. The curves obtained are shown in relation to the positions of the orifice and of the nozzle to compare the relative behavior of the gas as it passes throug each of these constrictions. Study of these curves indicates tha the velocity change for an orifice is somewhat different fro that for a nozzle. It may be observed that, for the nozzle, acce eration is complete, or very nearly so, when the fluid leaves t nozzle; whereas, in the orifice, acceleration continues for so distance beyond or to the region known as the vena contracta.

Blizard analyzes the acceleration of a particle in a gas strea by letting

v = velocity of the gas

u = velocity of particle

and assumes that, initially

$$v = v_0 = u_0$$

and that, at any later time

$$v = v_0 + cx \ldots\ldots\ldots\ldots [16$$

where

v_0 = velocity of gas before constriction
u_0 = velocity of particle before constriction
x = distance along center line of constriction
c = const

The sole force of any significant magnitude acting on the par ticle is

$$P = m \frac{du}{dt}$$

where

m = mass of particle

From Stokes's law

$$\frac{du}{dt} = 9/2 \frac{z}{\rho' a^2} (v - u)$$

where

z = absolute viscosity
ρ' = density of sphere
a = radius of sphere

Therefore

$$\frac{du}{dt} = C' (v - u) \ldots\ldots\ldots\ldots [17$$

where

$$C' = 9/2 \frac{z}{\rho' a^2}$$

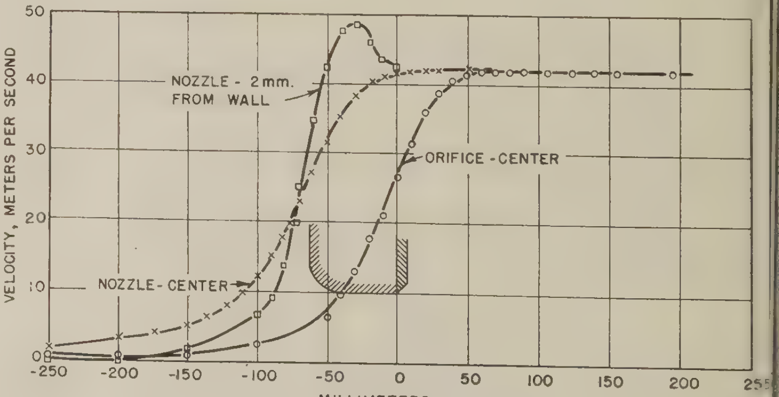

FIG. 10 CHANGE IN VELOCITY OF AIR PASSING THROUGH AN ORIFICE AND A NOZZLE

---

[8] Consulting Engineer, Foster Wheeler Corporation, New York, N. Y. Mem. A.S.M.E.

[9] "Die Strömung in Reaktionsstrahl," by Wilhelm Nusselt, *Zeitschrift für Flugtechnik und Motorluftschiffahrt*, vol. 6, 1915, pp. 179–184.

Consequently

$$P = m\frac{du}{dt} = mC'(v - u)$$

Differentiating Equation [17]

$$dv = 0 + c\,dx$$

or

$$\frac{dv}{dx} = C$$

By a conventional transformation

$$u\frac{du}{dx} = u\frac{du}{dv}\frac{dv}{dx} = u\frac{du}{dv}C \ldots\ldots\ldots\ldots [18]$$

Now since

$$u = \frac{dx}{dt} \ldots\ldots\ldots\ldots\ldots\ldots [19]$$

and

$$\frac{du}{dx} = \frac{du}{dv}\frac{dv}{dx}$$

we can write

$$u\frac{du}{dx} = \frac{dx}{dt}\frac{du}{dv}\frac{dv}{dx}$$

and, by Equation [19]

$$\frac{dx}{dt}\frac{du}{dx} = u\frac{du}{dv}\frac{dv}{dx}$$

from which, using Equation [18]

$$\frac{du}{dt} = u\frac{du}{dv}C$$

from Equation [17]

$$uC\frac{du}{dv} = C'(v - u)$$

and

$$\frac{du}{dv} = \frac{C'}{C}\left(\frac{v - u}{u}\right) = b\left(\frac{v}{u} - 1\right)$$

when

$$b = \frac{C'}{C}$$

Now, let

$$Z = \frac{u}{v}$$

or

$$vZ = u$$

Differentiating

$$vdZ + Zdv = du$$

or

$$\frac{du}{dv} = v\frac{dZ}{dv} + Z$$

Equating this with the previous result

$$v\frac{dZ}{dv} + Z = b\left(\frac{1}{Z} - 1\right)$$

or

$$\frac{u}{dv} = \frac{b(1 - Z) - Z^2}{Z\,dZ}$$

or

$$\frac{-du}{v} = \frac{Z\,dZ}{Z^2 + bZ - b}$$

Integrating by means of tables of integration

$$-\log u + K = \tfrac{1}{2}\log(Z^2 + bZ - b) - \frac{b}{2}\frac{1}{\sqrt{b^2 + 4b}}\log\frac{Z + \frac{b}{2} - \sqrt{\frac{b^2}{4} + b}}{Z + \frac{b}{2} + \sqrt{\frac{b^2}{4} + b}}$$

Let

$$p = \sqrt{b + \frac{b^2}{4}} - \frac{b}{2}$$

and let

$$q = -\sqrt{b + \frac{b^2}{4}} - \frac{b}{2}$$

Thus

$$\log u + K = \frac{b}{2(p - q)}\log\frac{Z - p}{Z - q} - \frac{1}{2}\log(Z^2 + bZ - b)$$

However, since $Z > 0$ and $b > 0$

$$Z^2 + bZ - b = |Z - p||Z - q|$$

Therefore

$$\log v + K = \frac{b}{2}\left(\frac{1}{p - q}\right)\log\frac{Z - p}{Z - q} - \frac{1}{2}\log|Z - p|\,|Z - q|$$

For initial conditions, $v_0 = u_0$, thus

$$Z_0 = u_0/v_0 = 1$$

Solving for constant of integration

$$\log v_0 + K = \frac{b}{2}\left(\frac{1}{p - q}\right)\log\left(\frac{1 - p}{1 - q}\right) - \frac{1}{2}\log|1 - p|\,|1 - q| \ldots\ldots\ldots [20]$$

$|1 - p||1 - q| = 1$, when values for p and q in terms of h are inserted in Equation [20]. Therefore the constant of integration

$$K = -\frac{1}{2}\log 1 = 0$$

The difference between the velocity at any point and the initial velocity is then

$$\log v - \log v_0 = \frac{b}{2}\left(\frac{1}{p - q}\right)\log\left(\frac{Z - p}{Z - q}\right) - \tfrac{1}{2}\log|Z - p||Z - q| - \frac{b}{2}\left(\frac{1}{p - q}\right)\log\left(\frac{1 - p}{1 - q}\right)$$

or

$$\log\frac{v}{v_0} = \frac{b}{2}\left(\frac{1}{p - q}\right)\log\left|\left(\frac{Z - p}{Z - q}\right)\right|\left|\left(\frac{1 - q}{1 - p}\right)\right| - \frac{1}{2}\log|Z - p|\,|Z - q| \ldots\ldots\ldots [21]$$

Values were given to $Z = u/v$ between 0.632 and 1.00 in Equation [21], for various values of p and q, corresponding to values of b from 1 to 6, and the resulting values of log v/v_0 were plotted against u/v, with b as a parameter, as shown in Fig. 11 of this discussion.

The curves shown in Fig. 11 indicate that the difference in velocity between a particle and its conveying medium depends upon the viscosity of the conveying medium, the density of the particle, and the size of the particle, which are contained in the parameter b.

Using these relations, an attempt has been made to assign values to C and C' to represent a practical case. Assuming a nozzle diameter 0.7 of the pipe diameter, the velocity at the throat will be $v_0/(0.7)^2$. Assuming also that the nozzle is constructed in such a way that the formula $v = v_0 + c\ x$ holds for any point x in the nozzle, and letting

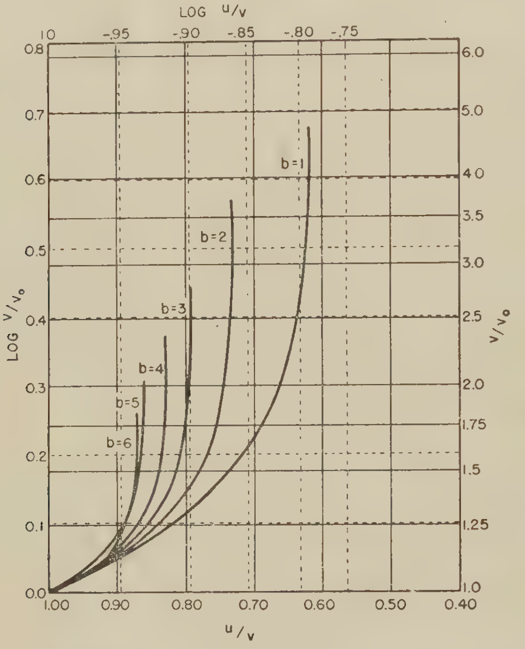

Fig. 11 Comparison of Air-Stream and Particle Velocities for Values of Parameter b

$$v_0 = 3600 \text{ fpm} = 60 \text{ fps}$$

and

$$L = 2 \text{ ft}$$

then

$$v_L = \frac{3600}{(0.7)^2} = 7340 \text{ fpm} = 122.5 \text{ fps}$$

Solving for C at $x = L = 2$, in $v_L = v_0 + C\ x$ gives $C = 31.25$.

Solving for

$$C' = 9/2\left(\frac{z}{\rho'\ a^2}\right)$$

under the conditions where

z = 12.7×10^{-6} lb sec per ft^2 for air at 70 F
ρ' = 85 lb per cu ft
a = 20 microns = 6.55×10^{-5} ft.

then

$$C' = 156.8 \text{ and } b = 5.05$$

Taking this value for b and calculating the velocity of the air at 3-in. intervals through the nozzle, and then referring to the $b = 5.05$ curve in Fig. 11, the corresponding particle velocities were obtained as in Table 1.

TABLE 1 CALCULATION OF PARTICLE VELOCITIES

x, ft	$v = v_0 + C\ x$	v/v_0	u/v, from curve, Fig. 11	u, fps
0.25	60 + 7.75 = 67.75	1.31	0.93	63
0.50	60 + 15.5 = 75.5	1.26	0.89	67
0.75	60 + 23.25 = 83.25	1.39	0.88	73
1.00	60 + 31 = 91.0	1.52	0.87	79
1.25	60 + 38.75 = 98.75	1.65	0.87	86
1.50	60 + 46.5 = 106	1.77	0.86	91
1.75	60 + 54.25 = 114.25	1.91	0.86	98
2.00	60 + 62 = 122.0	2.03	0.86	105

Fig. 12 is a plot of the tabulated results, giving the relation of the velocity of the particle and of the velocity of the conveying air with distance. The two velocity curves show that the velocity of the particle is somewhat less than that of the air at all points within the nozzle. The assumptions made do not permit extrapolation beyond the throat of the nozzle.

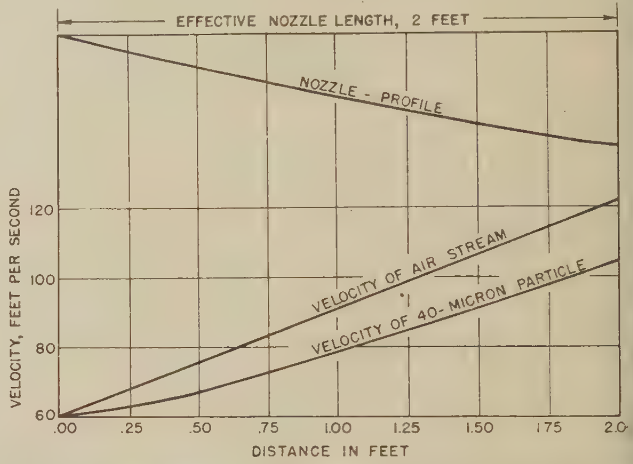

Fig. 12 Comparison of Air-Stream and Particle Velociti Through a Nozzle

This discussion supports previous findings of the difference i velocity between the heavier coal particles and the conveying ai as the mixture passes through a constriction. It does not a tempt to prove the principle of the meter, namely, that the o fice measures only the air, whereas the nozzle measures bo the air and solid. However, the fact that there is a difference o the basis of Nusselt's work in the velocity pattern through a orifice as compared to a nozzle may be a contributing factor t the successful operation of the meter.

J. M. Cunningham.[10] The meter combination presented i this paper is of considerable interest, and the application of th rubber-faced orifice is unique. While the method of employin two meter elements connected in a flow circuit for the purpose o amplifying the indication at one of the elements has been used both in flow measurement and position indication, on those devices the variation of the indication at one meter element resulted in an amplification of the indication at the other mete element. In the subject meter combination, the indication c an air-coal flowing mixture is obtained by comparison of th pressure drop, across a long-radius nozzle with the pressure dro across a sharp-edged plate orifice, using radius taps at both mete elements.

The theory of operation advanced by the authors stresses difference of acceleration of the coal particles through the two meter elements, and a corollary is given that the distance required for a particle of a given material to accelerate to a given velocity is independent of the fluid velocity. This is equivalent to stating that the particle motion is independent of the fluid velocity.

---

[10] Gulf Research & Development Company, Pittsburgh, Pa.

Considering the theory of effects of difference in acceleration of the coal particles, the mass velocity of air and coal across any section along the flow path must be constant from the condition of continuity. In design, the velocity through the nozzle is less than the velocity through the orifice, and both velocities are greater than the pipe velocity; thus the acceleration of a coal particle from pipe to nozzle velocity will be less than the acceleration of a coal particle which must exist from pipe to orifice velocity. In other words, the greatest acceleration of the coal particle must occur at the orifice entrance unless the coal particles can redistribute themselves in the flow pattern and travel at some uniform velocity independent of the air velocity, which is highly improbable. Following the nozzle outlet there will be a zone of deceleration of coal particles back from nozzle to pipe velocity. Then, if it is assumed that the coal particles do not have sufficient time to accelerate in the orifice entrance in proportion to the mass velocity of the coal which must flow through the orifice from the condition of continuity, it appears that any difference in acceleration of the coal particle would produce at least a concentration and possibly an accumulation of coal particles at the orifice entrance. It is doubtful that this latter effect occurs.

From consideration of acceleration effects it would appear that the orifice readings would give the indication of the coal content which effect is contrary to test results. Another theory for the difference in coal indication between the nozzle and orifice elements of the meter combination may be the friction and viscosity effects of the mixture flow. While friction and viscosity effects are considered indirectly in the flow coefficients of the meter elements, the friction effects will be more pronounced in a nozzle where the fluid completely fills the boundaries, whereas the fluid in flow through an orifice makes contact only at the entrance.

The coal fineness should have some influence on the friction effects and be more pronounced in the flow in the nozzle for a constant coal/air ratio. With increasing fineness, the effect in supposition will be similar to increasing the fluid viscosity, and further, this effect would be greater as the coal/air ratio is increased. The curves in Figs. 4 and 5 of the paper are in agreement with these conclusions.

Considering a suspended coal particle as a free body, the laws of its motion are given by D'Alembert's principle. One of the forces acting upon the particle is the frontal drag which is related to the particle shape, the fluid density, and fluid velocity, which, in turn, would indicate that the motion of the particle is not independent of the fluid velocity. While the corollary of constant accelerating distance has been given previously in the literature, the effects may have been the result of distortion in the flow pattern.

The fundamental equation given in the paper for gravimetric flow through a nozzle or orifice applies to uncompressible fluids. For gases this hydraulic equation is modified to correct for compressibility effects through multiplication of the flow coefficient by an expansion factor Y in the case of an orifice, or by the phi coefficient ϕ in the case of a nozzle; also there is a correction for deviation from the gas law through multiplication of the gas density by the supercompressibility factor y. However, in particular instances where the differential pressure across the meter elements is a small per cent of the inlet pressure, the expansion factor Y, and phi coefficient ϕ, are very nearly unity. Also, where the operating pressure is less than 50 psi, the supercompressibility factor y, for air is approximately unity. The definitions and values of these factors are given in reference (10) of the paper, and elsewhere.[11]

In the development of the coal-flow equation, the assumed density of the coal-air mixture is greater than the actual density in the ratio of $\left(1 + \frac{\rho_a W_c}{\rho_c W_a}\right)$, where the symbols follow the nomenclature of the paper.

From this density ratio and with coal/air weight ratios of 1 or less, the resulting error through use of the assumed density is very small and the conclusions of the authors in this respect are justified.

All together the simplifying assumptions in the paper do not lead to any appreciable error for the range of flow rates indicated. For example, recalculating the first portion of the example in the paper, having meter elements of 9.1-in-diam orifice and 10.5-in-diam nozzle, the over-all pressure differential, computed with corrections for compressibility effects and density of the coal-air mixture, was determined to be 11.04 in. water as compared with a pressure differential of 10.47 in. water in the paper. In these calculations a value for the coal density was taken as $87^1/_2$ lb per cu ft.

It is noted that there is no distinction in the calibration of the apparatus given for use in horizontal and vertical installations. One would expect these calibrations to differ somewhat due to the distortion of the flow pattern in horizontal runs.

Another minor point in question is the dimension used for a coal particle through 200-mesh screen. In the paper, a coal-particle size is given as 3.1×10^{-5} ft radius, which is approximately 19 microns diam. Other investigators have indicated in the literature a particle size of the order of 74 microns diam for particles through 200-mesh screen. Again, a rough check of the particle size as scaled from Fig. 1 of the paper, indicates a minimum diameter on the larger particles of the order of 0.6 in., which, when reduced by the magnification factor of 6000, gives a diameter of 0.0001 in., or approximately $2^1/_2$ microns. This value does not correlate when compared with a size of coal particle given in the literature which is of the order of 43 microns diameter for 300 mesh.

It would be of interest to know whether the authors in the course of their experimentation have obtained any data with the positions of the nozzle and orifice interchanged in the flow circuit. It is believed that the orifice will produce greater mixing of the coal-air flow components than obtained by the nozzle, with the result of a more uniform flow pattern.

In conclusion, the authors are to be commended on the presentation of their findings and for the use of conventional flow formulas. This meter combination should find application in the pneumatic conveyance of coal, cement, and grain.

W. E. Young,[12] J. T. Perry,[12] and A. E. Hershey.[13] The information presented in this paper regarding a method for measuring the instantaneous rate of flow of a suspension of finely pulverized solid material in a gas is particularly timely, in view of the widespread interest in processes requiring the "fluidization" of solid reactants. Anyone who has struggled with the problem of sampling such suspensions, in order to determine flow rates, must be deeply in debt to the authors for the extent and detail of the information which they have made available.

In an investigation of feeding and burning pulverized coal, we

---

[11] "Fluid Meters," fourth edition, ASME, 1937.

[12] Research Laboratories, Westinghouse Electric Corporation, East Pittsburgh, Pa.

[13] Research Engineer, Research Laboratories, Westinghouse Electric Corporation. Mem. ASME.

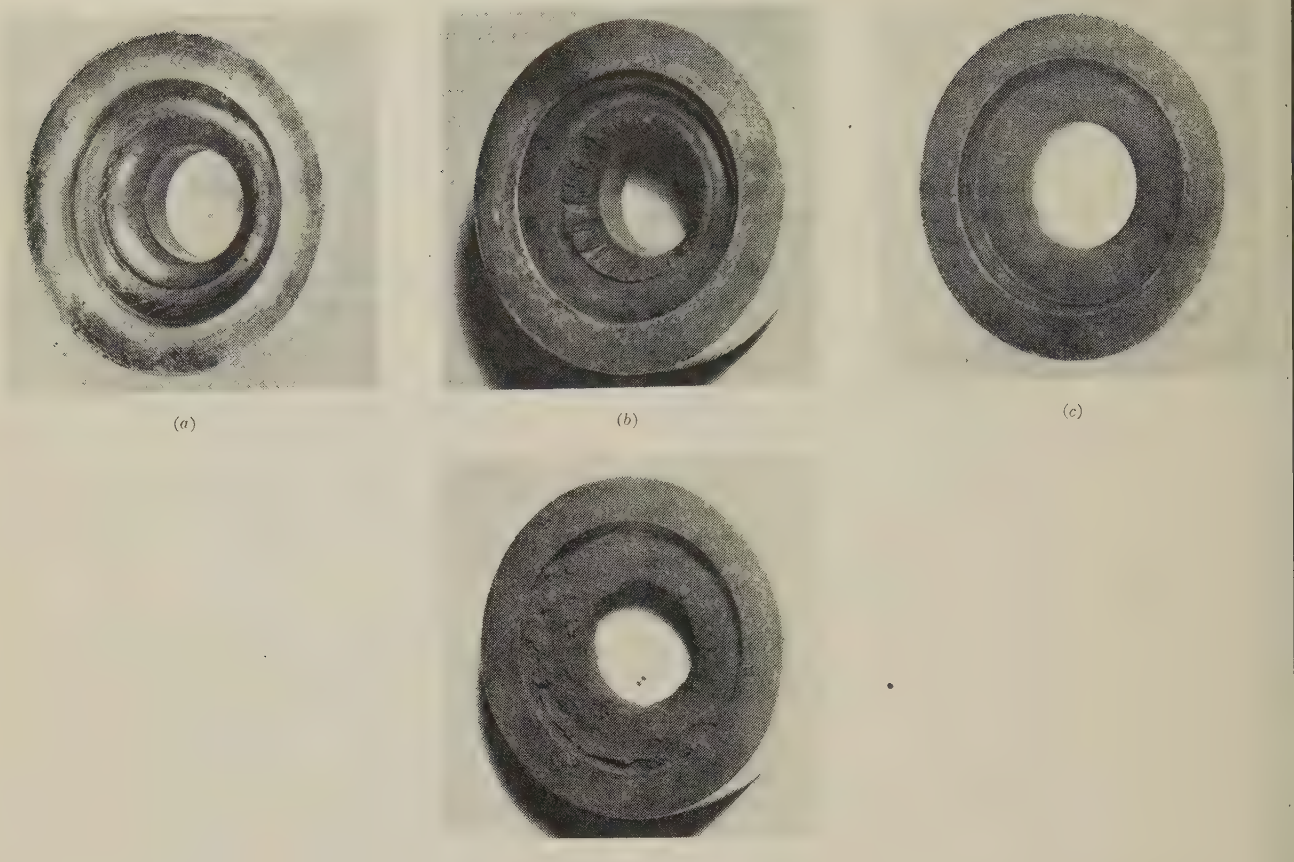
(a) (b) (c) (d)

Fig. 13 Views Showing Accumulation of Coal on Rubber Facing of Orifice and on Rounded Approach of Nozzle

have been using a flowmeter of this type for several months, and as a result of this experience, as well as reading the paper, some questions have arisen which may be of general interest.

The first explanation of the operating principle of the flowmeter which the authors have advanced, appears to be somewhat questionable. Photographs of the path lines approaching an orifice and a nozzle such as those given by Rouse[14] and others, indicate relatively little difference in these lines for the two types of constriction. Hence the second explanation, that the rounded approach of the nozzle provides "solid surfaces to guide the flow," would seem to be preferable. This comment would be rather trivial were it not for the conclusion that a nozzle with reversed curvature, such as those proposed by Moss,[15] may offer some advantages over the long-radius design indicated in Fig. 2 of the paper.

In metering suspensions of pulverized coal with a fineness of 95 to 99 per cent through 325 mesh, some difficulty with coal accumulations has been experienced. Both the orifice and nozzle have a diameter of 0.55 in. and they were installed in a $^3/_4$-in. line. Fig. 13 of this discussion shows the accumulation of coal on both the rubber facing of the orifice and the rounded approach of the nozzle after operating a total of about 3 hr. The coal on the orifice was soft and the face was easily cleaned. The coal on the nozzle approach was very hard and deeply striated. The coal fed to this line tested about 1 per cent moisture and 33 per cent volatile matter. The air was carefully dried and oil from the compressor was trapped out. The sharp edge on the rubber-faced orifice was eroded by the coal-air mixture and tended to round off.

Pressure pulsations in the combustor have made it extremely difficult to obtain manometer readings which are reliable, so that no test data can be presented. This of course implies no criticism of the flowmeter.

The test results represented by the curves in Fig. 3 of the paper raise another question. According to the differential acceleration principle, if the meter is calibrated for material with a given size distribution and then used to measure flow rates of a material which is more finely pulverized, the indicated flow should be less than the actual, because, as the particle size decreases the pressure drop at the orifice should approach that at the nozzle. The curves in Fig. 3 indicate the contrary, since the indicated flow with 92 per cent through 200 mesh is greater than that for 85 per cent through this screen. Do the authors have any information indicating that this trend is maintained with material in the subsieve size range?

Authors' Closure

In reply to the discussion by J. M. Cunningham, Mr. Cunningham correctly deduces that the theory advanced in the paper of differential acceleration of coal and air requires that there be an increased concentration of coal at the orifice. Although this may be improbable it is not impossible as, for example, in a centrifugal separator or pipe bend the dust concentration increases near the outer wall. As to Mr. Cunningham's alternate theory, involving friction and viscosity effects, originally the meter was thought to require a very long-throated nozzle as stated in the paper, and a meter was constructed with straight throat lengths of 5 and 10 diameters. Except for differences in the clean-air coefficient, no difference in meter performance was noted. The authors believe that if friction were an important factor these two lengths would have shown a difference in meter performance.

---

[14] "Fluid Mechanics for Hydraulic Engineers," by H. Rouse, McGraw-Hill Book Company, New York, N. Y., 1938, p. 262.

[15] "Measurement of Flow of Air and Gas With Nozzles," by S. A. Moss, Trans. ASME, vol. 50, 1928, paper no. APM-50-3.

Although in the paper emphasis is given the differential acceleration theory because of the known lag of particles suspended in an accelerating stream, mention is also made of an alternate theory less founded on calculation or experimental results, but perhaps nearer the fact that a shift occurs in the position of the vena contracta of an orifice because of the presence of particles. As to the further discussion by Mr. Cunningham of the dependence of frontal drag on fluid velocity, it should be pointed out that the major effect here is relative velocity of the particle and not simply fluid velocity.

The authors appreciate Mr. Cunningham's verification of the validity of the assumptions made in the application of conventional flowmeter formulas to the coal-air meter.

In regard to the expected difference in calibration for horizontal and vertical meters owing to settling of coal in a horizontal line, this has not been found to be an appreciable effect. Perhaps at lower velocities this would become important.

The size of particle given in calculations in the paper which Mr. Cunningham has derived to be 19 microns was a result of an average size determination made by the Lea-Nurse permeability method on an actual sample of coal pulverized to 90 per cent through 200-mesh screen. Although the maximum size of the opening in the 200-mesh screen is approximately 74 microns, the size used in the calculations was taken as an average particle diameter of about 19 microns. An explanation for this seeming excessively small average size may be that additional pulverization took place in the continued recirculation of coal in test work.

In checking the distances required for acceleration of a 74-micron particle, it was found that 0.484 foot for laminar flow and 5.27 ft for turbulent flow were required as compared to 0.364 in. and 1.34 ft, respectively, for the 19-micron particle. The distance for turbulent flow changes considerably with size, but even for the small particles the acceleration distance is still appreciable.

The average size of particle quoted from the literature of 43 microns applies to a large proportion of the coal in practical use. The size of particle shown in Fig. 1 of the paper is of a sample pulverized much finer than in ordinary practice, and hence the maximum size shown is about 4 microns. This figure illustrates shape rather than size.

With regard to nozzle and orifice sequence the authors have tried both arrangements but, because of the smaller disturbance of flow after the nozzle, it is usually placed before the orifice to make the meter as short as possible. It is probably true that an orifice gives better mixing.

In reply to the discussion by Messrs. Young, Perry, and Hershey, the reference in the paper to the guiding surfaces was intended to apply only to the straight section of the nozzle. It may well be that employing a reverse-curvature nozzle as suggested would be effective and eliminate accumulation at the entrance to the nozzle.

The meter installed in the $1^1/_2$-in. line at Battelle has operated approximately 100 hours using coal of 95 per cent through 200 mesh for 50 hours and coal of 97 per cent through 325 mesh in recent tests. This meter was disassembled and examined; some hard striated accumulation of coal was found at the mouth of the nozzle and very little accumulation on the upstream face of the orifice. If the coal continues to build up at the entrance to the nozzle, it may be necessary to coat this portion of the nozzle with rubber to prevent this accumulation. Abrasion of the orifice edge was not perceptible, but in this case the rubber bond between the metal and rubber face had separated. The reason for this is not apparent.

Recent work on a coal-air branch flow circulating system, in which small meters were installed in $1^1/_2$-in. branch lines, indicates that small meters are subject to greater errors than those installed in the 2 and 4-in. lines. Although the reasons for this difference in accuracy have not been fully established, there are indications that the greater friction effect in smaller pipe sizes and the lower Reynolds numbers for a given flow velocity in smaller pipes are factors which contribute to this difference in accuracy.

Attention was called to an apparent contradiction in Fig. 3 of the preprint which showed that flow indication using coal with a fineness of 92 per cent through 200-mesh screen was greater than for 85 per cent through this screen. This was the result of an error in the placing of symbols on the legend of Fig. 3 and has since been corrected. It is true that flow indication with the finer consists is less than with coarser consists of coal. The authors are not able to say whether this trend continues to any marked degree in the subseive sizes because no actual test work has been done on coal of this fineness, but the meter has apparently operated satisfactorily in an installation where coal 95 per cent through 325 mesh was used.

Test Data on Gas-Side Sulphate-Type Deposits on Tubes Beyond Boiler Furnace[1]

By J. F. Barkley,[2] L. R. Burdick,[3] and A. A. Berk[4]

Owing to accumulations of troublesome deposits on the gas side of tubes in one of the boilers at the Naval Gun Factory in Washington, a thorough study of the formation of the deposits was undertaken. From this work an improved method of analyzing products of combustion for SO_2 and SO_3 content was developed, details and procedure for which are given in the paper.

A TYPE of boiler and fuel-burning equipment (boiler No. 1), installed at the Naval Gun Factory, Washington, D. C., is shown in Fig. 1. The location where unusual, dense, troublesome deposits accumulated on the gas side of the tubes is indicated. The deposits resembled somewhat those often found in economizers, but these occurred in the boiler even at the end of the first pass of the gases through the tubes. Fig. 2 shows a typical specimen of the deposits, a dark-gray, very hard and tenacious, consolidated, somewhat stratified accumulation that was little affected by the soot blowers. It was quite different from the ordinary accumulation of slag or ash. It was very difficult to remove, caused much draft loss, and was corroding the tubes. A typical analysis of the deposit, which consisted largely of sulphates, is given in Table 1.

TABLE 1 TYPICAL ANALYSIS OF BOILER-TUBE DEPOSIT

	Per cent
Moisture at 105 C	2.0
Combined water	2.4
Silica, SiO_2	20.9
Aluminum oxide, Al_2O_3	8.8
Total iron, calculated as Fe_2O_3	9.3
Calcium oxide, CaO	1.0
Magnesium oxide, MgO	0.3
Sulphur trioxide SO_3	38.3
Alkalies, calculated as Na_2O	13.2
Water-soluble material, approximately	40.0

Filtered solution obtained by extracting 1/2 g of deposit with 50 ml water at room temperature for 1/2 hr showed a pH of 2.6.

A very low-sulphur coal was burned which analyzed as given in Table 2, while Table 3 shows the ash analysis.

TABLE 2 ANALYSIS OF LOW-SULPHUR COAL

		Per cent
Moisture, as-received		1.8
Volatile matter, dry basis		21.0
Fixed carbon, dry basis		71.8
Ash, dry basis		7.2
Sulphur		
Sulphate	0.004	
Pyritic	0.133	
Organic	0.463	
Total, dry basis		0.6
Btu, dry basis		14520
Ash fusion (approx.)		2660 F

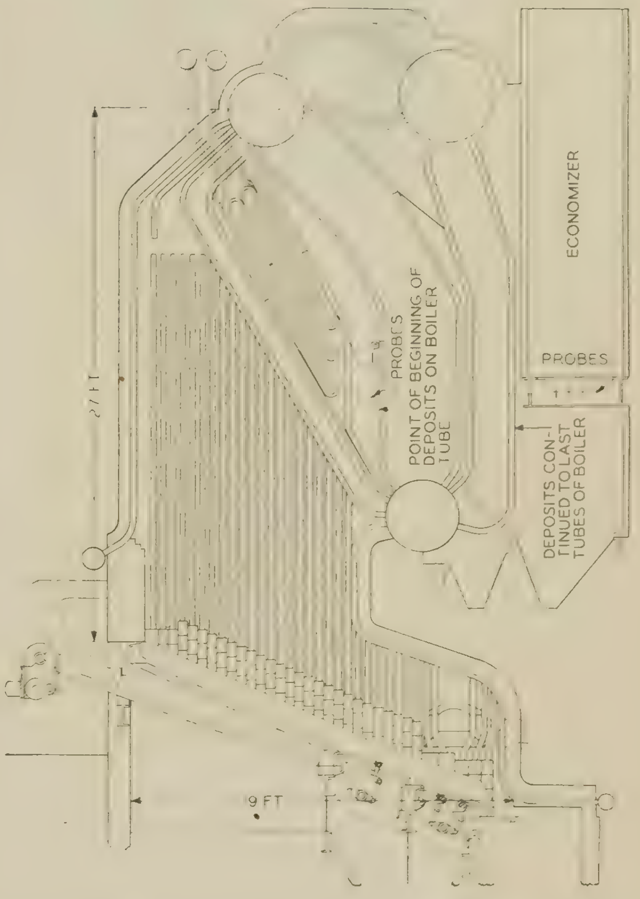
ECONOMIZER
PROBES
POINT OF BEGINNING OF DEPOSITS ON BOILER TUBE
PROBES
DEPOSITS CON-TINUED TO LAST TUBES OF BOILER
27 FT
9 FT

Fig. 1 Boiler No. 1 Showing Location Where Unusual, Hard, Consolidated Sulphate-Type Deposits Accumulated on Gas Side of Tubes

(Boiler heating surface 10,000 sq ft; waterwall surface 2013 sq ft; superheater surface 1520 sq ft; operated with superheater by-pass opened wide.)

TABLE 3 ASH ANALYSIS

	Per cent
Loss on ignition at 800 C	0.4
Silica, SiO_2	50.3
Aluminum oxide, Al_2O_3	31.4
Ferric oxide, Fe_2O_3	9.9
Calcium oxide, CaO	1.4
Magnesium oxide, MgO	1.3
Sulphur trioxide, SO_3	1.3
Alkalies, by difference, $Na_2O + K_2O$	4.0

The boiler was operated at 195 psi pressure, or a saturated-steam temperature of 386 F, with a superheated-steam temperature of 570 F. Although designed for a load of about 140,000 lb of steam per hr, the average 24-hr load was about 68,000 lb of steam per hr. The average amount of coal burned per square foot of projected grate surface was about 22 lb; a CO_2 of not less than 14 per cent was carried.

Fig. 3 shows another type of boiler (boiler No. 3) at the same plant, using the same coal and operating at the same steam pressure, with a superheated-steam temperature of 480 F, which gave

---

[1] Published by permission of the Director, Bureau of Mines, U. S. Department of the Interior, Washington, D. C.

[2] Chief, Fuels Utilization Division, Bureau of Mines, Washington, D. C. Mem. ASME.

[3] Supervising Engineer, Bureau of Mines, Washington, D. C. Mem. ASME.

[4] Supervising Chemist, Bureau of Mines, Washington, D. C.

Contributed by the Fuels and Power Division and presented at the Semi-Annual Meeting, Chicago, Ill., June 16–19, 1947, of The American Society of Mechanical Engineers.

Note: Statements and opinions advanced in papers are to be understood as individual expressions of their authors and not those of the Society.

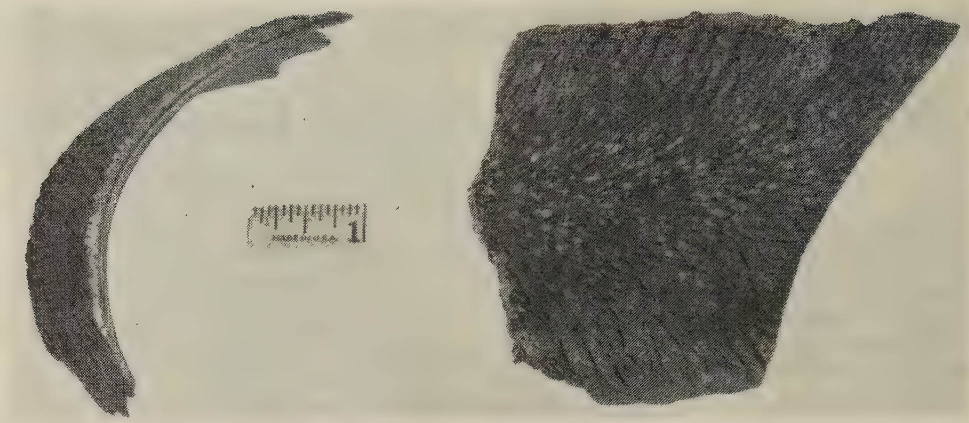

Fig. 2 Hard, Consolidated, Sulphate-Type Deposit That Accumulated on Gas Side of Boiler Tubes

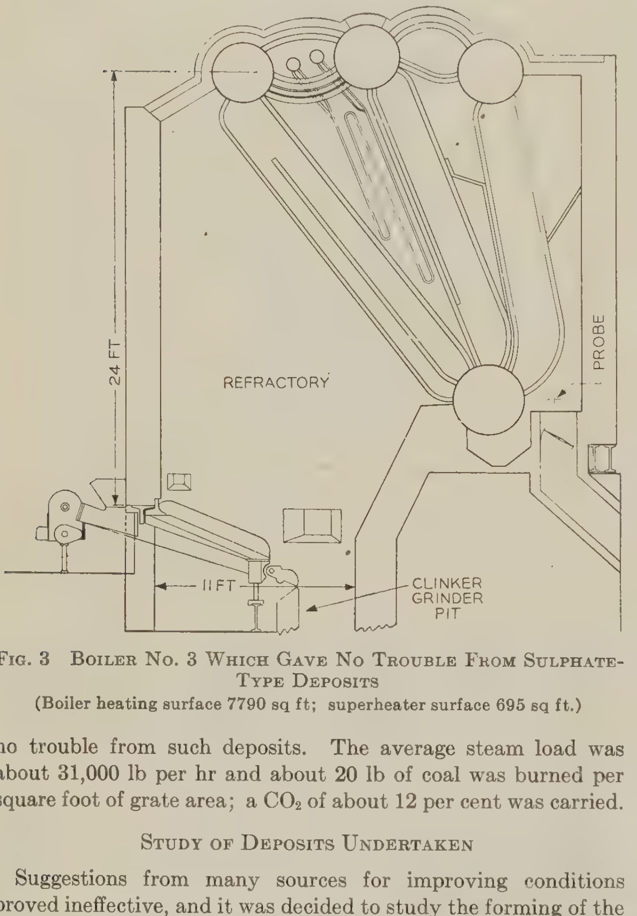

Fig. 3 Boiler No. 3 Which Gave No Trouble From Sulphate-Type Deposits
(Boiler heating surface 7790 sq ft; superheater surface 695 sq ft.)

no trouble from such deposits. The average steam load was about 31,000 lb per hr and about 20 lb of coal was burned per square foot of grate area; a CO_2 of about 12 per cent was carried.

Study of Deposits Undertaken

Suggestions from many sources for improving conditions proved ineffective, and it was decided to study the forming of the deposits by means of 6-ft 4-in. tubular probes made of $1^1/_2$-in gas pipe, devised as shown in Fig. 4. Piping was arranged so that either saturated steam or water at various temperature could be used to hold the probes at any chosen temperature Figs. 1 and 3 show where the probes were inserted in the boiler settings.

Table 4 gives results obtained with the probes. In summary it shows that, for boiler No. 1, the formation of deposits at the end of the first pass essentially ceased and appreciably decrease at the entrance to the economizer when a CO_2 of 9 per cent wa carried. As the CO_2 increased, the deposits at both points in creased. For the same conditions, the cooler the probe the mor the deposit. The probes also showed that for boiler No. 3 th same type deposit that did not accumulate on the boiler tub would accumulate at the boiler outlet on a probe cooled well be low boiler-tube temperature.

The deposit on the cooled steel probe characteristically ha against the probe a white layer which was largely ferrou sulphate. The remainder of the deposit consisted chiefly of sul phates and silica, such as would be formed from entrained fl ash acted upon by sulphuric acid. The iron of the inne layer appeared to come largely from the probe as it continuall lost metal as from corrosion. The action is shown typically by comparison of deposit analyses A and C for test 1. Samples and C were obtained by scraping off as carefully as possible top layer of the deposit for C, and then, after continued scraping taking a sample of the layer that first formed against the pip Sample C shows an increase of silica and alumina and a decrea of iron and sulphur trioxide. The C analysis, in this respect heads in the general direction of a typical analysis of the fly as or dust which had high ratios of silica and alumina to iron an very low sulphur trioxide as shown in Table 5.

Both samples E taken from the side of the probe toward th gases for tests 3 and 5 at the end of the first pass showed a sligh

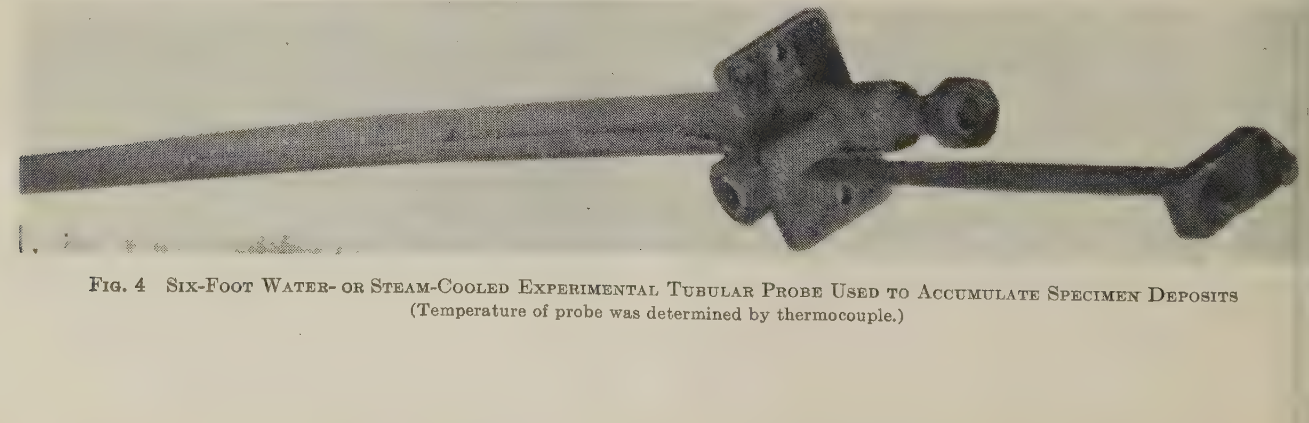

Fig. 4 Six-Foot Water- or Steam-Cooled Experimental Tubular Probe Used to Accumulate Specimen Deposits
(Temperature of probe was determined by thermocouple.)

TABLE 4 RESULTS OBTAINED FROM THE USE OF PROBES IN BOILERS 1 AND 3

Test No.		1				2		3		4	5		6	7
Boiler No.		1				1		1		1	1		1	3
Duration	hrs.	107				164		313		313	312		312	106
CO_2 at boiler outlet	%	12				15		9		11	13		15	12
Boiler water temperature	°F.							386 average						386
Steam temperature leaving superheater	°F.							570 average						480
End of 1st boiler pass:														
Gas temperature - approximate	°F.							1250 average						
Steel probes		Cooled			Not cooled	Cooled	Not cooled	Cooled		Cooled	Cooled		Cooled	
Temperature of outside face of tube	°F.	157			877	162	826	438		429	416		416	
Analysis of deposit:		A		C		D	D	E	F	D	E	F		
1. Moisture at 105°C	%	2.3		6.3		2.6	1.9	8.3	5.4	5.7	2.4	2.4		
2. Combined water	%	9.9		7.1		6.2				4.8	2.8	2.3		
3. Silica, SiO_2	%	1.7		7.3		15.1	51.8	13.6	17.2	15.5	17.1	18.7		
4. Aluminum oxide, Al_2O_3	%	2.6		6.0		7.7	21.0	11.9	13.8	10.7	11.6	11.7		
5. Total iron, calculated as Fe_2O_3	%	40.4		25.9	powdery	18.6	14.0	10.0	11.5	8.7	9.7	10.9		
6. Calcium oxide, CaO	%	0.1		0.5		0.6	2.6	1.6	1.9	1.1	1.5	1.3		
7. Magnesium oxide, MgO	%	0.0		0.2		0.4	1.1	0.3	0.5	0.3	0.4	0.4		
8. Sulfur trioxide, SO_3	%	45.2		40.1		31.1	13.5	36.3	27.8	34.4	35.0	31.5		
9. Water soluble material*	%	-		-		-	-	44.4	41.6	59.5	47.6	41.6		
10. pH of filtered solution from water solubility test	pH	3.1		2.8		2.8	3.0	2.9	2.9	2.7	2.8	2.8		
Relative quantity of deposit on probe		8			trace	10	powdery very small	very small		3	5		10	
Entrance to economizer:														Boiler outlet
Flue gas temperature	°F.	571				543		978		575	552		552	500
Steel probes cooled					(Non-metallic probe not cooled)						(Non-metallic probe cooled)			
Temperature of outside face of tube	°F.	154				154		241		235	165	245	257	150
Analysis of deposit:		A	B	C		A	C	E		D	D			D
1. Moisture at 105°C	%	17.8	9.8	7.3		2.8	2.8	13.8		7.3	5.8			1.3
2. Combined water	%		7.5	6.7		7.1	6.1			5.4	6.1			4.4
3. Silica, SiO_2	%	1.5	13.1	14.3		21.4	23.4	5.7		11.1	14.9			29.3
4. Aluminum oxide, Al_2O_3	%	1.8	6.6	11.9		14.2	14.4	6.1		8.4	8.9			20.4
5. Total iron, calculated as Fe_2O_3	%	38.0	14.1	11.8	water soluble,	13.7	11.6	21.3		16.5	9.9			17.4
6. Calcium oxide, CaO	%	0.0	1.1	1.2	grey, powdery	1.6	1.4	0.9		0.7	0.3			2.3
7. Magnesium oxide, MgO	%	0.0	0.2	0.3		0.6	0.6	0.2		0.2	3.3			0.8
8. Sulfur trioxide, SO_3	%	43.3	33.3	34.3		25.6	20.8	44.7		37.7	34.5			13.9
9. Water soluble material*	%	-	-	-		-	-	68.1		66.7	65.2			-
10. pH of filtered solution from water solubility test	pH	2.3	2.5	2.6		2.8	2.8	2.6		2.6	2.6			2.8
Relative quantity of deposit on probe			X		trace	XII		III		V	small	VIII	X	

* ½ gram extracted with 50 ml water at room temperature for 1/2 hour.

A Deposit next to probe
B Middle part of deposit
C Outside part of deposit
D All of deposit
E Deposit on gas side of probe
F Deposit on side of probe away from gas

TABLE 5 TYPICAL ANALYSIS OF FLY ASH OR DUST

	Per cent
Moisture at 105 C	0.1
Loss on ignition (less moisture)	48.5
Silica, SiO_2	22.6
Aluminum oxide, Al_2O_3	16.6
Total iron, calculated as Fe_2O_3	8.6
Calcium oxide, CaO	1.1
Magnesium oxide, MgO	0.7
Sulphur trioxide, SO_3	1.2

tendency to have more sulphur trioxide than samples F taken from the side of the probe away from the gases.

Much smaller deposits collected on uncooled probes. For example, for test 1 at 12 per cent CO_2 at the end of the first pass only a trace of deposit was present; not enough for analysis. It was powdery and probably differed little from fly ash. For test 2 at 15 per cent CO_2, enough deposit was formed to provide a sample; it was powdery and contained 13.5 per cent SO_3.

To determine if a steel tube was necessary to cause the deposit, the probe was wrapped tightly with a thickness of $^1/_{16}$ in. asbestos gasket material to form a nonmetallic probe. The analysis of the deposit for test 5 at the entrance of the economizer showed a typical acid high sulphur-trioxide deposit; it had, however, a relatively lower iron content and was less consolidated than deposits formed on a steel probe under similar conditions. The trace of deposit found on the uncooled nonmetallic probe of test 1 appeared to be the same type of deposit.

Very little importance can be attached to the moisture content of the deposits. When the probe was removed from the boiler, the deposit appeared quite dry. In a few minutes after being in the air, however, it became quite moist, showing the relatively new deposit to be quite hygroscopic which is typical of some sulphates, particularly of iron sulphate in the presence of small amounts of sulphuric acid. This characteristic prevented satisfactory weighing of the deposits. As shown in Table 4, quantities were judged visually and expressed on a relative basis. The deposit of the probe was removed easily and cleanly with water, leaving a shiny metal showing corrosion. The old deposit on the boiler tubes did not take up water so readily, nor was it readily dissolved. The rate of dissolution appeared to be affected greatly by the age of the deposit and its physical condition.

The physical nature of the deposit was affected greatly by its SO_3 content and also somewhat by the pounding action of the gases and fly ash. Hard consolidated deposits showed relatively high SO_3 content; powdery deposits showed relatively low SO_3 content. The test deposits on the probes toward the gases were harder than those on the back side, which were almost fluffy during the earlier stages of formation. The color was greatly affected by the quantity of soot entrained, ranging from white, against the iron, to gray, and on to virtually a black.

The 106-hr deposit of test 7 of boiler No. 3 showed appreciably higher SO_3 content than that of fly ash. It was not much consolidated, but its general appearance evidenced the beginning of the sulphate type of deposit.

In general, the probes indicated that under the proper conditions of saturation of the sulphurous gases and the moisture of the products of combustion, in which temperature is involved, the iron of the boiler tube and entrained fly ash are attacked, corroding the tube and altering the chemical and physical nature of the fly ash, causing the formation of a dense hard deposit. Since boiler No. 1 formed some deposit at 12 per cent CO_2 at the end of the first pass which boiler No. 3 did not, another factor was involved which apparently was a function of the equipment or its operation.

Wide Range of Operating Conditions Investigated

Experiments were made on changing the moisture contents of the products of combustion by operating with and without a continuous flow of cooling water in the ash pit of boiler No. 1. The boiler was also operated without the use of soot blowers for a period of 2 weeks. No measurable effects on the formation of the deposits were evidenced, the relative quantities of moisture involved being too small.

A study was next made of the SO_2 and SO_3 contents of the gaseous products of combustion. To analyze for SO_2 and SO_3, the method described in the ASME Power Test Code,[5] was carefully followed and found to be quite unsatisfactory and unreliable. An aspirator and orifice meter were used, drawing gas at the rate of 0.1 cu ft of 32 deg F, 29.92 in. Hg dry gas per minute for 30 min to give the 3 cu ft recommended for low-sulphur gases; the latter were absorbed in sodium hydroxide containing benzyl alcohol as directed. Trial tests were made with mixtures of SO_2 and air to check the apparatus and laboratory work. The volume of SO_2 calculated from these trials agreed satisfactorily with the volume fed, and no sulphate was found in the absorption solution, indicating satisfactory inhibiting action of the benzyl alcohol. However, when products of combustion were analyzed by the same methods, higher SO_3 values were obtained than anticipated and the total amount of sulphur in the gases was more than could have been present had all the sulphur in the coal gone into the gases.

When tests were made under operating conditions producing appreciable smoke, which occurred at times at 15 per cent CO_2, the small tuft of glass wool used for the filter permitted much of the fine carbon to get through and the absorbing solution became so dark that the titration end point was very difficult. The filter material was increased to 6 times the original amount which provided a colorless solution for titration, but resulted in much lower values of SO_3, particularly after soot had collected on the filter.

The values obtained for the SO_3 in the flue gases varied with the length of time the gas was drawn through the absorbing solution. By special tests of analyses of the rinse of the sampling tube and also of the bubbling tube, it was found that the SO_3 variation did not take place in either but did occur in the solution in the absorption bottle. When a sample of flue gas was drawn through the absorption bottle for a time period of 15 min, the SO_3 content shown for the gases by the solution was quite different from that shown for a time period of 45 min. The 15-min value was always much less—often less than one third, depending upon the nature of the flue gas.

The benzyl alcohol was not preventing the oxidation of sulphite to sulphate. Several changes in procedure were tried, such as dropping benzyl alcohol into the solution continuously during the test, the use of a straight instead of a right-angled bubbling tube, maintaining the absorbing solution temperature at 50 F, and cooling the gases before entering the bubbling tube; but none of these expedients was helpful.

Work in the laboratory with mixtures of SO_2 and CO_2 in air indicated that CO_2 did not interfere with the inhibiting action of the benzyl alcohol. All evidence pointed to the fact that some unknown element in the products of combustion was poisoning the inhibitor. Laboratory work with SO_2-CO_2-air mixtures showed that benzyl alcohol would not prevent the oxidation of an appreciable amount of the sulphite to sulphate in the absorption bottle when a very small quantity of copper ion was present. To a lesser extent, in the order named, other substances such as platinum, oxides of nitrogen, manganese, titanium, cobalt, nickel, and vanadium also produced this effect.

When the flue gases from the boiler were drawn through distilled water and the resulting solution evaporated, copper was found to be present in the residue. The copper was coming from the coal; special laboratory analyses of the coal ash showed it to contain 0.04 per cent copper. Therefore a search was made for an inhibitor that would be effective in the presence of copper and also any other substances which might be coming from the coal that would cause such trouble.

---

[5] "Instruments and Apparatus, Part 10, Flue and Exhaust Gas Analysis."

It is quite probable that some coals are free from metals or substances which might affect the inhibitor. However, since there are so many minerals of all types in relatively small quantities in coal, a scheme of analysis had to be used that would insure satisfactory results.

Method of Analysis Developed

The apparatus, reagents, and procedure finally adopted differed from the ASME Code in the following particulars:

The Sampling Tube. This consisted of a 19-mm-OD Pyrex glass tube, closed at the end, having four $^1/_{16}$-in. inlet holes on 4-in. centers along one wall of the tube. No filtering material used in tube; two 5-mm-OD Pyrex tubes for connection between the sampling tube and bubbling tubes.

The Bubbling Tubes. Two bubbling tubes were used, each having extra-coarse sintered-glass immersion filter to prevent high pressure drop across the two absorption bottles.

The Orifice Meters. An orifice meter was used to measure the gas from each absorption bottle.

Procedure. One hundred milliliters of 0.1 normal NaOH, 5 ml c.p. benzyl alcohol, a known amount of Na_2SO_4 equivalent to about 10 ml N/50 NaOH, and 1 drop of benzaldehyde (if required) were put in the absorption bottle. Thirty milligrams of P-amino-phenol-HCl were added to the solution exactly 2 min before the start of the test; the P-amino-phenol-HCl was mixed with mannitol in the proportion of 1 to 35 to facilitate measurement of small quantities with a spoon or scoop; 100 ml of 0.1 normal NaOH was used instead of 50 ml of 0.2 normal NaOH primarily to dilute any undesirable impurities absorbed from the gases.

A pH meter was used instead of brom-cresol-green to determine the end point of the titration at 4.6 with 0.2 N HCl.

One absorption bottle was used during half of the test period, and one for the full test period, thus giving evidence as to the action of the inhibitor. It was found that all c.p. benzyl alcohol as purchased in bottles did not have exactly the same inhibiting action. It was necessary to add a drop of benzaldehyde, an impurity frequently found in benzyl alcohol, to obtain the desired action in all cases except one. Its addition to one bottle of the alcohol was found to be detrimental. Using the two absorption bottles protected the test by indicating when the data of the test were satisfactory.

During the laboratory work with SO_2-CO_2-air mixtures, the volume of SO_2 indicated by the tests failed to check the volume of SO_2 fed to the apparatus. Tests with a CO_2-air mixture gave an acid titration of 49.0 ml instead of the 50 ml blank, showing that at the end point chosen a correction for CO_2 effect should be made in the calculation for SO_2 when the method is used for boiler flue gases. By using 49 instead of 50 in the ASME formula for the calculation of SO_2 volume, test values for the volume of SO_2 in SO_2-CO_2-air mixtures checked the actual volume of SO_2 closely. This correction accounted in part for the excessive total sulphur found in the flue gases during the early tests.

Test Results and Comparisons

Table 6 shows a comparison of the results obtained at the Naval Gun Factory with the ASME and the improved procedure. It is believed that with the new procedure, the volume of SO_2 determined by the analysis is within an accuracy of about 2 per cent of itself and that the maximum error in the determination of the SO_3 is ±0.0002 per cent SO_3.

Table 7 shows results typical of many analyses of the products of combustion for SO_2 and SO_3 at the boiler outlet. The SO_2 value for different CO_2 contents for boiler No. 1, as would be expected, increased with the CO_2, the excess air being considered merely a diluent. The reverse was true of the SO_3; it increased as the CO_2 decreased, that is, increased with the oxygen as if more oxygen burned more SO_2 to SO_3. This oxidation is considered to increase continuously the SO_3 formed as the gases pass through the boiler.

TABLE 6 COMPARISON OF ANALYSES FOR SO_2 AND SO_3 WHEN USING ASME AND NEW PROCEDURE; 30-MIN SAMPLES

	Per cent SO_2 by volume		Per cent SO_3 by volume	
Per cent CO_2	ASME	New procedure	ASME	New procedure
9.4	0.033	0.031	0.0054	0.0020
11.8	0.040	0.036	0.0052	0.0012
11.8	0.039	0.034	0.0044	0.0012

TABLE 7 SO_2 AND SO_3 CONTENTS OF GASES AT BOILER OUTLET OF BOILERS NOS. 1 AND 3

Boiler no.	Per cent CO_2	Per cent SO_2 by volume	Per cent SO_3 by volume	$\frac{\% SO_2}{\% SO_3}$
1	9	0.033	0.0031	11
1	12	0.039	0.0025	16
1	15	0.045	0.0015	30
3	12	0.034	0.0012	28

A study of the dew points of the 9 per cent CO_2 gases and the 15 per cent CO_2 gases showed that although the SO_3 content of the 9 per cent gas was about twice as high, its dew point was only about 20 F higher, because of its lower moisture content, the diluting air having much lower moisture than products of combustion with no excess air.

Table 4 shows that there was only about one third as much deposit with the 9 per cent CO_2 gas at the boiler outlet as with the 15 per cent CO_2 gas, although their dewpoints were about the same. Comparing the 12 per cent CO_2 sample of boiler No. 1 with that of boiler No. 3, both of which had about the same oxygen and moisture content, for the gas of boiler No. 1 somewhat higher SO_2 is shown, much higher SO_3, and a correspondingly lower SO_2/SO_3 ratio. This again points to a factor which was due to some difference in equipment or operation.

Fly-Ash Sampling

There is considerable general belief among operators that relative difficulties from the sulphate deposits are greater for underfeed stokers and less for spreader stokers and pulverized-fuel equipment. One factor related to such equipment which definitely varies inversely is the quantity of fly ash entrained in the gases. A number of fly-ash samples were taken at the boiler outlet of representative installations of underfeed stokers, of one traveling-grate stoker, and of several spreader stokers, all burning about 0.7 per cent sulphur coal. As an extreme case, a sample was taken at the outlet of the air preheater of a wet-bottom pulverized-fuel boiler using a 2 to 3 per cent sulphur coal. The following shows average analyses of the samples:

Equipment	SO_3	pH
Underfeeds....................	1.44	3.68
Traveling grate...............	1.50	3.70
Spreaders.....................	1.17	5.23
Wet-bottom pulverized........	1.00	11.50

The more the fly ash, the less was the SO_3 content and the acidity.

Because of the unusually long rear arch of boiler No. 1, much less fly ash was entrained in the gases than for boiler No. 3. A study was made of the fly ash from boiler No. 1, as shown in Table

8. The fly ash for 9 per cent CO_2 had less sulphur than that for 15 per cent CO_2 and was less acid. The fine sizes passing the 325-mesh screen for all cases had more sulphur and were more acid than the corresponding coarse sizes. It appears reasonable to assume that the sulphurous gases act on the fly ash in the gas stream, and that relatively more action would occur on the greater surface of the fine sizes. The coarser fly ash, however, retained on the 50-mesh screen had more SO_3 than the original nonsieved sample. This would indicate that the middle sizes were lower in SO_3, which did not at first appear to be reasonable.

TABLE 8 SULPHUR CONTENT AND ACID CONDITION OF FLY ASH FROM BOILER NO. 1

	9 per cent CO_2 test		15 per cent CO_2 test	
	Boiler hopper	Economizer hopper	Boiler hopper	Economizer hopper
Sieve analysis of fly ash, per cent:				
Retained on No. 16 sieve	9.2	5.9	2.4	0.9
Retained on No. 30 sieve, passing No. 16 sieve	33.3	29.7	20.2	12.4
Retained on No. 50 sieve, passing No. 30 sieve	30.4	32.2	32.7	30.5
Retained on No. 100 sieve, passing No. 50 sieve	18.0	21.4	27.7	33.1
Retained on No. 200 sieve, passing No. 100 sieve	5.1	7.4	10.3	15.5
Retained on No. 325 sieve, passing No. 200 sieve	1.4	1.6	2.4	2.8
Passing No. 325 sieve	2.6	1.8	4.3	4.8
Chemical analysis of fly ash:				
Sulphur as SO_3				
Nonsieved sample, per cent	0.9	1.1	1.0	1.2
Sample retained on No. 50 sieve, per cent	1.1	1.3	1.2	1.4
Sample passing No. 325 sieve, per cent	1.4	1.9	2.8	3.4
pH				
Nonsieved sample	5.3	4.2	4.0	3.8
Sample retained on No. 50 sieve	5.0	4.5	4.4	4.1
Sample passing No. 325 sieve	4.6	4.3	3.2	3.1
Fly ash per hr, lb	25.1	20.1	6.4	4.6
Sulphur in fly ash per hour, lb	0.090	0.088	0.026	0.022
Coal fired per hour, as fired, lb	6130		5470	
Per cent sulphur in coal, as fired, per cent	0.7		0.7	
Sulphur in coal fired, per hour, lb	42.9		38.3	
Sulphur in fly ash, per cent of sulphur in coal, per cent	0.2	0.2	0.07	0.06

Microscopic study, however, of the coarse sizes showed that coarse platelets of sulphate-type deposits were mixed with the fly ash, and also that the coarse particles of fly ash had embedded in them particles of the same deposit. This indicated that the fly ash was cutting into any deposit formed, thus retarding its accumulation. For both tests the sulphur in the fly ash and the fly-ash acidity increased as the ash moved through the boiler passes. There was also much more fly ash at 9 per cent CO_2, about 4 times as much being caught per hour in the ash hoppers. Although the fly ash caught at 9 per cent CO_2 had less sulphur in per cent, it took out a greater poundage of sulphur than the fly ash caught at 15 per cent CO_2. Table 8 also shows that the amount of sulphur in this fly ash was exceedingly small, as compared to the total amount in the coal burned. This would also be true of the amount in the fly ash leaving the boiler.

Summary and Conclusions

An improved and satisfactory method of analyzing products of combustion for SO_2 and SO_3 content is given.

The data of this continuing investigation to date indicate the complexity of the action resulting in the accumulation of the sulphate-type deposits on the tubes. Many factors are involved, such as the temperature of the collecting surface, the temperature of the gases, the quantity, size, and chemical analysis of the fly ash, the relative amount of burning of SO_2 to SO_3, and the relative saturation of the moisture and of the sulphurous gases which depends upon the CO_2 carried and the amount of sulphur coming from the coal. The term "sulphurous gases" is used because the relative action of the SO_2 and the SO_3 has not yet been satisfactorily determined. Any one of these factors might be the governing one under a particular set of conditions.

Table 4 shows for boiler No. 1 more deposit at the economizer inlet with 15 per cent CO_2 than with 9 per cent CO_2, although the dew points of the gases are nearly the same; evidently the sweeping action of the greater amount of fly ash, together with its higher traveling speed, for the 9 per cent CO_2 was a big factor in retarding the accumulation. The acidity of any fine fly ash entrained in the deposit for the 9 per cent CO_2 was appreciably less than for the 15 per cent CO_2.

The deposit on ferrous tubes characteristically had an inner layer of white deposit of ferrous sulphate, formed largely from the iron of the tube and sulphuric acid; the remainder of the deposit consisted chiefly of sulphates and silica, such as would be formed from fly ash entrained and acted upon by sulphuric acid.

The deposit can form on nonferrous equipment, showing that the initial action of sulphurous gases on iron is not necessary. The fact that the deposit can form at temperatures so much higher than are ordinarily anticipated from dew-point considerations calls for more study.

When boiler No. 1 is operated at 12 per cent CO_2, some deposit builds up even at the end of the first pass; when boiler No. 3 is operated at 12 per cent CO_2, no deposit builds up anywhere in the boiler. Factors functioning to cause the difference are the much higher quantity of fly ash in boiler No. 3 which physically sweeps on the tubes, and the apparent action of this greater amount of fly ash in taking out a greater amount of sulphurous gases from the products of combustion. It appears reasonable to assume that the fly ash takes out SO_3 in preference to SO_2. Although the amount of sulphur taken out is not much of the total sulphur involved, it could be enough of the SO_3 to result in an appreciably lower dew point of the gases. Just what effect, if any, the boiler No. 1 type of furnace, with its greater water cooling, has on the production of SO_3 as compared to the boiler No. 3 type of furnace is not now known. Just what bearing, if any, the slightly higher superheater temperature of boiler No. 1 has on the problem is not now known.

As an operating matter, it was found that by dropping the CO_2 from above 14 per cent for boiler No. 1 to about 12 per cent

CO_2, a year's operation could be had without draft loss and with only a small accumulation of deposit which was effectively removed by an off-the-line water-washing procedure devised by the plant personnel.

Possibly the answer, at least in part, to the question asked repeatedly in the last few years as to why sulphate-type deposits have recently become so much more troublesome, may be that higher CO_2 content is, in general, being carried, resulting in many cases in appreciably less fly ash; lower-grade coals such as were received during the war, having higher moisture or sulphur contents, would also be a contributing factor.

ACKNOWLEDGMENTS

These studies were made possible through the capable co-operation and advice of Earl Griggs, Master Mechanic in charge of the Naval Gun Factory power plant. Dr. Elias Bielouss of the Navy, and N. E. Rogers and W. A. Selvig of the Bureau of Mines, assisted on the analytical work. D. J. Mosshart and A. C. Stark of the Westinghouse Electric Corp. gave helpful assistance.

Discussion

EARL GRIGGS.[6] A brief outline of the boiler deposits from an operator's viewpoint follows:

Boilers Nos. 1 and 2, both identical, were purchased new and put on line January 24, 1942, and January 25, 1943, respectively. Designed for 405 psig, 700 F, they are operated at about 195 psig, 600 F. Due to local reducing-valve conditions, loading is limited by total temperature of 600 F. This results in a maximum loading of 90,000 lb per hr.

The deposit appears to have the same expanding and contracting qualities as the tubes. It is very hard and brittle on the gas-stream side, and somewhat softer with powdery tendency on the opposite side. In general, after removal the tubes have a bright appearance, thus showing corrosion, but no pitting is visible. Eighteen pilot tubes are measured with micrometer from time to time; to date tube wastage is not appreciable.

Due to draft loss caused by build-up of deposit, it is necessary to wash the tube surface with water at 40 to 50 psig and normal flow temperature, say, 60 to 90 F. The superheater and economizer are also washed at this time. Three men per 8-hr shift for 3 continuous shifts are required. Various lengths of pipe equipped with standard pipe fittings are arranged to enter tube lanes so water will reach each tube in the bank. While the entire deposit is not soluble in water, apparently sufficient water is absorbed to loosen the bond. After washing, all visible surfaces are free of deposit.

Immediately after washing, the boiler is filled with 220 F water and a wood fire is maintained for a minimum of 72 hr, then the coal fire is "lit" off and the boiler cut in the line. In this way the boiler is dried at once to avoid the possibility of any water of appreciable acid content causing accelerated corrosion. This is most apt to occur in rather inaccessable places where insufficient water reaches the area.

A reinjector system has recently been installed on boiler No. 1 to inject contents of sifting, boiler outlet, and economizer hoppers into the combustion area. The effect of this installation in retarding deposit build-up has not yet been noticeable.

Opinions have been expressed that the length of the back arch is conducive to deposit and should be reduced appreciably to assist in decreasing the amount of deposit. As this is a major change and costly, it is not contemplated at this time.

The study to date has revealed that operation at 12 per cent CO^2 retards the build-up rate. However, it is hoped that further steps which will be not too costly can be taken so that 14.5 per cent CO_2 can be carried without appreciable deposit.

W. F. HARLOW.[7] The crux of the problem presented in this paper is the origin of the sulphur trioxide which is clearly the cause of the deposits. This particular deposit trouble is only one of several injurious effects which arise from the presence of sulphur trioxide in flue gases, the reasons for which have been under close investigation by the writer's company for a number of years. This question was dealt with in a paper[8] by the writer in 1943, in which it was shown that sulphur trioxide can be formed by the passage of flue gases over heated oxidized iron, the amount depending upon the temperature of the metal and the condition of its surface.

These findings were based on actual measurement of the condensed acid on temperature-controlled surfaces, thus avoiding contentious chemical methods of flue-gas analysis which, as this paper shows, may give misleading results.

The writer submits that the passage of flue gases over unprotected iron surfaces at elevated temperatures is the major cause of the sulphuric-acid production in boiler plants and suggests that the case under discussion is no exception and that the sulphur trioxide is chiefly formed on the superheater tubes. Although the temperature of these tubes, as judged by the steam temperature, is considerably below that at which any considerable formation of sulphur trioxide has been shown to occur, it should be realized that the metal temperatures may often be much higher than the steam temperatures would indicate, owing to unfavorable conditions existing on the inside and/or the outside of the tubes. Internal scale will of course elevate the metal temperature, and external deposits can cause unequal distribution of the gases, resulting in local overheating of some tubes above the average temperature. An even more important factor affecting the metal temperature is the possibility of unburned gases reaching the superheater, resulting in surface combustion on the tube surface. This will elevate the skin temperature considerably above that which would exist if the gases were inert. Restriction of flame impingement on superheater tubes has been found to reduce considerably the amount of acid in flue gases.

The difference in acid content of the gases from boilers Nos. 1 and 3 could be explained adequately by the higher superheat temperature of boiler No. 1, together with the possible variations in the other factors referred to.

The writer has seen deposits of the type described in a boiler constructed with a two-stage superheater arranged across the unit. The deposit was much heavier on the boiler tubes in line with the secondary or high-temperature superheater than with those in line with the primary superheater, showing that the superheater-tube temperature was the controlling factor, since all other conditions were identical.

Any reduction in the operating temperatures of the superheater tubes can be expected to reduce the acid production and consequent deposit formation. The introduction of secondary air has been found to have a beneficial effect in this respect by accelerating the process of combustion in the gases so that this is completed before the tubes are reached.

It will be seen that since the acid content of flue gases is a function of the temperatures of the surfaces over which they pass, any comparison of the acidity produced by different types of combustion equipment may be misleading unless the boiler temperatures are identical. For this reason it is necessary to know the particulars of the boilers from which the figures for acidity were obtained for the relative merits of the different types of combustion equipment to be assessed correctly.

---

[6] Master Mechanic, Power Plant, Naval Gun Factory, Washington, D. C.

[7] International Combustion Limited, Derby, England.

[8] "Causes of High Dew-Point Temperatures in Boiler Flue Gases," by W. F. Harlow, Proceedings of The Institution of Mechanical Engineers, vol. 151, 1944, pp. 293–298.

Hilmer Karlsson.[9] The authors should be congratulated on developing an improved method for determination of SO_2 and SO_3 content in flue gases, the accurate determination of which will permit a better understanding as to the relative importance of these constituents in flue gases as it affects the low-temperature surface of a steam generator and its auxiliary heat-recovery equipment.

The authors' findings that deposits of ferrous sulphate will take place even on nonferrous types of surface is interesting and confirms findings in connection with a study now in progress of the different types of deposit formed at the cold end of air-preheater surface.

The findings by the authors that fly ash passing a No. 324 sieve or particles less than 44 microns in diameter are higher in acidic content than the larger particles indicates that particle size is one important item to consider in investigations of factors causing corrosion of the low-temperature surface in a steam-generating plant.

The authors' investigations further prove that the method of firing, in the case of coal fuels, is an important factor in the rate of corrosive attack to be anticipated by the gases of combustion from any given coal and confirm the knowledge now available.

It is hoped that the work started by the authors may be continued so as to permit a more accurate evaluation of the different factors affecting corrosion of air preheater, economizer, and boiler heating surface.

It may not be amiss to mention in this connection that the company with which the writer is associated, presently has a co-operative program under progress with the Bureau of Mines, the results of which, when published, it is hoped will throw further light on the problem under discussion, especially as it affects the low-temperature zones of the flue-gas system, which includes air-preheating surface.

W. T. Reid.[10] The importance of deposits on heat-receiving surfaces of steam-generating equipment is rightly stressed by the authors. However, unlike the usual case where interference with the transmission of heat is the principal problem experienced with boiler-tube deposits of coal ash or slag, they point out that draft loss and corrosion are the most objectionable features of the thick, consolidated, and tenacious coatings described. The occurrence of sulphate deposits of this type has been noted only in recent years, but most of the trouble observed has resulted from external corrosion of furnace-wall tubes in pulverized-coal-fired furnaces.[11] In some instances, corrosion in such furnaces has been so severe as to necessitate tube replacement, but the authors do not state the extent or degree of corrosion in the stoker-fired furnace shown in their Fig. 1. Such information would be valuable not only in comparing the activity of sulphate-type deposits in the two types of furnaces and under different conditions but also in pointing out the hazards to be expected in allowing such deposits to form on boiler tubes.

Of particular interest is the similarity between the composition of the deposits described by the authors and those found on furnace-wall tubes, as shown in Table 9 of this discussion.

TABLE 9 COMPARISON OF BOILER-TUBE AND FURNACE WALL-TUBE DEPOSITS

	Typical boiler-tube deposit, per cent		Typical furnace-wall tube deposit, per cent[a]	
	As received	Ash-free	As received	Ash-free
Moisture at 105 C	2.0	...	0.2	...
Combined water	2.4	...	...	...
Silica, SiO_2	20.9	...	8.3	...
Aluminum oxide, Al_2O_3	8.8	...	6.2	...
Total iron, as Fe_2O_3	9.3	15.3	16.6	20.3
Calcium oxide, CaO	1.0	...	2.7	...
Magnesium oxide, MgO	0.3	...	0.2	...
Sulphur trioxide, SO_3	38.3	63.0	36.5	44.6
Alkalies, as Na_2O	13.2	21.7	28.7	35.1
Water-soluble	40.0	...	90.8	...
pH of 1 per cent solution	2.6	...	3.6	...

[a] Sample C-9, reference noted.

The calculation of the ash-free composition is based on the fact that the compound $K_3Fe(SO_4)_3$ is known to be present in large amounts in the water-soluble portion of these deposits. Although solid solution of other components such as Na_2SO_4 and SO_3 may occur, there is little likelihood that silica, alumina, or other normal constituents of coal ash play any real part in the production of the deposit, and thus they can be neglected in evaluating its formation. Presumably the process is one of developing a liquid surface by reaction of alkali metals, SO_3, and iron oxides supplied either by the tube metal or occurring in coal ash, with fly ash adhering to this sticky surface to increase the bulk of the deposit. Although some of the Fe_2O_3 shown by the analysis undoubtedly occurs in the fly ash physically held in the deposit, the iron oxides cannot be distinguished from those in chemical combination as $K_3Fe(SO_4)_3$; thus all the Fe_2O_3 is included in the ash-free composition.

The essential differences in the two deposits is in the relative proportions of SO_3 and alkalies. For the boiler-tube deposit the SO_3/Na_2O ratio is 2.90; for the deposit from the furnace-wall tube, it is 1.27. As has been shown,[12] the alkali metal ferric trisulphates are particularly sensitive to the presence of SO_3, reacting readily with the gas at low temperatures, and evolving SO_3 at high temperatures. At temperatures below about 600 F, reaction with SO_3 occurs readily to form pyrosulphates; from 700- 1000 F, the compounds are relatively stable; while at temperatures above 1100 F, they are almost quantitatively decomposed into Na_2SO_4 and K_2SO_4, Fe_2O_3 and SO_3. It would appear, therefore, that the boiler-tube deposit contains a larger amount of S because the temperature at which it is deposited is in the ran 400–450 F. This would also explain why the deposit was h groscopic and rapidly became damp when exposed to the atmosphere, and would indicate as well that it would be high corrosive. The lower pH of a solution of the boiler-tube depo is additional evidence of the formation of pyrosulphates. Th higher temperatures of 600–800 F, normal for furnace-wall tubes decrease the formation of pyrosulphates, and thus less SO_3 i present in the deposit.

It seems probable that the deposits described by the author should not be classed with those found in economizers or ai heaters, where the dew point of the gas undoubtedly plays an important part. Rather, they should be considered as similar i nature to those found on furnace-wall tubes, despite the differences in composition resulting from moderate changes in temperature.

The authors' recommendations regarding modification of th ASME Power Test Code method for analyzing flue gas fo SO_2 and SO_3 clear up some of the vexing points regarding thi difficult analysis. The recognition of copper as a major interfering element will simplify any further developments of the tes

---

[9] Chief Engineer, The Air Preheater Corporation, Wellsville, N. Y. Fellow ASME.

[10] Supervisor, Battelle Memorial Institute, Columbus, Ohio. Mem. ASME.

[11] "External Corrosion of Furnace-Wall Tubes—I. History and Occurrence," by W. T. Reid, R. C. Corey, and B. J. Cross, Trans. ASME, vol. 67, 1945, pp. 279–288.

[12] "External Corrosion of Furnace-Wall Tubes—II. Significanc of Sulphate Deposits and Sulphur Trioxide in Corrosion Mechanism, by R. C. Corey, B. J. Cross, and W. T. Reid, Trans. ASME, vol. 6 1945, pp. 289–302,

Although the proposed method is shown to yield more consistent results than the Test Code procedure, the necessity of using two absorption bottles for different total times of sampling as a check on the action of the inhibitor, indicates that further work on the analytical method will be necessary. Because the presence of SO_3 in flue gases plays such an important role in the formation of deposits and in causing corrosion, it is hoped that the authors will be able to carry on their researches in still further improving this analytical procedure.

Authors' Closure

The authors wish to express their appreciation for the added value to the subject matter given by the discussions.

The description of washing the tubes given by Mr. Griggs should be of interest to operators; his statement as to the amount of tube corrosion adds important information.

Mr. Harlow mentions a number of conclusions reached from his long study of the general subject matter which is much appreciated. His statement that "the sulphur trioxide .... is clearly the cause of the deposits" and that "the acid content of flue gases is a function of the temperature of the surfaces over which they pass," no doubt gives factors in the production of deposits and formation of SO_3. However, as the data show, a number of other factors were also at work. The superheat temperature of boiler No. 1 was only about 90 F higher than that of boiler No. 3; it would appear that a greater difference of temperature would be needed to produce substantial differences. Both of these superheaters were not clean during the tests and neither had exposed "heated oxidized iron."

The authors greatly appreciate the emphasis on the importance of phases of the work given by Mr. Karlsson.

Mr. Reid's question as to the severity of the corrosion of the deposits on the boiler tubes is covered in Mr. Griggs' discussion. The comparison of these deposits to those found on furnace wall tubes is interesting and his explanation of chemical similarities and of possible mechanisms of formation is a valued contribution. In regard to the required use of two absorption bottles in testing for SO_2 and SO_3 in flue gases, attention might be called to the fact that the use of the two bottles not only checks the inhibitor but also gives a check reading which is usually desirable in test work. Until information is built up on many coals, the authors consider that two bottles should be used at the start in testing gases from any new coal. Having checked the inhibitor for that coal, only one bottle need be used for further tests. A new bottle of benzyl alcohol should also be checked by the use of two absorption bottles. Improvements in the test method will of course be made as found possible.

Additional work has been done since this paper was written. In the study of deposits produced by another coal from a different coal-mining area, it was found that a hard-bonded layer deposit was produced that apparently was cemented by boron phosphate which constituted more than 50 per cent of the layer. This find has broadened the scope of the study.

Progress Report No. 1 on Tool-Chip Interface Temperatures

By K. J. TRIGGER,[1] URBANA, ILL.

The author presents some of the results of a series of tests in which the principal phase of study concerned the temperature developed at the contacting surface of the tool and the chip. This tool-chip interface temperature is referred to as the "cutting" temperature. The determination of the tool-chip interface temperature was by means of the Herbert-Gottwein tool-work thermocouple wherein the steel workpiece constituted one member of a thermocouple and the cemented-carbide insert the other member. This principle has been used in the study of cutting temperatures, the investigation of friction between unlike metals, the study of surface temperatures of brass wire drawn through steel dies and for investigation of surface temperatures of mating gears of unlike metals.

INTRODUCTION

PREVIOUS reports (1, 2, 3, 4)[2] on the application of the tool-work thermocouple to determine cutting temperatures have been based largely upon the cutting of steel with high-speed-steel tools. The cutting speeds were restricted to that range within the capacity of high-speed steel and to cutting temperatures not in excess of 1000 F.

This paper is based upon the cutting of steel with a suitable grade of cemented carbide, and on cutting temperatures in the approximate range of 1100 to 1800 F. Another point of difference lies in the fact that in previous tests both the workpiece and he tool were iron-base alloys of similar basic lattice structure—a actor which may have significant effect upon the tendency of the hip to adhere to the tool. It is to be expected, therefore, that he results herein discussed may differ materially from those preiously reported.

TEST ARRANGEMENT

The test arrangement is illustrated in Fig. 1. The standard arbide tool has a hole drilled in the shank through which a rod of arbide, 3, insulated from the shank, is placed in contact with the arbide insert, 2, the assembly being electrically insulated from he tool post. Details of the tool tip are shown in Fig. 2.

The brush, 4, insulated from the machine frame, was made rom a section of the workpiece. Iron-wire leads, 5 and 6, with uitable connectors were attached to the potentiometer binding osts 7. The completed arrangement thus consisted of several hermocouples, namely, 1–2, 3–6, and 4–5. Couples 6–7 and –7 were of no consequence since any parasitic emf's developed ould cancel one another. Since the lead wires were at constant emperature during any test, the reference junction was at ouples 3–6 and 4–5, and the temperature at these points was maintained essentially constant during any calibration or cutting test.

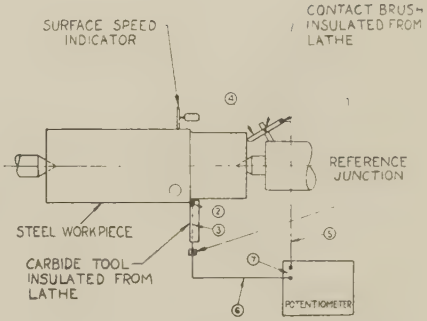

FIG. 1 DIAGRAM OF TEST ARRANGEMENT

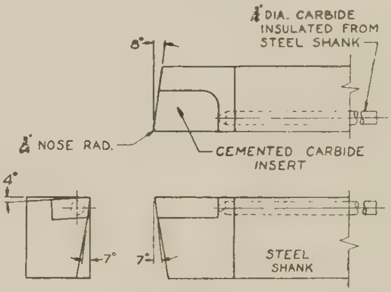

FIG. 2 DETAIL OF TOOL TIP

No thermocouple existed at 2–3 since the carbide insert, contact rod, and calibration strip were made from the same batch of carbide mixture. Similarly, junction 1–4 was of no consequence since both metals in contact were from the same bar.

Thus the hot junction of the thermocouple circuit was at 1–2, and the reference junction at 3–6 and 4–5.

The validity of the operating principle of the tool-work thermocouple may be affected by several factors: (*a*) The effect of chip force upon the tool face; (*b*) the electrical effect of chip deformation; (*c*) the triboelectric effect due to friction of the steel rubbing on the carbide; (*d*) the temperature gradient at the contacting surface of the chip and the tool; and possibly by (*e*), the dissimilarity of temperature gradients during calibration, as compared with those during cutting.

The effect of chip force was investigated by slowly forcing a carbide strip into a steel strip under a bearing stress of over 100,000 psi. No electrical effect was observed at the potentiometer. The thermoelectric effect of chip deformation was investigated by substituting a bar of the workpiece for the tool. When this bar and the workpiece were brought together under simulated cutting conditions, only a very slight (0.04 to 0.05 mv negative) emf was noted even though the bar was smeared on the workpiece by the rubbing action. When two pieces of chemically identical high-speed steel were substituted for the tool and workpiece, an indication of the same magnitude was observed. Since the local deformation was severe and, further, since the effect is within the limits of reproducibility and reading accuracy of the

---

[1] Professor, Department of Mechanical Engineering, University Illinois. Mem. ASME.

[2] Numbers in parentheses refer to the Bibliography at the end of he paper.

Contributed by the Special Research Committee on Metal Cutting ata and Bibliography and presented at the Semi-Annual Meeting, hicago, Ill., June 16–19, 1947, of THE AMERICAN SOCIETY OF MEHANICAL ENGINEERS.

NOTE: Statements and opinions advanced in papers are to be nderstood as individual expressions of their authors and not those of he Society.

potentiometer, it was concluded that any deviation introduced by chip deformation is inconsequential. The triboelectric effect was evaluated on a "Metalsorter,"[3] using a bar of the test stock and the carbide calibration bar as the two metals in contact. The observed deflection was 27 mm positive corresponding to 0.03 mv. It was concluded that the triboelectric effect was negligible and, in fact, tended to cancel any error introduced by chip deformation. Since the range of readings was 11 to $19^1/_2$ mv during the cutting tests, it was apparent that these minor deviations were insignificant.

Observations were made for the purpose of determining whether the tool surface and chip surface would attain a stable temperature. A strip of carbide 0.20 in. × 0.25 in. × 11 in. was ground as a tool bit on one end, insulated from a supporting steel bar and used as a cutting tool. The millivolt reading was 12.97 at the beginning of a test and virtually the same reading prevailed during a 45-sec duration of cut. It was concluded that the contact surface of the tool and chip reached, at least, a state of quasi-equilibrium almost immediately after a cutting test was started. Therefore it was assumed that the separating surface of the chip and the face of the tool reached essentially the same temperature during a cutting test.

That the temperature gradients along the calibration strips during calibration were not the same as those during a cutting test seemed to be of no consequence in the light of the so-called "law of the homogeneous circuit," which states as a corollary, "if one junction of two dissimilar homogeneous materials is maintained at a temperature T_1 and the other junction at a temperature T_2, the thermal emf developed is independent of the temperature gradient and distribution along the wires" (5). While steel and cemented carbide cannot be considered as homogeneous materials they may be thought of as being uniformly unhomogeneous and the law of the homogeneous circuit would apply. As a result of these preliminary investigations, it was concluded that the possible errors were not of sufficient magnitude to outlaw the tool-work thermocouple as a means—perhaps the only means—of evaluating the temperature where tool failure is instigated.

In considering the experimental results it must be remembered that the tool-work thermocouple consists, in reality, of a number of thermocouples in parallel so that the emf observed is an average emf of all points of contact (thermocouples) of the tool and the chip. Cutting temperatures so determined would represent an average temperature at the tool-chip interface.

Calibration Procedure

The general calibration arrangement is shown in Fig. 3 and details in Fig. 4.

The steel member was prepared from a portion of the workpiece and had a rounded end so as to provide line contact with the carbide calibration strip. A $^1/_{16}$-in. hole was drilled within 0.010 in. of the contact area for the reference chromel-alumel thermocouple. Contact between the carbide and steel was maintained by means of a small clamp and blocks of ceramic insulation.

The assembly was placed in an electric furnace through a hole in the door so that the opening could be packed with asbestos yarn and alundum cement. The cold ends of both steel and carbide members projected about 2 in. beyond the door so that cooling water could be applied to keep the cold junction at the desired reference temperature. The lead wires connecting the cold junction to the potentiometer were the pair used in the cutting tests.

During the calibration, a protective furnace atmosphere of nitrogen gas was used for temperatures above 350 F to prevent oxidation or decarburization. The cold-junction temperatu was kept constant by cooling water, the temperature of whic was the same as that prevailing at the potentiometer bindin posts. Thus each calibration curve had a reference temperatu to which all results from the cutting tests were corrected.

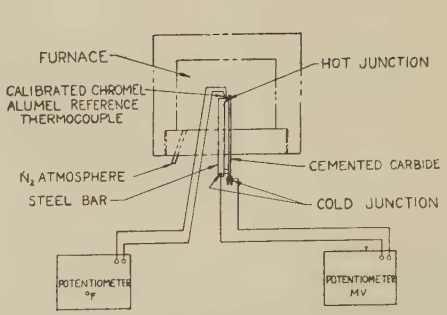

Fig. 3 Diagram of Calibration Arrangement

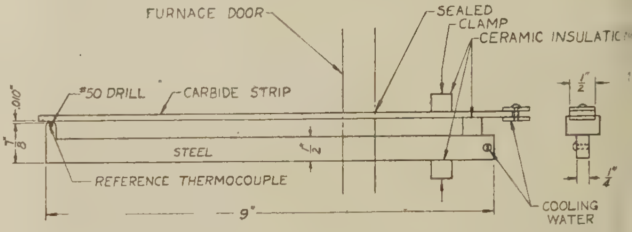

Fig. 4 Detail of Calibration Thermocouple

After establishing uniformity of temperature, simultaneou readings of reference thermocouple temperatures and tool-wor thermocouple millivolts were taken in following increment 5-deg F intervals to 100 F; 50-deg F intervals from 600 to 13 F; 25-deg F intervals during the allotropic transformation the steel, and 50-deg F intervals to the maximum temperatu attained during a particular calibration. A typical calibrati curve is shown in Fig. 5. It may be noted that the temperatu millivolt relationships are straight lines in the ranges show The change of slope at 1400 F is evidence of the allotropic chan in the steel either as it affects the thermocouple proper or as causes variation in the structure along the steel member. A fe points were checked on cooling to determine whether any carburization had occurred in the steel at the contact poi Generally, the points were found to be on the curve though some calibrations the points were slightly higher than the corr sponding ones obtained during heating.

In applying the calibration curve for cutting temperatures extended portion of the curve was used, since by the time 15 was indicated the cutting speeds were such that there was sufficient time for the allotropic transformation to occur whi the chip was in contact with the tool. A metallographic e amination of the separating surface of the chip revealed the sam type of structure as that in the annealed bar. Thus it was co cluded that transformation did not occur, and the extended po tion of the curve in Fig. 5 was used for temperatures in excess 1400 F.

Numerous calibration tests were conducted with the ste member of the tool-work thermocouples in various conditio such as mill-annealed, normalized, heat-treated to 300 Bhn, a cold-worked to 50 per cent cross section. The temperatu millivolt relationships were affected very little (less than 0.10 m by changes in the steel member, probably because the same t phases, ferrite and carbide, existed in the steel and were alter only in their distribution. Thus the same calibration cur was used for all conditions of a particular steel and althou slight errors may have resulted, these were considered to negligible.

---

[3] Control Equipment Company, Pittsburgh, Pa.

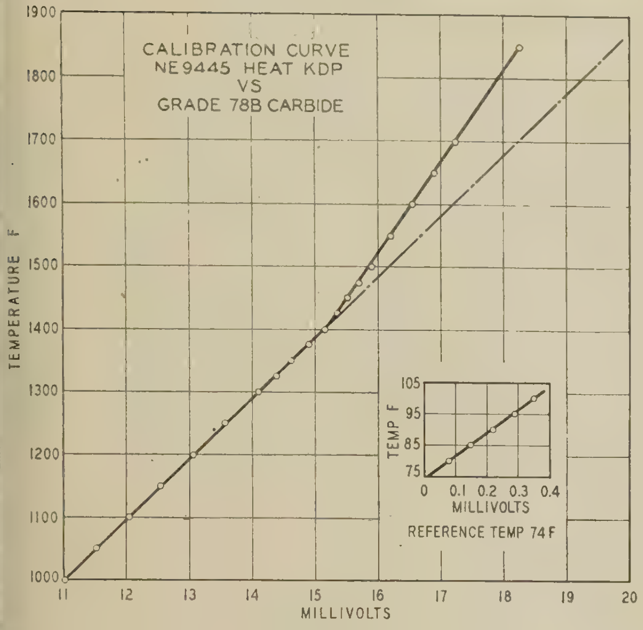

FIG. 5 TYPICAL CALIBRATION CURVE

TEST PROCEDURE

. Tests were conducted on a 16-in. × 54-in. lathe, equipped with a 10-hp motor and having 27 speeds in the range of 18 to 1000 rpm. The feed was held constant at 0.01 in. per revolution, and the same grade 78B Carboloy tool was used throughout the test. Except for one negative-rake test, the tool shape was held constant with specifications as follows: Back rake, 0 deg; side rake, 4 deg; end relief, 7 deg; side relief, 7 deg; end cutting-edge angle, 8 deg; side cutting-edge angle, 0 deg; and nose radius, 3/64 in. All tests were conducted without coolant.

Tool preparation was made on 120-grit and 320-grit diamond wheels, and finishing was done with a 400-grit diamond hone. The setting angle was 90 deg in all tests, and the cutting edge of the tool was set on the center line of the workpiece by means of shims and a gage attached to the tailstock of the lathe.

Surface speeds were measured with a calibrated Metron type 25B indicator having ranges of 0–200, 0–400, and 0–1000 fpm.

During a test the chip was kept from coming in contact with any part of the lathe to avoid grounding the thermocouple. All tests were of 12- to 15-sec duration.

Workpiece materials consisted of NE9445 mill-annealed and as heat-treated to 401 and 311 Bhn; NE8640 mill-annealed; and sulphite-treated NE 8640, mill-annealed. The test logs were from 4 to 6 in. diam and 2 ft long. The compositions and physical properties are shown in Tables 1 and 2, respectively.

RESULTS OF TESTS

In this report the effects of the different variables are compared by noting the cutting speed which results in a selected cutting temperature. A number of factors affect the elevated temperature hardness (hot hardness) of cemented carbides, the principal ones being the grain size, the type of carbide, and the amount of cobalt binder.

W. Dawihl (6) reports the conical indentation hardness of a steel-cutting grade of cemented carbide as being 1170 kg$\sqrt{mm^2}$ at 1290 F, whereas hardened high-speed steel was reported as 1230 kg$\sqrt{mm^2}$ at room temperature. Thus it appears that this particular carbide could be used above 1290 F and still be of adequate hardness for metal-cutting purposes.

E. W. Engle (7) presents curves of Rockwell A hardness values for cemented carbides at elevated temperatures. For the carbide composition used in these tests, interpolation of Engle's curves gives a hardness of 80 R_A at 1300 F, 79 R_A at 1350 F, and 77 R_A at 1400 F. The respective R_c equivalent hardnesses are 58, 56, and 52.

An R_c of 56 to 58 is generally considered as a satisfactory hot hardness for metal cutting. At temperatures above 1350 F, the hardness decreases quite rapidly, and on this basis 1350 F was tentatively selected as the highest cutting temperature for economical tool life. The cutting speed which resulted in a cutting temperature of 1350 F was denoted as the "permissible" cutting speed.

The results of the cutting speed-cutting temperature tests with the different variables are shown in Tables 3 to 7, inclusive, and the relationships are plotted on logarithmic co-ordinates in Figs. 6, 7, 9, and 10.

TABLE 1 CHEMICAL COMPOSITION AND MICROSTRUCTURE OF STEELS USED IN TEST

Steel	Heat no.	C	Mn	Phos	S	Si	Ni	Cr	Mo	Grain size
NE9445............	KDP	0.48	1.18	0.023	0.025	0.49	0.42	0.43	0.11	Fine
NE8640............	X839	0.43	0.82	0.020	0.028	0.32	0.51	0.46	0.19	Fine
NE8640 sulphite-treated..........	X838	0.43	0.82	0.020	0.049	0.32	0.51	0.46	0.19	Fine

Steel	Heat no.	Microstructure
NE9445............	KDP	Fine spheroidized with some lamellar pearlite
NE8640............	X839	Approximately 40 per cent lamellar pearlite; balance spheroidized
NE8640 sulphite-treated..........	X838	Approximately 60 per cent lamellar pearlite; balance spheroidized

TABLE 2 PHYSICAL PROPERTIES OF WORK MATERIALS

(0.505-in. × 2-in. test specimen)

TRANSVERSE SECTION

Steel	Yield strength, psi (drop-of-beam method)	Ultimate strength, psi	Elongation in 2 in. per cent	Reduction in area, per cent	Bhn
445..........	40700	90075	24.5	36.6	183
640..........	38750	85450	20.0	22.5	178
640 sulphite-treated......	38900	83250	15.5	16.3	174
LONGITUDINAL SECTION					
E9445.......	42500	89750	27½	52.3	183
E9445.......	136500	152700	17	46.9	311[a]
E9445.......	178000	192600	11	35.8	401[a]

---

[a] Quenched in oil from 1550 F, tempered 5 hr at 850 F and 1050 F for 401 nd 311 Bhn. respectively.

VARIABLE DEPTH OF CUT

Figs. 6 and 7 show the relation of cutting speed to cutting temperature as the depth of cut was increased from 0.050 in. to 0.150 in. at a constant feed of 0.01 in. per revolution.

The cutting temperature - cutting speed relationships are straight lines on logarithmic co-ordinates, indicating that the cutting temperature is a power function of the cutting speed in accord with the general equation $T = CV^n$, wherein T is the cutting temperature, deg F; C a constant; V the cutting speed, sfpm, and n the exponent.

TABLE 3 CUTTING SPEED-CUTTING TEMPERATURE RESULTS

Variable depth of cut
Steel: NE9445 annealed 183 Bhn
Tool: Grade 78B carbide. 0-4-7-7-8-0-3/64
Feed: 0.01 in. per revolution. Cut: Dry

Depth of cut 0.050 in. Cold-junction temperature, 77 F			Depth of cut 0.075 in. Cold-junction temperature, 75 F		
Cutting speed, sfpm	Corrected mv*	Cutting temperature, deg F	Cutting speed, sfpm	Corrected mv*	Cutting temperature, deg F
112½	11.04	1003	112½	12.34	1128
129½	12.24	1110	134	12.80	1173
134	12.33	1127	156	13.24	1217
157	12.78	1173	180½	13.70	1262
182	13.21	1218	213	14.19	1309
214	13.69	1261	254	14.62	1350
256	14.16	1307	293	15.05	1392
293	14.69	1357	348	15.57	1442
339	15.15	1400	408	16.12	1496
351	15.23	1410	471	16.62	1543
413	15.75	1460	529	17.01	1582
475	16.19	1503	561	17.27	1607
544	16.74	1555	652	17.82	1660
645	17.29	1609	748	18.42	1718
658	17.49	1628	...	...	...
760	18.02	1680	...	...	...

* Millivolt readings corrected to calibration reference junction temperature.

TABLE 4 CUTTING SPEED - CUTTING TEMPERATURE RESULTS

Variable depth of cut
Steel: NE9445 annealed 183 Bhn
Tool: Grade 78B carbide. 0-4-7-7-8-0-3/64
Feed: 0.01 in. per revolution. Cut: Dry

Depth of cut, 0.125 in. Cold-junction temperature, 80 F			Depth of cut, 0.150 in Cold-junction temperature, 75 F		
Cutting speed, sfpm	Corrected mv	Cutting temperature, deg F	Cutting speed, sfpm	Corrected mv	Cutting temperature, deg F
112	12.69	1163	112	12.74	1168
128	13.12	1205	133	13.20	1213
133½	13.20	1213	155	13.72	1263
152	13.52	1244	164	13.77	1267
155	13.66	1257	180	14.05	1296
177	13.98	1288	212	14.42	1332
180	14.04	1295	252	14.93	1381
211	14.40	1329	291	15.31	1417
242	14.82	1368	344	15.91	1475
251	14.90	1378	404	16.44	1527
287	15.24	1410	466	17.04	1585
334	15.47	1451	548	17.69	1648
395	16.42	1524	624	18.16	1695
464	16.90	1572	663	18.27	1705
535	17.47	1625	768	19.05	1778
630	17.97	1675	...	...	...
717	18.67	1744	...	...	...
732	18.80	1756	...	...	...
835	19.41	1816	...	...	...

TABLE 5 CUTTING SPEED - CUTTING TEMPERATURE RESULTS

Variable back-rake angle
Steel: NE9445 annealed 183 Bhn
Tool: Grade 78B carbide.
Feed: 0.01 in. per revolution. Depth of cut: 0.100 in. Cut: Dry

Tool shape: 0-4-7-7-8-0-3/64 Cold-junction temperature, 77 F			Tool shape: Neg. 2° 20′-4-7-7-8-0-3/64 Cold-junction temperature, 78 F		
Cutting speed, sfpm	Corrected, mv	Cutting temperature deg F	Cutting speed, sfpm	Corrected mv	Cutting temperature, deg F
130	12.91	1184	124	12.81	1175
137	13.12	1206	146	13.39	1233
151	13.44	1235	169	13.83	1275
175	13.89	1279	188	14.17	1307
206½	14.31	1321	197	14.38	1328
237	14.65	1354	236	14.90	1377
245	14.89	1377	273	15.57	1442
284	15.34	1420	323	16.16	1498
335	15.88	1471	378	16.57	1540
394	16.36	1516	415	17.02	1583
455	16.75	1555	437	17.10	1592
520	17.38	1618	490	17.72	1651
540	17.50	1626	515	17.75	1655
600	17.93	1673	575	18.32	1710
626	18.11	1686	595	18.37	1715
685	18.43	1721	...	...	...
715	18.70	1745	...	...	...

TABLE 6 CUTTING SPEED-CUTTING TEMPERATURE RESULTS

Variable hardness
Steel: NE9445, quenched and tempered
Tool: Grade 78B carbide, 0-4-7-7-8-0-3/64
Feed: 0.01 in. per revolution. Depth of cut: 0.100 in. Cut: Dry

Quenched and tempered at 1050 F to 311 Bhn Cold-junction temperature, 77 F			Quenched and tempered at 850 F to 401 Bhn Cold-junction temperature, 78 F		
Cutting speed, sfpm	Corrected mv	Cutting temperature, deg F	Cutting speed, sfpm	Corrected mv	Cutting temperature, deg F
61	12.21	1116	43	12.56	1151
71	12.50	1144	51½	13.16	1209
84	12.93	1187	61	13.59	1250
98½	13.28	1222	71	14.09	1300
113½	13.62	1253	85	14.42	1331
136	14.01	1292	99	14.80	1368
161	14.51	1340	115	15.17	1403
183	14.87	1375	137	15.63	1448
220	15.45	1430	162	16.02	1487
256	15.87	1472	186	16.37	1520
296	16.28	1511	221	17.07	1588
351	16.90	1572	...	...	...

TABLE 7 CUTTING SPEED - CUTTING TEMPERATURE RESULTS

Variable steel
Tool: Grade 78B carbide. 0-4-7-7-8-0-3/64
Feed: 0.01 in. per revolution. Depth of cut: 0.100 in. Cut: Dry

Steel: NE8640 sulphite-treated annealed 174 Bhn Cold-junction temperature, 84 F			NE8640 annealed 178 Bhn Cold-junction temperature, 78 F		
Cutting speed, sfpm	Corrected mv	Cutting temperature, deg F	Cutting speed, sfpm	Corrected mv	Cutting temperature, deg F
117	13.21	1112	128½	13.45	1160
136	13.69	1156	153	14.03	1215
163	14.31	1213	181	14.53	1265
188	14.73	1251	208	15.00	1307
220	15.10	1285	256	15.41	1345
261	15.64	1335	289	15.98	1400
304	16.22	1386	334	16.42	1441
353	16.57	1418	395	17.00	1498
415	17.22	1475	460	17.50	1545
485	17.75	1525	530	18.03	1598

The equation of the lines are as follows:

Depth	Equation
0.050 in.	$T = 366\ V^{0.23}$
0.075 in.	$T = 402\ V^{0.219}$
0.100 in.	$T = 416\ V^{0.217}$
0.125 in.	$T = 421\ V^{0.216}$
0.150 in.	$T = 421\ V^{0.216}$

There is a slight decrease in the slope of the line as the depth of cut is increased above 0.050 in., although the effect is slight at depths in excess of 0.075 in. Very likely an important factor which may account for the change of slope of the 0.050-in. li is that the nose radius is nearly equal to the depth of cut wh would constitute, in effect, a change in the setting angle of tool.

The dotted portion of the line for 0.050 in. depth of cut inc cates the result of an excessive built-up edge on the tool. T effect of the built-up edge is to remove some of the many par leled thermocouples from the separating surface and thus to lowe the indicated emf. The separating surface of the chip is bac torn whenever the built-up edge is significant, which in the pr sent series of tests, existed only at the lowest speed for the lighte (0.050-in.) cut.

Figs. 6 and 7 show that with cutting speed and feed held co stant, the cutting temperature increases with increase in dept of cut up to 0.100 in., beyond which there is no appreciable rise cutting temperature as the depth of cut is increased to 0.150 in.

Results for the 0.125-in. and 0.150-in. depths are plotted as single line in Fig. 7. In fact, one half of the points for the 0.10 in. depth plotted in Fig. 6 could be placed on the line in Fig. It could be concluded that under the conditions of the test, th cutting temperature is independent of the depth of cut, at lea in the range from 0.100 in. to 0.150 in., and very probably beyo this limit. This is shown in Fig. 8.

Permissible cutting speeds for the different depths of cut a as follows:

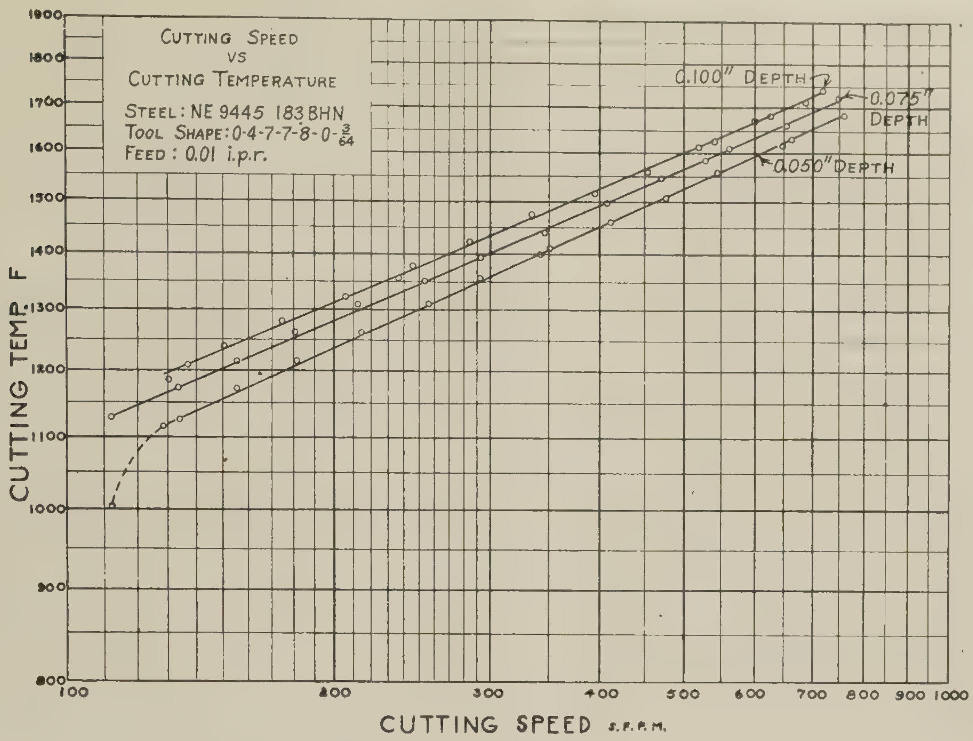

FIG. 6 CUTTING SPEED VERSUS CUTTING TEMPERATURE

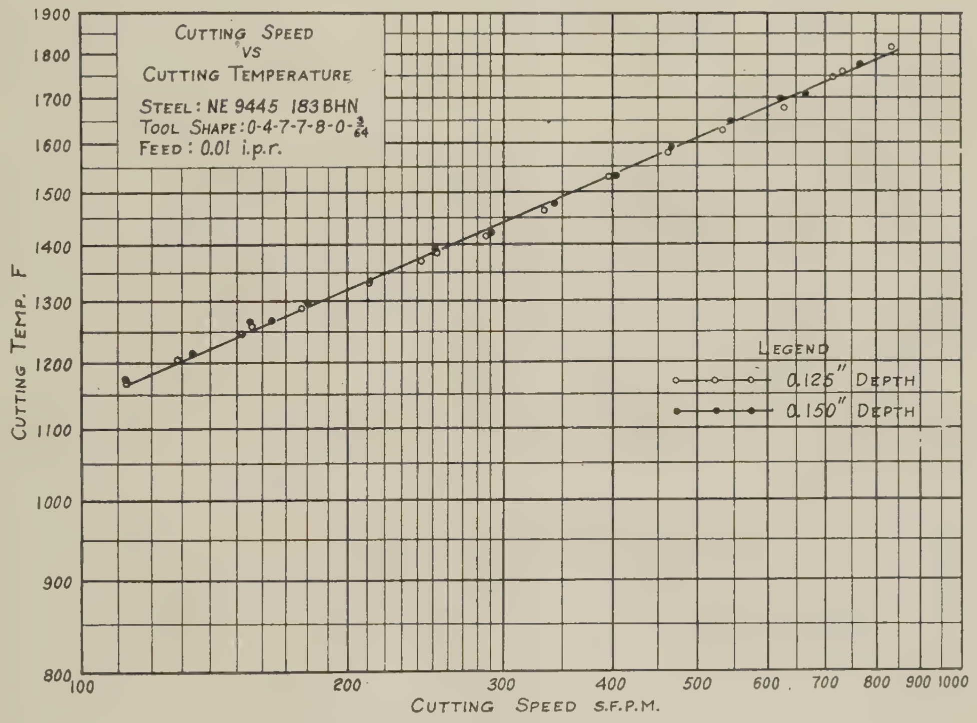

FIG. 7 CUTTING SPEED VERSUS CUTTING TEMPERATURE

Depth	Cutting speed, sfpm
0.050	293
0.075	253
0.100	227
0.125	222
0.150	222

the cutting temperature is considered as the criterion for tool e, the indications are that increasing the depth of cut from 0.100 in. to the maximum value reported will result in very little, if any, increase in the rate of tool failure. As a consequence, more metal may be removed between grinds.

In a paper (8) which included the effect of variable depth of cut at constant feed when turning annealed SAE 3140 with high-speed-steel tools, Messrs. Boston, Gilbert, and Colwell observed that, with a nose radius of $^3/_{64}$ in., increasing the depth of cut

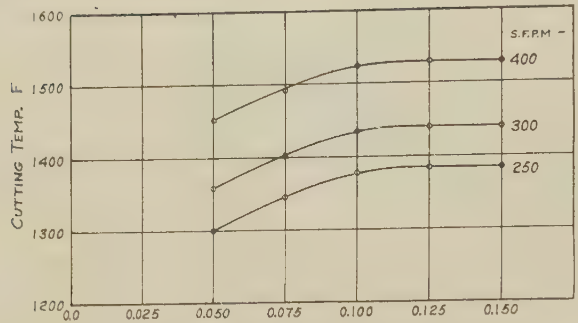

Fig. 8 Depth of Cut Versus Cutting Temperature
(Steel: NE9445 183 Bhn. Feed: 0.01 in. per revolution.)

beyond 0.100 in. at a feed of 0.0125 in. per revolution had comparatively little effect on the tool life. To quote from this report: "This indicates that when the depth of cut exceeds eight times the feed (i.e., 0.100 in.), a further increase in depth will not reduce the tool life to any great extent—indicating that the increased depth beyond 0.100 in. has little effect upon the cutting speed (for a given tool life) and, therefore, is a desirable proportion of cut."

The excellent agreement of the cutting-temperature tests with the tool-life tests by Boston, Gilbert, and Colwell suggests that the respective results are a manifestation of the same factor, namely, that once the depth of cut is significantly greater than the nose radius, the heat concentration per unit length of cutting edge is virtually constant, and therefore the cutting temperature and tool life are relatively unaffected by the depth of cut.

Variable Back-Rake Angle

Table 5 and Fig. 9 show the effect of a negative back-rake angle of 2 deg, 20 min, when cutting annealed 9445 steel at 0.100-in. depth of cut, and 0.01-in per revolution feed.

The introduction of a negative back-rake angle increases the cutting temperature for a given cutting speed, and also increases the slope of the cutting speed - cutting temperature curve. This indicates that the rate of temperature rise becomes greater with an increase in cutting speed. The negative rake angle has a minor influence at the low range of speeds where the two lines converge, but the effect is pronounced at higher cutting speeds. For example, the difference in cutting temperature is 15 deg F at 200 fpm and slightly over 50 deg F at 500 fpm. The permissible cutting speeds are 227 sfpm and 213 sfpm for 0 back-rake and negative 2 deg 20 min back-rake, respectively. It is to be expected that greater negative back-rake angles would result in further increase in both the cutting temperature for a chosen cutting speed, and the slope of the cutting speed-cutting temperature curve. Operational difficulty was encountered in the negative rake tests, particularly at low speed, since the chip curled back in contact with the workpiece and interfered with the tool-work thermocouple circuit. Hence the present report contains the results of only one negative-rake test although further work on rake angles is contemplated.

Variable Brinell Hardness

Tables 5 and 6, and Fig. 10 show the effect of variable hardness upon the cutting speed - cutting temperature relationships of NE9445 steel at a depth of cut of 0.100 in. and feed of 0.01 in. per revolution.

Comparison of the curves for the steel, as annealed to 183 Bhn, and as quenched and tempered to 311 and 401 Bhn, reveals a pronounced effect of an increase in hardness upon the cutting temperature for a selected cutting speed.

The increment of temperature rise is much less for an increase from 183 to 311 Bhn than it is for the smaller increase from 311 to 401 Bhn, when compared at 150 sfpm, for example. The permissible cutting speeds are 227, 164, and 92 sfpm, for hardnesses of 183, 311, and 401 Bhn, respectively. Evidently the cutting speed must be reduced in somewhat other than a linear relationship as the Brinell hardness is increased. Cutting speed-cutting temperature equations for the quenched and tempered steels are $T = 498\ V^{0.196}$ and $T = 592\ V^{0.182}$ for 311 and 401 Bhn, respectively.

During these cutting tests a few measurements of chip thickness were made with micrometers. While no complete program was followed in this respect, the brief data on the variation of chip thickness with (*a*) hardness of the steel, and with (*b*) the cutting speed, may shed some light on the behavior of the cutting speed-cutting temperature relationship. Table 8 shows the chip thickness at the different hardness levels and for several cutting speeds.

It may be noted that, at constant cutting speed, the chip thickness decreases as the hardness is increased, and also that the chip thickness decreases as the cutting speed is increased, up to a limit, with other factors remaining constant.

The variation of the chip thickness at the permissible cutting speed, where any temperature effect on the mechanism of shear presumably is minimized, indicates that, as the hardness is increased, the cutting action is concentrated on less area of the tool. As a consequence, higher cutting temperatures result.

If the chip thickness is compared at a fixed cutting speed, for example, 135 fpm, so that the rate of chip removal is constant, it may be noted that the decrease in chip thickness parallels the decrease in permissible cutting speed as the hardness is increased.

The foregoing remarks on chip thickness are based on comparatively few observations and point to a field of future study with the same steel over additional hardness ranges.

Variable Steel

NE8640 annealed and sulphite-treated NE8640 annealed were cut at 0.100-in. depth of cut and 0.01-in per revolution feed. The cutting temperatures for the 8640 steels were obtained from appropriate calibration curves. The results are shown in Fig. 10 together with those of the annealed and heat-treated NE9445 steel.

A comparison of the annealed 9445 and 8640 reveals that the latter may be cut at somewhat higher speeds for the same cutting temperature. The permissible speeds are 227 and 246 sfpm for the 9445 and 8640, respectively. Considering the difference in the carbon content, the hardness, and the ductility of the two steels, the moderate increase in cutting speed is of the expected magnitude.

Sulphite-treated NE8640 may be cut at 273 sfpm for 1350 F cutting temperature. The chemical composition differs from the

TABLE 8 CHIP-THICKNESS DATA

Hardness, Bhn	Permissible cutting speed, sfpm	Per cent	Chip thickness, in.					
			At permissible cutting speed	Per cent	At 135 sfpm	Per cent	At 220 sfpm	Per cent
183	227	100	0.035	100	0.042	100	0.035	100
311	164	72.2	0.023	65.7	0.026	61.8	0.021	60
401	92	40.5	0.020	57.0	0.017	40.5	0.015	42.8

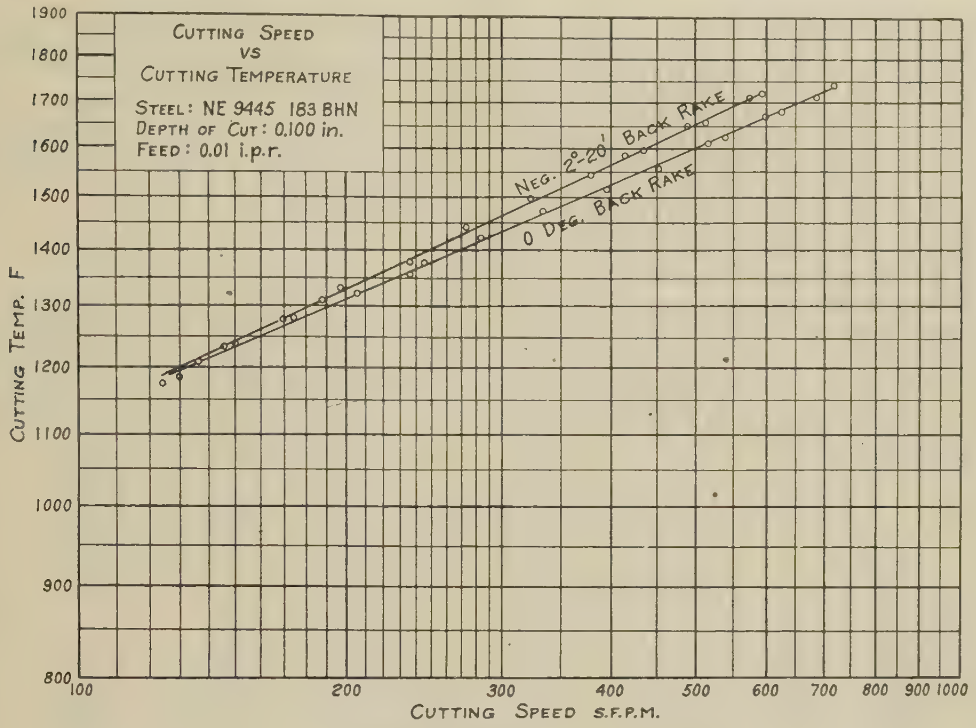

Fig. 9 Cutting Speed Versus Cutting Temperature

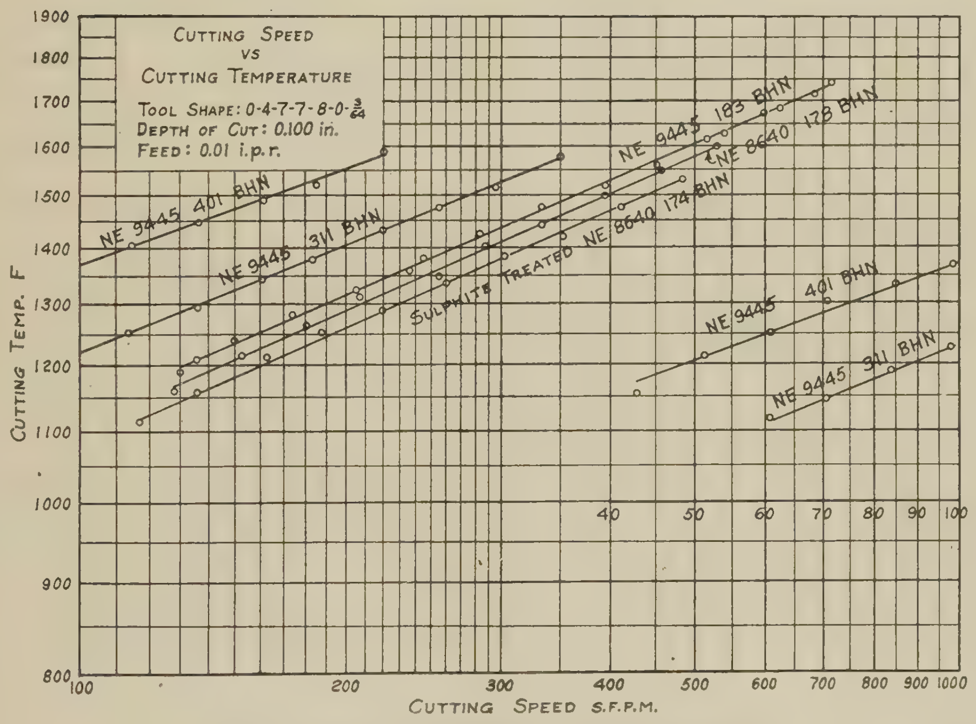

Fig. 10 Cutting Speed Versus Cutting Temperature

E8640 only in the sulphur content, but the major point of ifference was considered to be the method of sulphur addition. a paper before the AIME, Ramsey and Graper (9) dis-ussed the function of sulphite compounds as a means of sulhurizing steels for prevention of hot shortness and for improveent of the machinability.

Commenting on the particular action of sulphite compounds, they note that "the sulphur dioxide is added to the steel by means of the decomposition of an anhydrous sulphite principally sodium sulphite or sodium bisulphite. In general, sulphites upon being heated decompose easily into sulphur dioxide and the oxide of the metal (sodium). The addition of sodium sulphite to molten metal causes a vigorous reaction, liberating sodium dioxide which is taken up by the metal, and sodium oxide which is a strong base and reacts readily with the oxides of the deoxidation reactions, forming a fluid slag which rises to the top of the steel." They report further that the slag analysis of sulphite-treated steels revealed that large amounts of refractory inclusions had been washed from the steel. It was claimed that the removal of the abrasive inclusions and more uniform distribution of the sulphide compounds would give improved machinability from the standpoint of cutting speed, accuracy, finish, and tool life.

Within the limits of these tests the improvement in the machinability attributable to the sulphite treatment supports the contention of Ramsey and Graper.

A very common measure of machinability is the tool life between grinds and, since a principal reason for tool failure is softening of the cutting surface due to high local temperatures at the tool-chip interface, it is logical to rate the machinability of a steel by comparing the cutting speed which causes a permissible maximum cutting temperature.

TABLE 9 SUMMARY OF EXPERIMENTAL DATA AND RESULTS

Steel	Bhn	Back-rake angle,	Depth of cut, in.	Cutting speed-cutting temperature equation	Permissible cutting speed, sfpm	Relative machinability, per cent
NE9445........	183	0	0.050	$T = 366\ V^{0.23}$	293	...
NE9445........	183	0	0.075	$T = 402\ V^{0.219}$	253	...
NE9445........	183	0	0.100	$T = 416\ V^{0.217}$	227	100
NE9445........	183	0	0.125	$T = 421\ V^{.0216}$	222	...
NE9445........	183	0	0.150	$T = 421\ V^{0.216}$	222	...
NE9445........	183	−2° 20′	0.100	$T = 378\ V^{0.237}$	213	...
NE9445........	311	0	0.100	$T = 498\ V^{0.196}$	164	72.2
NE9445........	401	0	0.100	$T = 592\ V^{0.182}$	92	40.5
NE8640........	178	0	0.100	$T = 397\ V^{0.222}$	246	108.3
NE8640, sulphite-treated.......	174	0	0.100	$T = 388\ V^{0.222}$	273	120.2

Table 9 which is a summary of Figs. 6, 7, 9, and 10, shows the permissible cutting speeds for all conditions of these tests. For those tests at 0.100 in. depth of cut and constant tool shape, the relative machinability is listed, and it is based on the permissible cutting speed with the annealed NE9445 serving as the datum.

CONCLUSIONS

1 Within the range of this investigation the cutting temperature is a power function of the cutting speed in accord with the general equation $T = CV^n$.

2 At a feed of 0.01 in. per revolution and with other factors constant, the cutting temperature increases with increase in depth of cut up to 0.100-in. depth and is relatively unaffected as the depth is increased to 0.150 in.

3 A change in the back-rake angle from 0 deg to negative 2 deg 20 min increases the cutting temperature at any but low speed ranges, and increases the rate at which the temperature rises with increased cutting speed. It is expected that greater negative rake angles would cause further increase in the cutting temperature, as well as increase the slope of the cutting speed-cutting temperature curve.

4 An increase in the Brinell hardness results in higher cutting temperatures and the increment of cutting temperature becomes greater as the hardness is increased.

5 As the hardness of the steel is increased, the chip thickness decreases for constant cutting speed, feed, and depth of cut, thus concentrating the heat on a smaller area of the cutting tool and causing more rapid tool failure.

6 The sulphite-treated NE8640 may be machined at higher speeds than regular NE8640 for the same cutting temperature.

7 The relative machinability of steels may be rated by the cutting speed necessary to develop a permissible cutting temperature.

ACKNOWLEDGMENTS

The author herewith expresses his appreciation to the Carboloy Company, Inc., which supplied the cemented-carbide tools and calibration strips, and to the Wisconsin Steel Company which supplied the NE8640 steels used in these tests.

Acknowledgment is also made to Mr. T. S. Chang and Mr. W. H. Chen, graduate students at the University of Illinois, for their valuable help during the investigation.

BIBLIOGRAPHY

1 "The Measurement of Cutting Temperatures," by E. G. Herbert, Proceedings of The Institution of Mechanical Engineers, vol. 1 1926, pp. 289–329.

2 "Die Messung der Schneidentemperatur biem Abdrehen von Flueseisen," by K. Gottwein, *Maschinenbau*, vol. 4, 1925, pp. 1129 1135.

3 "Cutting Temperatures Developed by Single-Point Turning Tools," by O. W. Boston and W. W. Gilbert, Trans. ASM, vol. 23 1935, pp. 703–726.

4 "A Method for Measuring Tool Tip Temperature," by B. A Crowder, Engineering Experiment Station, Institute of Technology University of Minnesota, Technical Paper No. 55, June, 1946.

5 "Thermoelectric Thermometry," by W. F. Roeser, *Journal o Applied Physics*, vol. 11, June, 1940, pp. 388–407.

6 "Investigation of the Processes in the Wear of Cemented Carbide Tools," by Walter Dawihl, *Zeitschrift für Technische Physik*, vol 21, no. 12, pp. 337–345. Translation by Henry Brutcher, Altadena, Calif.

7 "Powder Metallurgy," edited by John Wulff, American Society for Metals, Cleveland, Ohio, 1942, p. 444.

8 "The Effect of Size and Shape of Cut Upon the Performance of Cutting Fuids When Turning SAE 3140 Steel," by O. W. Boston W. W. Gilbert, and L. V. Colwell, Trans. ASME, vol. 61, 1939, pp 315–322.

9 "Observations in the Making and Use of Sulphite-Treated Steels," by E. L. Ramsey and L. G. Graper, Trans. AIME, Iron and Steel Division, vol. 150, 1942, pp. 127–130.

The Role of Meehanite Metal Castings in Engineering Production

By C. R. AUSTIN,[1] NEW ROCHELLE, N. Y.

The application of iron castings in engineering producion covers an extremely wide field which was extended reatly during the war years. Steel foundries and forging hops were heavily loaded, and it became necessary for the lesign engineer to seek other facilities, and other engieering materials. In the process, the engineer soon earned that cast irons were available which would replace ven with advantage many of the engineering parts which ad formerly been specified in fabricated steel or other naterials. The engineering facts concerning hightrength cast irons, their production techniques, and xamples of important applications are treated in this aper.

ENGINEERING production is always concerned with design and with selection of materials most suitable for the service required. The problem of design must be based on known nd established physical and mechanical properties of the particlar material selected, and it is for this reason that, in the past, e design engineer has tended to look toward fabricated-steel arts rather than to cast iron for his base material. This was a ise decision despite the decidedly unfavorable immediate ecoomic aspect of the selection.

For fabricated parts the metal is first poured into ingot form nd then, by various procedures, such as cogging, rolling, and rop forging or pressing, made to acquire a shape approximating ore or less the form of the design part. This is followed by achining operations which permit removal of much material here property requirements make its presence unnecessary or en undesirable.

In cast-iron parts the problem is totally different. Whether it either ordinary founding in sand molds, or die casting as plied to nonferrous metals, it is possible to place the metal itially where it is desired. Variation in metal section and sting configuration is immediately possible, and by the use of nventional cores hollow sections constitute normal everyday undry performance.

Thus the foundry has available techniques which will furnish e engineer the form of an engineering part directly in accordance th his proposed design. Until recent years, however, this fact ne did not answer completely the first part of his requirement, mely, a prescribed shape, since the requirement also implied me uniformity of metal density and property irrespective of riation in casting dimensions and casting form.

Modern research on this problem applied to high-strength irons s afforded a solution which will be discussed in the present paper. Once casting solidity and uniformity of properties over widely fering sections have been established, engineering production still concerned with the basic engineering properties of the tal and with the assurance that these properties can be mained in normal engineering production of castings.

Therefore it will be a further purpose of this paper to submit data on various engineering properties of the irons and to illustrate the utilization of such irons in many service applications.

Since the author of this paper is naturally familiar with engineering applications of Meehanite iron castings and since a large amount of engineering data and casting records are now available, the illustrations for the production engineer must be drawn largely from modern developments and applications of Meehanite iron castings.

It has already been pointed out that what may be termed "engineered castings" depend for their successful service application, not on any one fact alone. For production engineering it is important to consider many aspects of the subject. Among these the following are of major importance:

1 The selection of the proper iron in relation to casting section and to mechanical properties demanded.

2 The basic engineering properties of the irons in relation to service demanded.

3 The manner in which these specific properties can be utilized in designed castings.

These sections will be discussed in the order listed.

Selection of Iron in Relation to Casting Sections

At first sight this problem might be considered of little importance to the production engineer but since he usually has the very important duty of specifying the metal to be employed in his product it behooves him to give some attention to this matter.

In nonferrous metals he is concerned merely with the chemistry of the alloy and, consequently, specifies an alloy of given analysis with known and readily defined properties having little relation to casting section.

With cast irons the problem is a profoundly different one since the following two important factors must consistently be borne in mind:

1 The structure and properties of iron depend on the rate of cooling during solidification and hence on the section of the casting and its location in the sand mold into which the metal is to be poured.

2 The outer peripheral parts of heavier iron castings are ordinarily more dense than the inner parts where solidification takes place more slowly. Indeed, it is common experience to find the interior of heavy gray-iron castings exhibiting a porous open structure and having such low density compared to the exterior parts that there is a very great decrease in hardness and tensile strength of the iron.

These facts have been thoroughly recognized and brief reference to Meehanite practice, whereby control of both these variables can be effected, is needed in order that the engineer may have some notion of its importance in specifications.

Structure in Relation to Casting Dimensions. Two totally different cast irons, gray and white, are easily recognized by the engineer. The properties of the former are indicated by low hardness and easy machinability, and the structure consists of flake graphite distributed in a matrix of pearlite and free ferrite. The properties of the latter are indicated by high hardness, brittle-

---

[1] Meehanite Metal Corporation.

ontributed by the Metals Engineering Division and presented at Fall Meeting, Boston, Mass., Sept. 30–Oct. 2, 1946, of The ERICAN Society of Mechanical Engineers.

OTE: Statements and opinions advanced in papers are to be erstood as individual expressions of their authors and not those he Society.

ness, and nonmachinability, and the structure consists of massive free carbides or cementite and pearlite.

Fortunately for the user of gray-iron castings, some control of the "grayness" and hence the properties of the iron are available by what may be termed balancing the analysis of the irons. Thus in thin sections, which are prone to yield brittle white irons by virtue of rapid cooling, an increase in silicon content is made to assure a gray fracture despite high cooling rate. This procedure, however, has a deleterious reaction on the structure of heavy sections which solidify with a coarse open or porous structure.

It is control of the nature of the matrix along with solidity penetration which is so vital to the engineer demanding both constancy of properties and essential uniformity of properties independent of section. The lack of foundry control has clearly been the cause of the vagaries in the properties of cast iron which resulted in the design engineer looking elsewhere for his materials of construction.

As a result of much carefully planned and extensive development research, it is possible to control the structure of irons independent of casting dimensions, without profoundly changing the silicon content. One method of control is effective because of what has been termed a two-step process:[2]

Step (1) consists in computing and suitably preparing a charge of iron and steel which can be melted to a liquid constitution[3] having direct relation in terms of carbide balance to the amoun of primary carbide formed in the solidified casting.

Step (2) is concerned with the controlled decomposition of the primary cementite so as to insure a metal matrix consisting wholly of pearlite with absence of free cementite or free ferrite. Furthermore, control in size and distribution of the graphite is effecte so that in the higher engineering type of irons the cast structure may be likened to that of a normalized tool steel in which is uniformly distributed fine and short flake graphite.

Fig. 1 shows a typical structure of such an iron having optimum mechanical property characteristics.

Solidity Penetration. Having established the means of controlling structure and hence of controlling mechanical characteristics, it became necessary to control structure in terms of castings dimensions. By this practice it was discovered that there is a direct relation between the "constitution" of the iron and the thickness of the section of the casting to be made, and that it was possible to establish a ratio between what have been termed the constitutional and process wedge values in each casting which will insure uniformly dense sections and predetermined engineering properties.

This is of vital significance to engineering production, and i must be recognized if the engineer is to be able to make best use of the materials now at his disposal. A few examples should ai in stressing its importance.

By correlating the constitution of the iron with the section to be cast, essentially uniform hardness may be assured from cente to surface. This fact is demonstrated by factual data, submitted in Fig. 2, which were taken on a 45,000-psi tensile iron, cast in the form of a 12-in. square block, sectioned transversely through th center. The engineer is generally familiar with the open an relatively porous character of the structure obtained toward th

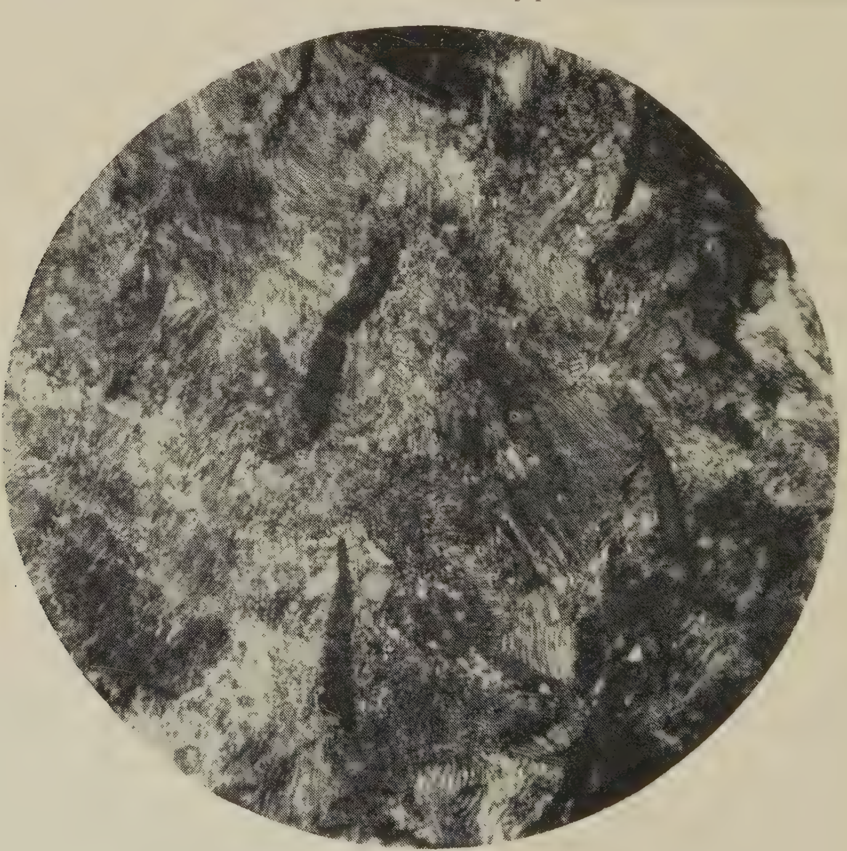

Fig. 1 Typical Microstructure of Meehanite Iron

---

[2] Letters Patent 2,371,654.

[3] The term "constitution" must not be confused with composition or chemical analysis. Constitution connotes the behavior of the iron in changing from the liquid to the solid state, in terms of the nature and distribution of the structural components and their effect on the physical and mechanical properties of the iron. Its measure affords an accurate method of control of casting production as outlined in Patent No. 2,371,654.

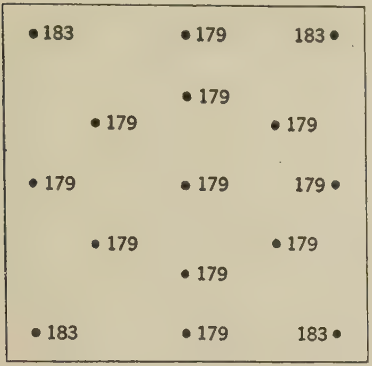

FIG. 2 HARDNESS DETERMINATION ON A 12-IN. BLOCK OF A 45,000-PSI IRON

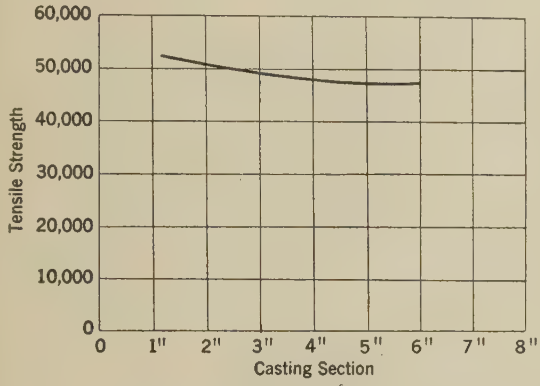

FIG. 3 TENSILE STRENGTH VERSUS CASTING SECTION OF 50,000-PSI IRON

center of such a cast block when proper control of the iron is not assured.

An examination of the tensile strength in relation to casting section also serves well to demonstrate the importance of mass influence. In an uncontrolled iron cast in sections varying from 1 in. to several inches, a tensile-casting section relation may exhibit a marked drop in tensile strength as the section of casting is progressively increased. By controlling the foundry practice as already outlined the relation becomes similar to that portrayed in Fig. 3.

In order to insure these property controls, foundry technique and control of the highest order are absolutely necessary, and it is clearly the duty of the casting producer constantly to exercise control of the product and to advise the type of metal most suited for any engineering production job. Nevertheless, there can be intelligent co-operation between the foundry and production engineer only if the latter has some knowledge and appreciation of the problems of the former, and of the fact that there are now available for his use "tailor-made" iron castings produced to do a specific engineering job.

The need for this co-operation has long been recognized in the fabricated-steel industry, but it is only recently that the production engineer or metallurgist and the utilization or design engineer have really begun to work together. That the control methods outlined are essential to the production of "engineered castings" is further exemplified when it is remembered that the constitution of the iron must be controlled in relation to casting section, the heavier the section the higher the constitution.

If too-high a constitution iron be poured in a section, the point of maximum solidity penetration is passed and the more rapidly cooled portions of the casting solidify with a white hard structure.

The production engineer recognizes this condition immediately, but he terms it hard or nonmachinable castings. By suitable adjustment of the constitution of the iron, a free-machining casting with maximum solidity penetration and uniform property characteristics results.

In this patented process the matter has been largely simplified for the production engineer by designation of engineering types with tensile properties ranging from 50,000 to 30,000 psi.

Specification is certainly one of the most important duties of the design or production engineer, and the relation of Brinell hardness and tensile strength to section thickness of the various types of engineering irons is shown in Figs. 4 and 5. This provides us with a most important lesson in specifications.

Types GD and GE[4] may be poured in thin sections $^3/_8$ in. or less and still retain their grayness or free-machining qualities, along with excellent tensile properties. If GA is poured in a casting less than $^1/_2$ in. section, its strength properties tend to fall, and machining problems may result.

An engineer may have a particularly important casting in which he desires high tensile strength and consequently specifies GA Meehanite or a 50,000-psi iron. This specification is correctly made if the casting sections are relatively heavy. However, assume a section of $^3/_8$ in., if type GA be employed a loss of tensile may result and machining problems are sure to arise. If, however, GC is specified, good tensile strength, Fig. 5, high hardness, Fig. 4, and free machinability result.

Fortunately, the modern foundry is equipped to advise on these matters, and it is necessary only for the production engi-

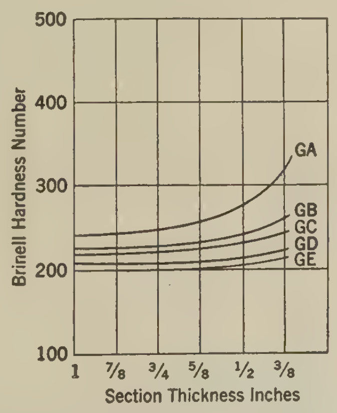

FIG. 4 GRAPH SHOWING INCREASING HARDNESS OF METAL WITH DECREASING SECTION THICKNESS

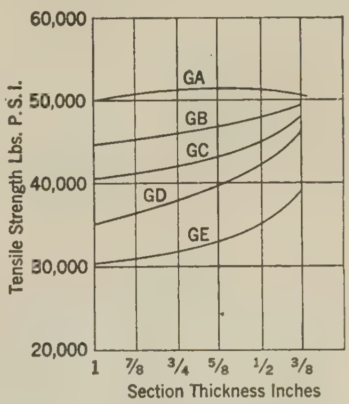

FIG. 5 GRAPH SHOWING CHANGE IN TENSILE STRENGTH WITH DECREASING SECTION THICKNESS

neer to be aware of the newer products at his command, and the need and reason for consultation with the foundry metallurgist or engineer.

---

[4] The chemical compositions may be varied, according to desired constitution and casting dimensions.

Basic Engineering Properties

Until more recent years cast iron was not considered a true engineering material which could be utilized on a design basis, and certainly little thought was given to its application in members for service at elevated temperatures, where loads of given magnitude must be maintained with plastic flow controlled within predetermined limits.

In this section of the paper attention will be directed to the properties of engineering irons of importance to the design engineer at normal temperature operation, as well as for service at elevated temperatures.

Properties at Normal Temperatures. Probably the characteristic of a metal of most service to the engineer is the tensile stress-strain curve, and it is beginning to be recognized that a simple statement of tensile strength, along with ductility, by no means provides a complete picture of serviceability. A comparison of the stress-strain diagrams of ductile steel and a 50,000-psi iron demonstrates this point.

In Fig. 6 are reproduced the stress-strain diagrams for these two engineering materials. The diagrams reveal three distinct areas, as follows:

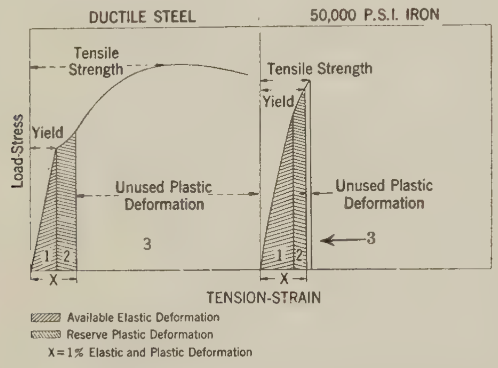
DUCTILE STEEL
50,000 P.S.I. IRON
Tensile Strength
Tensile Strength
Yield
Yield
Load-Stress
Unused Plastic Deformation
Unused Plastic Deformation
1
2
3
1
2
3
X
X
TENSION-STRAIN
▨ Available Elastic Deformation
▤ Reserve Plastic Deformation
X = 1% Elastic and Plastic Deformation

Fig. 6 Two Types of Stress-Strain Diagrams

1 Stress absorbed during elastic deformation. This has relation to the modulus and yield strength.

2 Stress absorbed during elastic and plastic deformation which has some relation to the reserve of plasticity available, against sudden fracture.

3 Plastic changes recording deformation during failure.

Areas 1 and 2 illustrate in a general way the relative capacity of both materials to absorb working stresses in service up to approximately 1 per cent plastic deformation, which is about all that much engineering construction can endure.

Accordingly, the relative tensile strength or ultimate breaking load of the steel and the iron provides little information on the useful properties of the material which can be used in unit design.

A typical stress-strain curve of a 50,000-psi iron is shown in Fig. 7.

Thus the old concept that cast iron should be regarded as "brittle" material without any true elastic properties no longe holds with the modern irons which can be made so that thei dependability and properties are accurately known and are reliable.

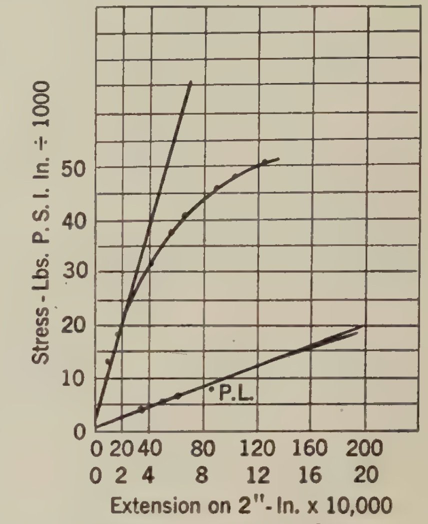

Chemical Analysis, Per Cent

TC	2.90
Mn	0.76
Si	1.66
P	0.13
S	0.107

Physical Properties

Y.P. 0.2 per cent plastic strain
P.L. = 14,000 psi
Y.P. = 46,000 psi
T.S. = 51,000 psi
Ext. = 0.5 per cent on 2 psi
Mod = 18.9×10^6
Bhn = 241

Fig. 7 Stress-Strain Curve of a 50,000-Psi Iron

In Table 1 are given the general engineering specifications f the various types of engineering irons. These values represen the normal minimum assured physical properties.

Attention has also been directed to the importance of mai tenance of tensile strength independent of casting section. Da on this point are given in Tables 2 and 3.

An important property of a metal is its toughness. Considera ble thought and experimental analysis have been given to th property, and no test is yet available which provides a satisfa tory measure of toughness. In fabricated steels an Izod o Charpy value on a 10-mm-square test bar has usually suffice whereas for tool steels such tests are meaningless and resort ha been made to torsion impact.

In the study of irons, a modified Izod impact made on an unnotched test piece, machined to 0.798 in. diam seems to hav found rather general favor. In Table 4 are given data obtaine in an extensive investigation on the general engineering types o iron.

The fatigue strength of a metal is also a very important cha acteristic of metal parts, and data are available for the variou irons discussed in this paper. Using the standard R. R. Moo

TABLE 1 GENERAL SPECIFICATIONS FOR VARIOUS ENGINEERING IRONS

Two-step process iron	Tensile, psi	Transverse		Bhn (min)	Compression strength, psi	Modulus elasticity	Fatigue[a] strength	Specific gravity
		1.2-in. bar, 18 in. center	Deflection, in.					
GA	50000	3100–3600	0.28–0.34	207	175000	21000000	22000	7.31
GB	45000	3000–3400	0.28–0.34	196	160000	19000000	19000	7.28
GC	40000	2900–3300	0.26–0.34	192	150000	17500000	17500	7.25
GD	35000	2600–3000	0.22–0.34	183	130000	15000000	15000	7.22
GE	30000	2000–2600	0.20–0.34	174	120000	12000000	13700	7.16

[a] Reversed bend.

TABLE 2 TENSILE STRENGTH IN RELATION TO SECTION THICKNESS OF 50,000-PSI IRON, ADJUSTED FOR SECTIONAL THICKNESS

Section of casting tested, in.	Tensile strength, psi
0.75	...
1.25	53500
2.00	54000
3.00	53000
4.00	50800
6.00	47500

TABLE 3 TENSILE STRENGTH IN RELATION TO THICKNESS OF BAR AND CASTING; 55,000-PSI TWO-STEP PROCESS IRON[a]

Casting	Thickness, in.	Tensile, psi; 1.2-in-diam bar	Tensile, psi; casting	Per cent of 1.2-in-diam bar
Cylinder liner	2¾	72010	66730	92.7
Cylinder liner	3½	71970	61630	85.6
Crankshafts	1⅜	60480	50400	83.5
Gears	2¾	64960	49280	76.0

[a] Figures are averages of a large number of examples.

TABLE 4 MODIFIED IZOD IMPACT-TEST RESULTS FROM ROUTINE TESTING OF 0.798-IN. UNNOTCHED TEST BARS

Two-step process iron	Impact, ft-lb to fracture
GA	25–35
GB	15–23
GC	12–20
GD	8–15
GE	6–12

type of fatigue-testing specimen and machine, values ranging from 22,000 psi for the 50,000-psi type down to 13700 psi for the 30,000-psi irons have been established.

Many other properties such as damping capacity and machinability rating are also of vital concern to the engineer but space precludes further discussion.

Properties at Elevated Temperatures. As the operating temperature of unit parts in engineering applications is progressively increased, the significance of normal temperature basic engineering tests becomes decreasingly important. It is for this reason that creep studies have been developed so extensively in recent years, n order that the design engineer might have specific knowledge of the behavior of materials at various temperature levels when subjected to defined stress conditions.

A vast amount of data have thus been accumulated on the behavior of fabricated steels and special alloys, but little information is available on the creep properties of cast irons.

During the past several years many creep tests have been conducted on engineering and heat-resisting irons, which are of direct interest and aid to the design engineer.

In this section of the paper a brief review of the subject will be given.

It must first be pointed out, however, that the creep rates of value to the engineer may vary widely, depending on the high-temperature service demanded. Two extreme cases may be ited. In steam-turbine design, one authority has quoted the gure 0.01 per cent elongation per year as being a satisfactory reep rate for high-temperature turbine parts. This is equivalent o 0.00000001 in. per in. per hr plastic flow. In the case of metals sed for cracking units in the petroleum-refining industries, the mount of visually observed bulging of the tubes, indicating several per cent elongation, has been utilized to designate the nd of the safe life period of serviceability.

Thus the desired sensitivity of creep tests or the order of mag-itude of the creep data, particularly with respect to irons, de-ends wholly on service applications. Up to temperatures of 700 · 800 F, serviceability frequently depends on the essential main-nance of dimensional stability, where data on load-strain rela-onships involving very low strain rates, are essential. At mperatures of 1000 to 1200 F and above, much greater strain tes can usually be tolerated, and often the information most needed includes the stress-temperature characteristics for some given life period within which freedom from failure by fracture is assured.

An initial general view of the effect of temperature on the ultimate and on the elastic modulus of a 50,000-psi iron is summarized in Table 5. Up to temperatures as high as 700 F, the tensile strength shows some increase, after which it shows a progressive drop as the temperature increases. There is a slight decrease in the modulus up to about 600 F, beyond which temperature the elastic modulus begins to drop rapidly.

It is well recognized, however, that the creep characteristics of metals are a more reliable index of their high-temperature strength, and such data furnish the engineer with information required for design purposes.

TABLE 5 EFFECT OF TEMPERATURES UP TO 1095 F ON THE ULTIMATE AND ELASTIC MODULUS OF A 50,000-PSI IRON

Temperature		Ultimate strength, psi	Modulus of elasticity, psi
deg C	deg F		
15	60	54000	19,200,000
230	445	57000	18,300,000
250	480	57000	....
300	570	59000	17,800,000
350	660	57200	....
400	750	46200	14,400,000
490	915	27900	10,600,000
590	1095	21100	....

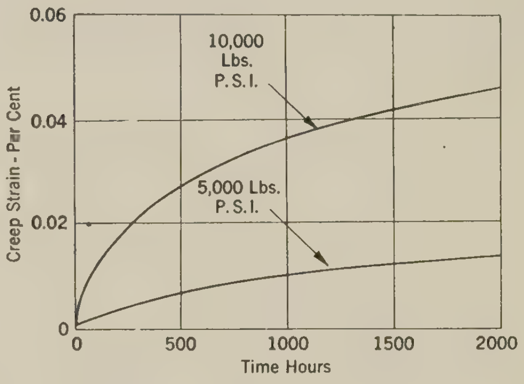

FIG. 8 CREEP TESTS AT 750 F ON 50,000-PSI IRON, GA TYPE

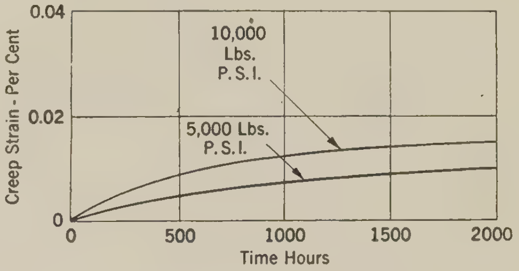

FIG. 9 CREEP TESTS AT 750 F ON 55,000-PSI IRON, GM TYPE

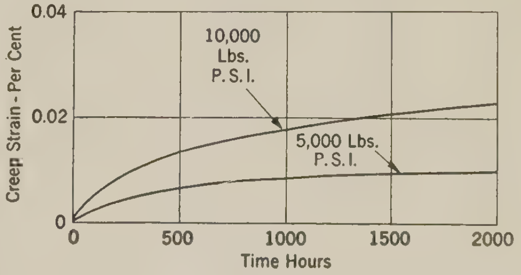

FIG. 10 CREEP TESTS AT 750 F ON HEAT-RESISTING SC-2 IRON

Creep Properties up to 850 F. The results of creep tests on GA, GM, and SC-2[5] iron at 750 F, have been reproduced in Figs. 8, 9, and 10, respectively. These castings were tested on a gage diameter of 0.358 in. over a gage length of 2 in., using stresses of 5000 and 10,000 psi.

TABLE 6 CREEP-RATE DATA ON ENGINEERING IRONS

Type	Stress, psi	Creep rate at 2000 hr in./in./hr	Creep rate at 2000 hr Per cent/-10000 hr	Strain or total elongation at 2000 hr, per cent
50000 psi	5000	3.0×100^{-8}	0.03	0.015
55000 psi	10000	7.5×10^{-8}	0.075	0.045
55000 psi	5000	1.5×10^{-8}	0.015	0.01
	10000	2.5×10^{-8}	0.023	0.015
Heat-resisting	5000	1.7×10^{-8}	0.017	0.01
	10000	5.0×10^{-8}	0.050	0.022

The data obtained from these curves have been included in Table 6, where it will be noted that the creep rates have been reported in the two forms most commonly used, namely, creep rate in inches per inch per hour and in per cent per 10,000 hr.

The results have established that any of these engineering materials can be utilized in applications where only extremely small creep rates can be tolerated. The creep rates are of the same general order of magnitude as those established for wrought carbon steels under similar temperature-strain conditions. They are also of the order of magnitude of interest to turbine engineers who demand a creep rate for certain operating parts not exceeding 0.01 per cent elongation per year or 1×10^{-8} in. per in. per hr.

These data should serve to emphasize the urgent need for review of such tentative specifications as ASTM A 278-44T, limiting iron castings for pressure-containing parts to temperatures up to a maximum of 650 F.

Some tests at 850 F on HB heat-resisting iron are also instructive and demonstrate the load-carrying capacity of these irons where creep rates of 0.05 to 0.1 per cent per 1000 hr are satisfactory for service applications. The curves for loads ranging from 7500 to 12,500 psi are given in Fig. 11.

Some very useful data on heat-resisting SC-type irons are included in Fig. 12. The tests were run at 730 F, under a 10,000-psi tensile load. The creep rates range from 0.023 up to 0.043 per cent per 1000 hr or a maximum of 4.3×10^{-7} in. per in. per hr. The duplicate tests show satisfactory agreement.

No microstructural changes could be observed in any of the tests reported within the stated temperature range.

Creep Properties Above 850 F. When tests are conducted on any metallic materials at temperatures where the microstructural constituents and their distribution are unstable, the measured elongation consists of the algebraic sum of two components. Elongation or contraction arising from structural change, and elongation (true creep) depend on plastic flow of the metal under stress. This idea is demonstrated by the curves in Fig. 13 drawn from tests conducted on a two-step process iron. Trace A represents the observed and recorded elongation-time relation for a test conducted at 1200 F under 2000-psi tensile load. Trace B represents a similar relationship with the stress reduced to a nominal 100 psi. The first curves show the elongation summation resulting from structural changes and from creep whereas the latter exhibits the elongation-time reaction from structural changes alone. By difference the true creep curve C was obtained.

Industrially we are usually interested in total dimensional changes as shown in curve A. However, it is common practice to "stabilize" fabricated steels by heating to a temperature slightly above service temperature prior to placing the part in actual service.

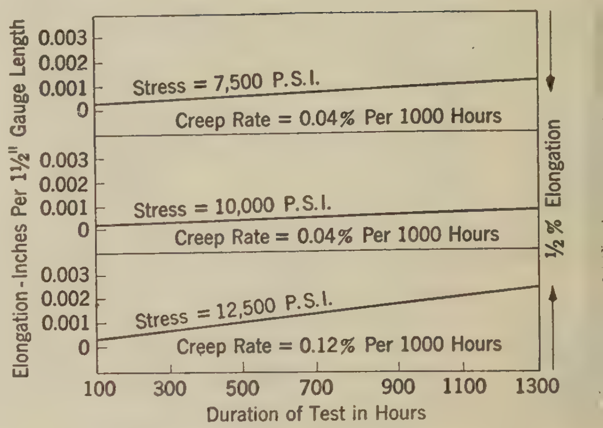

FIG. 11 HIGH-TEMPERATURE CREEP TESTS ON TYPE HB HEAT-RESISTING IRONS AT 850 F

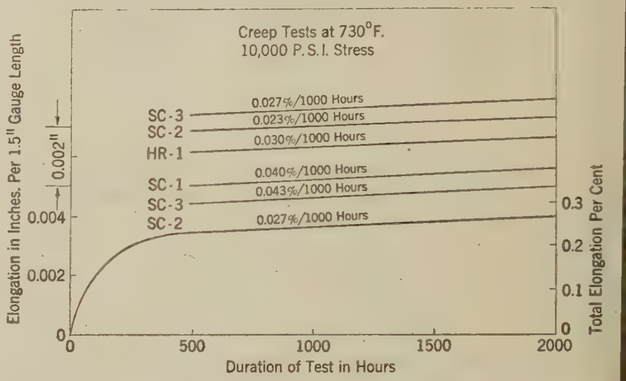

FIG. 12 CREEP TESTS ON HEAT-RESISTING SC-TYPE IRONS

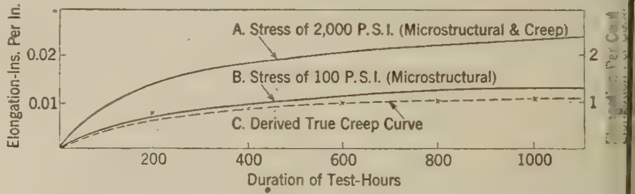

FIG. 13 ELONGATION-TRUE CURVES OF AN ENGINEERING-TYPE I TESTED AT 1200 F

In applications where amounts of deformation below 5 p cent introduce no difficulties, it is of interest to note the effect increasing the stress on cast test bars of an iron similar to tha considered in Fig. 13.

The behavior of the castings is shown in Fig. 14 which i cludes the creep-rate per cent measured at the end of test und the three stresses 2000, 3000, and 4000 psi, respectively.

In order to ascertain the strength properties of SC-typ irons at 1400 F, a few creep tests were run using loads of 1000 an 1500 psi. It was anticipated that the castings would fracture in relatively short time at the higher stress, but it was informati to have an index of ductility at this red-heat temperature.

The form of the creep curves is shown in Fig. 15 where it ma be noted that elongation at fracture resulting from a stress 1500 psi ranges from $1^1/_2$ to $3^1/_2$ per cent. Under a stre of 1000 psi at 1400 F, where the test bars resisted failure, SC showed a total elongation of approximately 0.7 per cent, an SC-5 a total elongation of a little more than 1 per cent.

Practical application of these data on a basis that a maximu elongation of 1 or 2 per cent per 1000 hr would serve as a sat

---

[5] Meehanite designation for heat-resisting irons—higher-silicon iron.

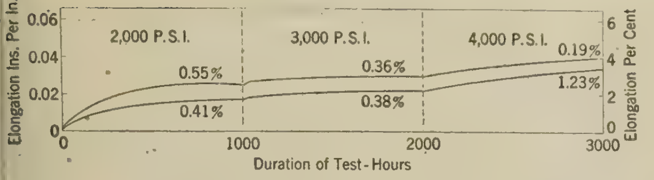

IG. 14 CREEP CURVES OF TWO SIMILAR ENGINEERING IRONS ESTED AT 1200 F UNDER STRESSES INCREASED FROM 2000 TO 4000 PSI

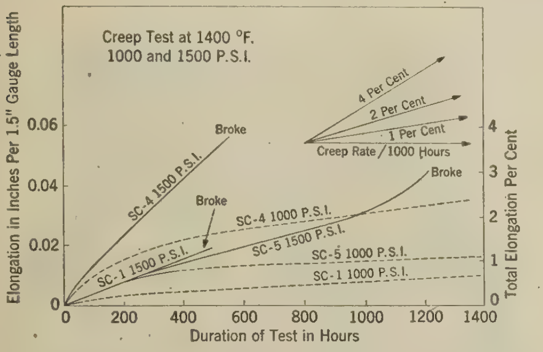

FIG. 15 CREEP CURVES FOR SC-TYPE HEAT-RESISTING IRONS

actory criterion, indicates that these irons might be stressed afely at loads up to 1000 psi at a temperature of 1400 F.

IRON CASTINGS IN ENGINEERING PRODUCTION

The applications of iron castings in engineering production over an extremely wide field which was extended tremendously uring the war years for at least two particular reasons, as follows:

1 On account of the burden imposed on already heavily aded steel foundries and forging shops, it became necessary for he design engineer to look for and turn to other facilities and other ngineering materials.

2 The engineer soon learned that cast irons were fortunately vailable which would replace even with advantage many of the ngineering parts which he had become accustomed to specifying n fabricated steel or other material.

Thus replacement was made in a wide variety of applications here such properties were demanded as pressure-resistant parts or steam, gas, oil, and water; sliding surfaces subject to friction here minimum galling tendency was necessary; effective dampng and high fatigue strength in systems subject to vibration, uch as crankshaft applications and cutter bodies; heat-treated arts where high hardness or wear resistance was essential; and any applications where varied property characteristics must be aintained at elevated temperatures.

Engineering applications of the various types of general engieering, heat-resisting, wear-resisting, and corrosion-resisting irons ere already extensive before the outbreak of war, and few fields f engineering remained in which the engineer, although rightly onservative, had not already benefited by adopting these castngs.

Despite the economies of the substitution of cast parts for abricated parts nothing is gained unless the new material proides the essential properties at least comparable to those obained in the material to be replaced. In many instances, howver, a much greater service life was obtained, and examples of the mportant role of these materials in engineering production will e illustrated and described in this last section of the paper.

These examples must necessarily be fragmentary because of pace limitation, but they should be of real service to the engineer n directing his attention to further developments where economy of initial cost and increased service life may be readily attained.

In the field of ordnance castings, Fig. 16 shows a howitzer wheel originally specified as steel but finally adopted in 50,000-psi iron after abnormal load tests. Many other examples could be cited but we are now more interested in directing attention to more normal engineering practice.

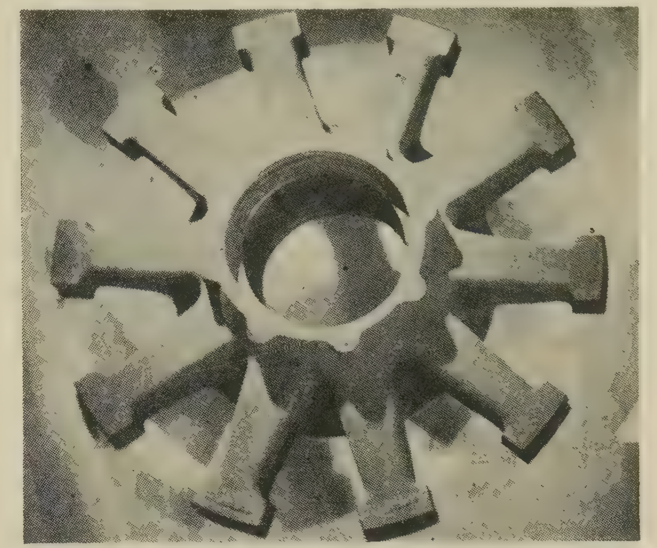

FIG. 16 HOWITZER WHEEL, ORIGINALLY MADE AS A STEEL CASTING, BUT AFTER BEING THOROUGHLY TESTED OUT WITH ABNORMAL LOADS, 50,000-PSI IRON WAS ADOPTED AS STANDARD

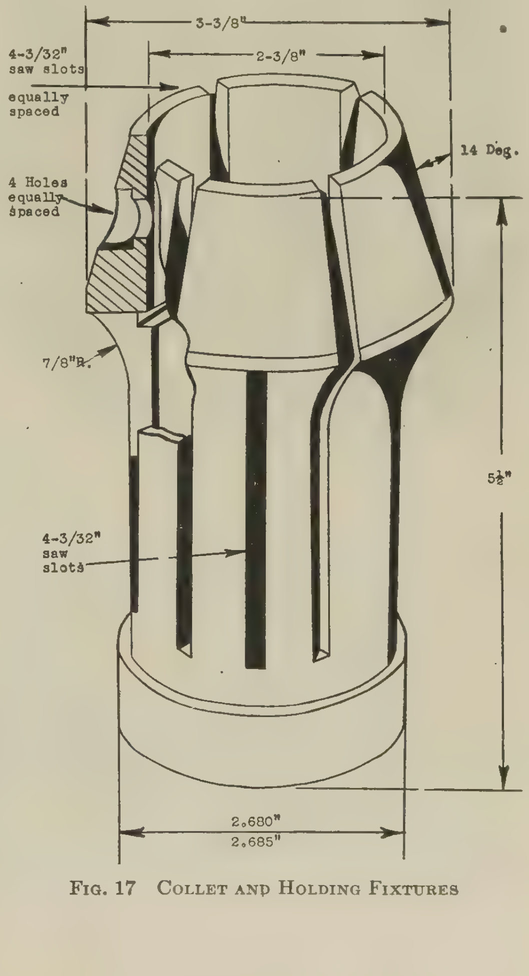

FIG. 17 COLLET AND HOLDING FIXTURES

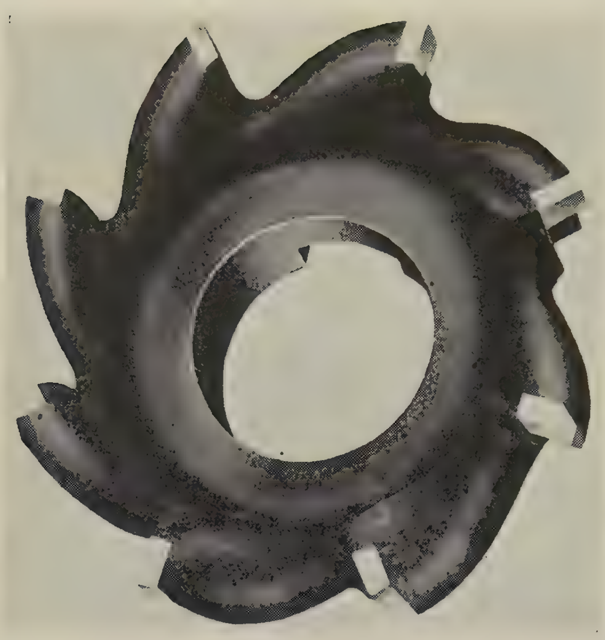

Fig. 18 Milling-Cutter Body

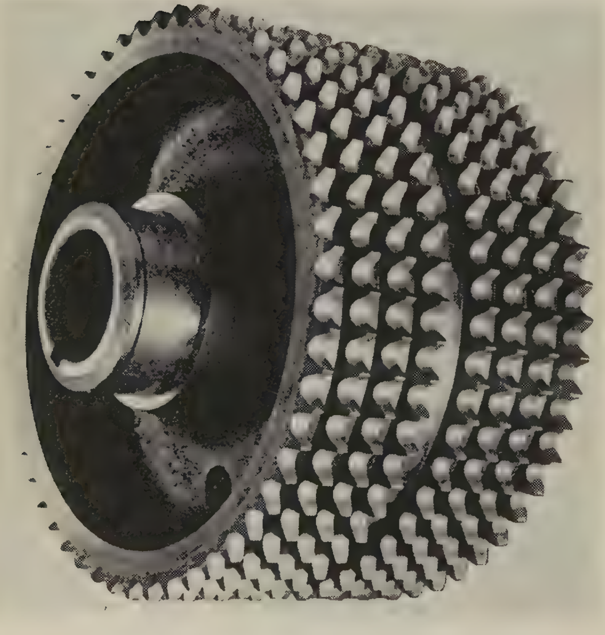

Fig. 19 Main Sprocket for Twin-Engine Ship-Propulsion Assembly

In machine and machine-tool applications, the wide adoption of iron castings has been the inevitable result of increased experience and better recognition of their engineering properties and reliability, as demonstrated in the field of serviceability.

In the collet and holding fixture, illustrated in Fig. 17, the elastic properties of these irons are utilized. In order to achieve the necessary spring temper, the collet was heat-treated after machining. It replaced a part previously machined from a solid bar of SAE 1045 steel. The casting weighs only 4 lb. with a $^1/_{16}$-in. machining allowance.

The use of this iron in tool shanks and milling-cutter bodies, Fig. 18, provides examples of superior performance because of increased vibration absorption combined with strength, rigidity, and better heat conductivity. Cast closely to shape, the shan and cutter bodies reduce machining operations and provi greater flexibility as to design.

An example of the main sprocket used in a propulsion assemb which was specified in a two-step process iron, is illustrated Fig. 19. The importance of these sprockets from the standpoi of performance, resistance to wear, strength, and toughness obvious in units of this type. All sprockets have cut teeth a the machining of a part of this type provides tangible evidence casting uniformity, solidity, freedom from defects, and good m chinability.

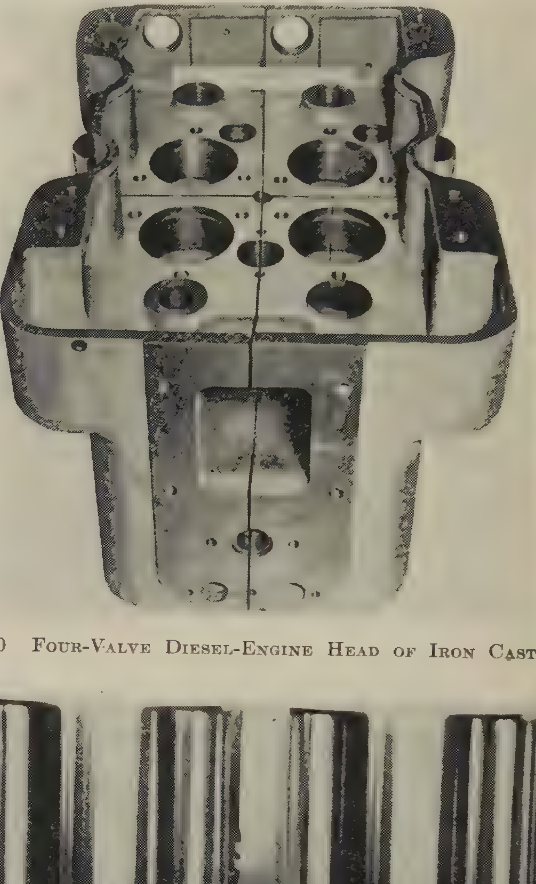

Fig. 20 Four-Valve Diesel-Engine Head of Iron Castin

Fig. 21 Cast Engine Liners for Diesel-Electric Locomotiv

An interesting example, where density and solidity are paramount, is illustrated in Fig. 20, which shows a large 4-valve Diesel-engine head made of iron castings. This casting contains sections ranging from $^1/_4$ in. in the frame head passages and cylinder walls to 2-in. on the firing face of the cylinder head. All passageways have to be watertight with close tolerances maintained.

Many examples may be cited in the field of engine design and pressure vessels but a few illustrations must suffice.

Fig. 21 depicts cast liners used in 1000-hp Diesel-electric locomotives where long wear and smooth operation are essential.

In the compressor shown in Fig. 22 castings were used for (1) casings; (2) rotors (silver-soldered to rotor shaft); (3) thrust-bearing housings. The rotors revolve at a top speed of 18,000 rpm, and extremely close tolerances, structural stability, and dimensional accuracy must be maintained. In operation, air enters the bottom of the casing at the right and bites of air are trapped by the pairs of helical lobes. Male and female lobes intermesh and compress the air until the discharge part is uncovered and air is squeezed out as a steady flow under compression.

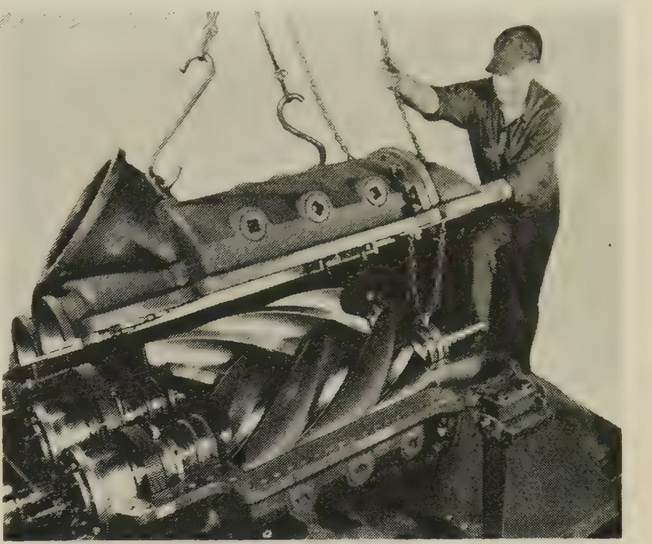

FIG. 22 COMPRESSOR CASINGS, ROTORS, THRUST-BEARING HOUSINGS OF TWO-STEP PROCESS CASTINGS

In the custom-built press for large tube-upsetting reproduced in Fig. 23 the following iron castings were used:

Part	Finished weight, lb
Horizontal ram	11500
Pistons	55 (each)
Pull-back covers	35 (each)
Vertical ram	7400
Rollers	115 (each)
Rails	270 (each)
Stripper ram	725 (each)

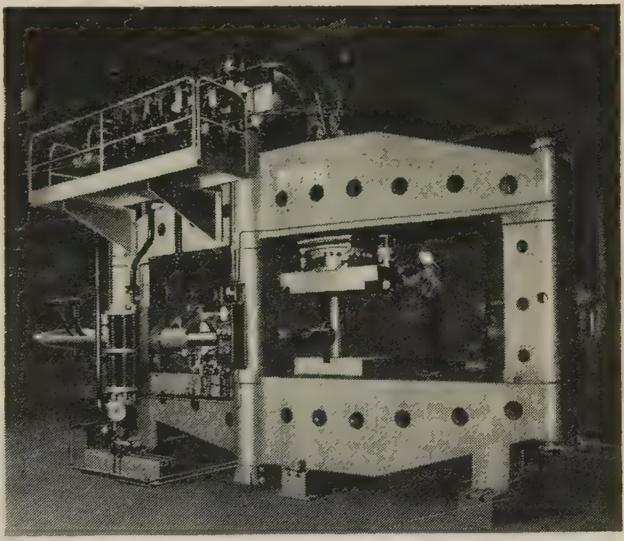

FIG. 23 CUSTOM-BUILT PRESS FOR TUBE UPSETTING

The new slide-valve design shown in Fig. 24 provides improved performance and reduction in production costs. The dense uniform structure of the iron containing finely dispersed graphite particles provides a self-lubricating bearing surface for a carburized and hardened-steel slide. Three rubber O-rings are used to fit the spacer in the aluminum housing, permitting the use of aluminum, steel, and iron in close conjunction, despite different coefficients of expansion. The unit has made it possible to hold the pressure drop to about one point at 3 gpm flow. The hydraulic valve was designed for use in fighter aircraft in connection with control of the autopilot.

An example of particular interest to the design engineer is the welded-steel and cast-iron Diesel block and base assembly reproduced in Fig. 25, where comparisons were possible for the economies involved. The finished weight of the cast unit was 10,620 lb, as compared with 11,442 lb for the welded unit. On the

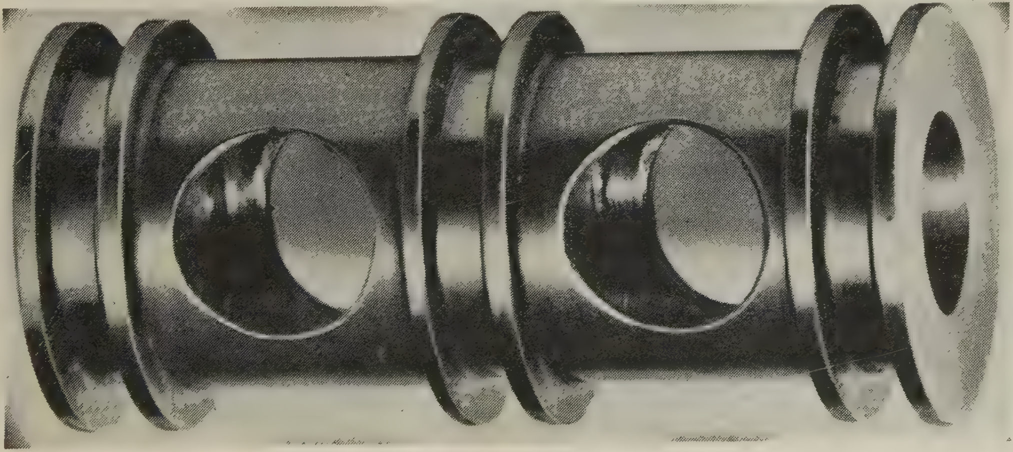

FIG. 24 SLIDE-VALVE DESIGN

basis of finished costs of the two-step process casting being 100, the finished welded assembly was 388.

Some factual data on this problem taken from an analysis on production engineering of these units follow:

	Cast	Welded
(*a*) Block and assembly base of 1000-hp Diesel engine:		
Finished weight, lb	10620	11442
Production rate per month	4	20
Finished cost	$1774	$6875
(*b*) Auxiliary drive housing for engine:		
Finished weight, lb	738	361
Production rate per month	4	20
Finished cost	$200	$385
(*c*) Diesel-exhaust manifold:		
Finished weight, lb	442	222
Production rate per month	4	10
Finished cost	$180	$345

It must not be inferred from these figures that the design en gineer should automatically turn from weldments to casting Very careful cost analysis of the problem together with con sultation with the foundry engineer should always be mad The figures submitted, however, indicate what can be e fected by application of correct design principles to a specif job.

Two examples of cast pressure vessels are shown in Figs. 2 27, and 28. It took 10,000-lb pressure to burst the compres unit in Fig. 26, whose normal working pressure is 1500 p Thus this body normally provides a factor of safety of over 60 per cent.

The hydraulic pump head, Fig. 27, is drilled with 16 holes b fore it is submitted to a routine test of 12,000 psi. Fig. 28 illu trates the pump head under test to a maximum pressure of 30,0 psi.

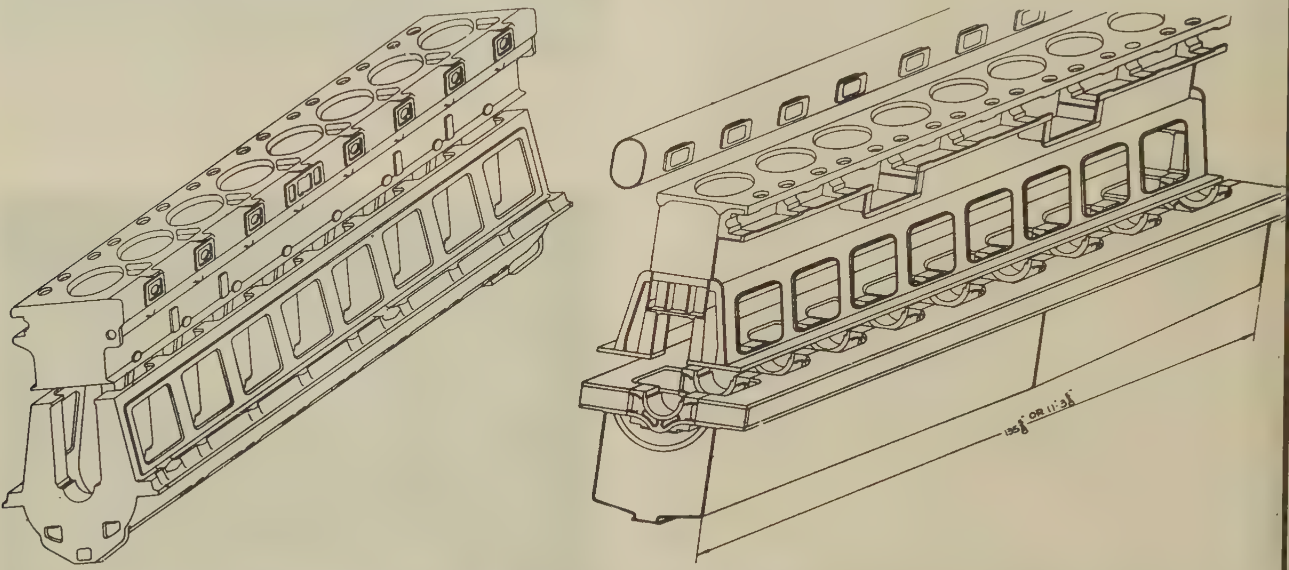

Fig. 25 Comparison of Welded-Steel and Cast-Iron Diesel Block and Base Assemblies

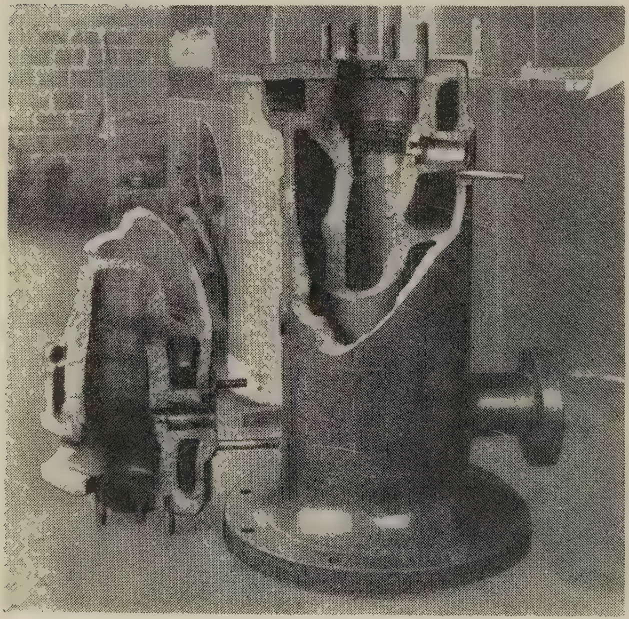

Fig. 26 Compression Unit Which Burst at 10,000 Lb Pressure

For many years these types of irons have served as a success die material for four basic reasons:

1 Cast dies may be produced closely to dimensions, redu required machining and expensive built-up constructions.

2 The graphite content of these iron dies provides self-lu cation in service, thus increasing die life.

3 Easy machinability with high strength properties.

4 Adaptability to heat-treatment and flame-hardening.

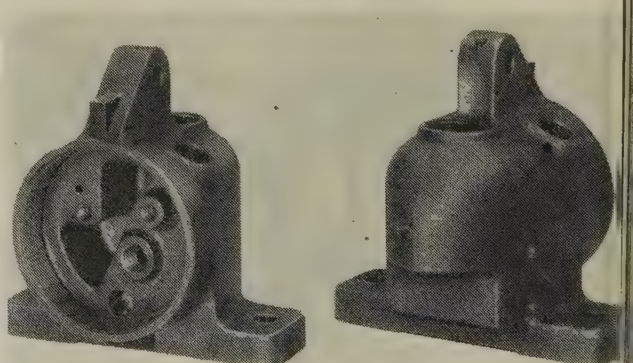

Fig. 27 Hydraulic-Pump Head

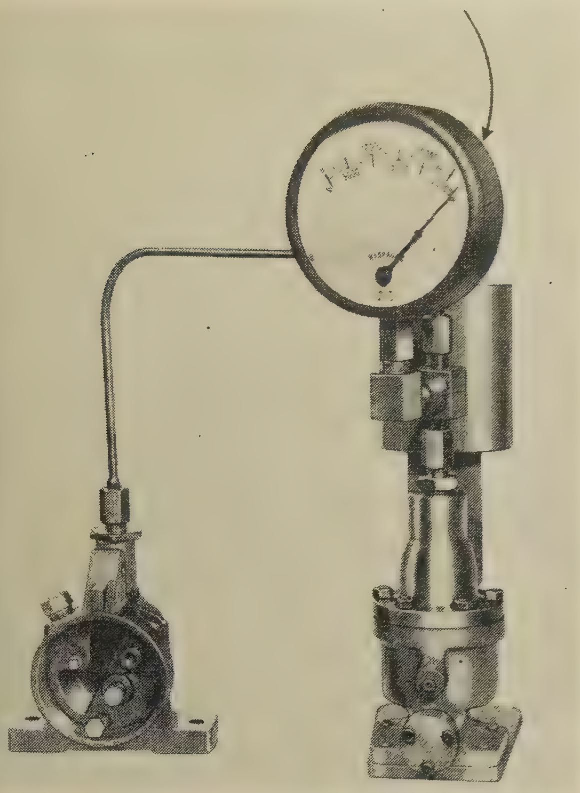

Fig. 28 Pump Head Under Test at 30,000 Psi

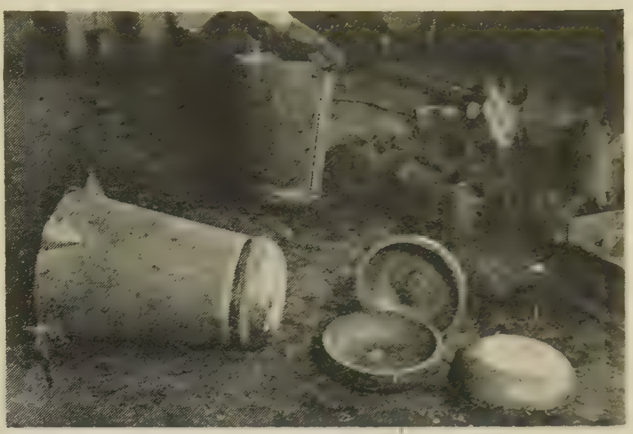

Fig. 29 Ladle Bottoms Hot-Formed on Iron Dies

A typical application includes ladle bottoms fabricated from 1-in. steel plate, Fig. 29, which were hot-formed on iron dies.

Examples of many other applications, including high-temperature and corrosion- and wear-resistant service conditions, could be cited. Thus Fig. 30 illustrates a 9-ft × 12-ft Marcy mill cast in wear-resisting-type iron and carrying a ball load of 50 tons. The weight of this mill on each trunnion is 70 tons.

Conclusion

It is hoped that the examples cited suffice to reveal clearly the varied characteristics of the modern new irons which are available to the production engineer in his search for more serviceable materials with increased economy of the finished product.

Fig. 30 Ball Mill Cast in Wear-Resisting Iron

Nozzle Flow Characteristics in Pneumatic Force-Balance Circuits

By D. B. KIRK,[1] PHILADELPHIA, PA.

A simple nozzle-diaphragm device for transmitting an ir pressure substantially corresponding to an applied rocess pressure is examined with respect to the factors ffecting nozzle clearance. Elementary gas-flow formulas re used to analyze these factors, and auxiliary circuit mponents are introduced which reduce substantially e variation in nozzle clearance as a function of the trans- itted air pressure.

PNEUMATIC transmitters are often used for converting process variables to air pressures for remote indication, recording or controlling, particularly in dealing with cor- sive or viscous fluids, or with extremes of temperature which ake impracticable direct transmission of the process medium the receiver. Transmitters may be of the displacement type, herein changes in the process variable result in mechanical otion which, in turn, actuates the pneumatic circuit. Or trans- itters may be of the force-balance type, wherein changes in e process variable result in force changes that are balanced di- ctly by air pressure. This discussion deals with the latter type.

FORCE-BALANCE TRANSMITTERS

Force-balance transmitters have been applied to the measure- ent and control of a number of variables, including force or ight, pressure, liquid level, specific gravity, flow, temperature, d motion or position. The direct-nozzle system, shown sche- atically in Fig. 1, illustrates one of the basic forms of a pressure nsmitter. Here the process pressure is applied to the upper e of a flexible diaphragm. Air is supplied to the opposite side the diaphragm through a fixed orifice. An escape nozzle rovided, so that excess air will be exhausted to the atmosphere. e diaphragm carries a seating member which restricts the v of air through the nozzle in accordance with the position of diaphragm.

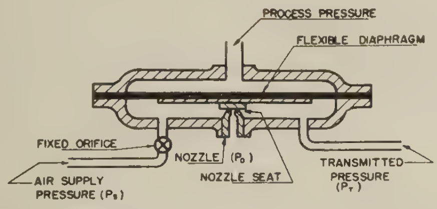

. 1 SIMPLE FORCE-BALANCE PNEUMATIC TRANSMITTER USING DIRECT-NOZZLE CIRCUIT

n operation, the process pressure tends to force the diaphragm l seat toward the nozzle to restrict the escape of air. But this ses the air pressure below the diaphragm to increase. Thus diaphragm will take a position which permits air to escape through the nozzle at the same rate at which it is supplied through the fixed orifice. Under these conditions the pressures on either side of the diaphragm will be substantially equal if negligible force is exerted by the diaphragm itself. The clearance between the nozzle and its seat, in this type of transmitter, must necessarily be a function of the transmitted pressure.

The relationship between nozzle clearance and the transmitted pressure has a very definite effect on the general performance of pressure-transmitting circuits. This subject therefore has been given considerable study in an attempt to improve transmitter performance. To obtain measurements of the nozzle clearance with an accuracy in the order of 0.00001 in. would be practically impossible by means of ordinary gaging equipment, even if the nozzle seat were accessible. But the problem is greatly simplified by taking advantage of the effects of changes in nozzle clearance on the transmission characteristic.

The spring rate of the transmitter was first determined by applying various known pressures to one side of the diaphragm and by measuring the corresponding deflection of the seat with a dial indicator. A graph was drawn of the seat displacement versus applied pressure, and the slope of the graph, through the normal operating range of the seat, was taken as the change in nozzle clearance resulting from unit change in differential pressure across the diaphragm.

The nozzle was then replaced and connections were made to operate the system as a pressure transmitter. This is shown in Fig. 2. A manometer, connected across the diaphragm, provided an indication of the differential pressure, from which the displacement of the nozzle seat could be calculated. By this means, with a diaphragm spring rate of 100 psi per in., changes in nozzle clearance in the order of 0.00001 in. were indicated on the manometer as approximately 0.03-in. changes in water column. The absolute value of the nozzle clearance was not given by this method, but was instead determined directly from the dial-indicator readings.

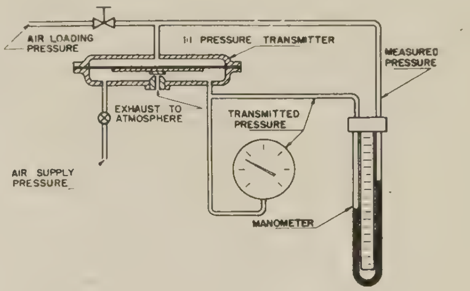

FIG. 2 CIRCUIT FOR MEASURING NOZZLE CLEARANCE AS FUNCTION OF TRANSMITTED PRESSURE

Fig. 3 shows the relationship between nozzle clearance and transmitted pressure as determined by laboratory measurements on a transmitter of the direct-nozzle type shown in Fig. 1. It will be noted that the nozzle clearance varies as a nonlinear function of the transmitted pressure. This deviation from linearity becomes significant in view of the fact that all practical transmitters use resilient members which exert a restraining force pro-

---

[1] Chief Engineer, Moore Products Company.

resented at first National Meeting of the Industrial Instruments Regulators Division, Pittsburgh, Pa., Sept. 16–18, 1946, of AMERICAN SOCIETY OF MECHANICAL ENGINEERS.

OTE: Statements and opinions advanced in papers are to be erstood as individual expressions of their authors and not those he Society.

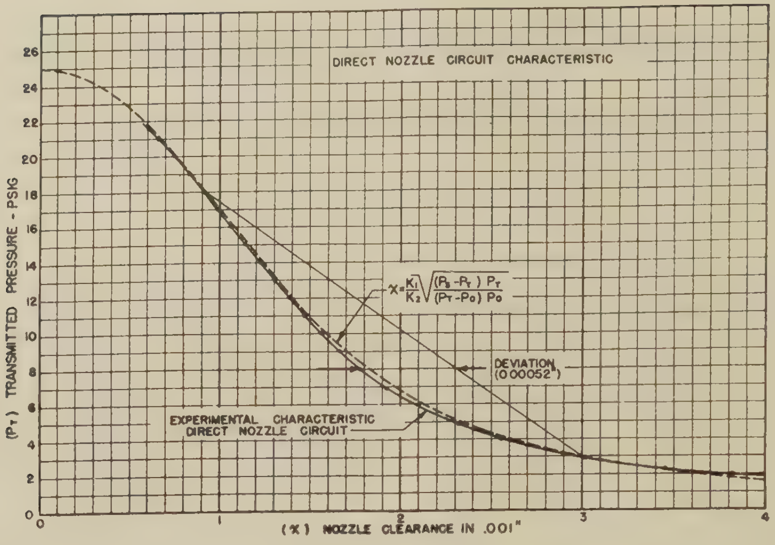

Fig. 3 Nozzle Clearance Versus Transmitted Pressure; Direct-Nozzle Circuit

portional to their displacement. The effect of this force is to prevent the transmission of pressure in an exactly 1:1 ratio. If the nozzle clearance bore a linear relation to the transmitted pressure, its effect would not be objectionable except in certain types of 1:1 transmitters. But the fact that the relationship is nonlinear means that the transmitted pressure will also be nonlinear with respect to the process pressure. Some idea of the nonlinearity may be obtained by comparing the straight line drawn through the usual limits of the transmitted-pressure range, that is, 3 and 18 psig. The deviation from linearity of the nozzle-clearance characteristic in this case is 0.00052 in. With a diaphragm spring rate of 100 psi per in., the deviation from linearity of the transmitted pressure is 0.052 psi, or 0.35 per cent of the total transmitted range of 15 psi.

The causes of nozzle-seat motion lie in the fundamental relations governing the flow of gas through an orifice. In the case of a fixed orifice, the flow of air is proportional to the square root of the pressure drop and to the square root of the absolute downstream pressure. This may be expressed by the relation

$$\text{Flow} = K_1\sqrt{(P_1 - P_2)P_2} \ldots\ldots\ldots\ldots\ldots [1]$$

In this expression K_1 is a constant combining temperature and density of the air, the orifice coefficient and area, and other constant factors depending on the units chosen for measuring the several variables. A similar relation holds for the nozzle and seat shown in enlarged cross section in Fig. 4. Here also, the flow is proportional to the square roots of the differential and downstream pressures. In addition, it is proportional to the nozzle clearance x, if this clearance is small compared with

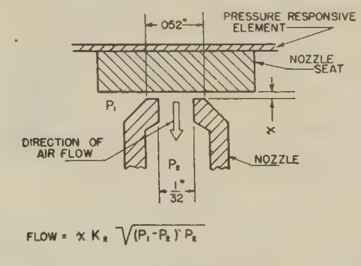

Fig. 4 Dimensions of Nozzle Used in All Transmitting Circuits

the nozzle diameter. The relation therefore for the nozzle a
seat combination is

$$\text{Flow} = xK_2\sqrt{(P_1 - P_2)P_2} \ldots\ldots\ldots\ldots\ldots [$$

K_2 is a constant, combining all fixed factors.

When the transmitter in Fig. 1 is operating under conditio
of equilibrium, flow of air through the orifice is equal to that e
hausted through the nozzle. It is therefore possible to combi
Equations [1] and [2], substituting the values for supply press
P_s, transmitted pressure P_t, and atmospheric pressure P_0
follows

$$\text{Flow} = K_1\sqrt{(P_s - P_t)P_t} = xK_2\sqrt{(P_t - P_0)P_0}$$

It is assumed that the air remains at constant temperatur
it flows through the supply orifice and the nozzle. This con
tion is closely approximated under practical conditions bec
of the good thermal contact made between the transmitter
relay bodies and the relatively small flow of air involved (appr
imately 0.1 scfm). Solving this for the nozzle clearance (x)

$$x = \frac{K_1}{K_2}\sqrt{\frac{(P_s - P_t)P_t}{(P_t - P_0)P_0}} \ldots\ldots\ldots\ldots\ldots$$

This expression holds in the range where no orifice is subject
critical-flow conditions, that is, where

$$1.89\,P_0 > P_t > 0.53\,P_s$$

For values of transmitted pressures above this range, Equati
[3] must be modified by substituting 53 per cent of the upstre
pressure for the pressure drop and also for the downstream pr
sure. Therefore we have

$$x = \frac{K_1}{K_2}\,\frac{1}{0.53\,P_t}\sqrt{(P_s - P_t)P_t} \ldots\ldots\ldots\ldots [$$

and for P_t less than 0.53 P_s, we have

$$x = \frac{K_1}{K_2}\,0.53\,P_s\sqrt{\frac{1}{(P_t - P_0)P_0}} \ldots\ldots\ldots\ldots [$$

The validity of Equation [3] is indicated in Fig. 3 by its agr
ment with the experimental curve. The values of K_1 and
were arbitrarily chosen so that the calculations resulted i

alue of 0.003-in. nozzle clearance at a transmitted pressure of psig. This condition, which is typical in the operation of cerain types of commercial force-balance transmitters, is the basis r comparison between the various circuits described in this aper.

Examination of Equation [3] shows that, with constant supply nd atmospheric pressures, the nozzle clearance depends upon ree factors which are functions of the transmitted pressure, as llows:

1 The pressure drop across the supply orifice ($P_s - P_t$).
2 The density of the air at the nozzle (P_t).
3 The pressure drop across the nozzle ($P_t - P_0$).

liminating the variation in any one, or all, of these factors would efinitely reduce the change in nozzle clearance as a function of e transmitted pressure.

One of the variables affecting nozzle clearance has been reuced by a major extent in the pneumatic circuit shown in Fig. 5

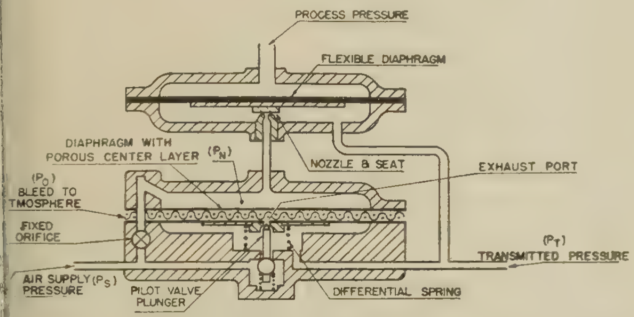
PROCESS PRESSURE
FLEXIBLE DIAPHRAGM
DIAPHRAGM WITH POROUS CENTER LAYER (P_N)
NOZZLE & SEAT
EXHAUST PORT
(P_0) BLEED TO TMOSPHERE
FIXED ORIFICE
(P_T) TRANSMITTED PRESSURE
AIR SUPPLY (P_S) PRESSURE
PILOT VALVE PLUNGER
DIFFERENTIAL SPRING

G. 5 Transmitter With Booster Pilot, Using Constant Differential Across Nozzle

this circuit, air is supplied through a fixed orifice to the upper le of the flexible diaphragm in a pneumatic relay. From there escapes through the transmitter nozzle to the underside of the aphragm in the transmitter. It returns to the pneumatic relay rough a separate connection, and may be either transmitted a receiver (not shown) or it may escape through the exhaust rt and the porous center section of the diaphragm to the atsphere. Air is also supplied, as required, through a valve ectly to the underside of the diaphragm in the transmitter.

An increase in the process pressure tends to force the diaphragm and seat toward the nozzle, causing the pressure in the upper chamber of the pneumatic relay to rise. The diaphragm in the pneumatic relay will then be moved downward to close the exhaust port and open the supply port. Whereupon, air admitted through the supply port is furnished to the underside of the transmitter diaphragm until it reaches a value substantially equal to that of the process pressure. At the condition of equilibrium, the nozzle seat is lifted lightly from the face of the nozzle to permit the air to flow through the nozzle at the same rate at which it is supplied through the fixed orifice. The diaphragm in the pneumatic relay is likewise in a state of balance since the pressure above this diaphragm must exceed that below it by an amount sufficient to overcome the force of the differential spring. This differential pressure is also effective across the nozzle in the transmitter and therefore prevents any significant change in the pressure drop across this nozzle as a function of the transmitted pressure. The pneumatic relay serves the additional purpose of increasing the transmission capacity of the system and therefore is commonly referred to as a booster pilot.

It may be noted that the direction of flow through the nozzle has been reversed in this circuit compared to that shown in Fig. 1. This reversal of flow has little significance other than to alter slightly the discharge coefficient of the nozzle. The effect was compensated for in these tests by making a corresponding change in size of the air-supply orifice.

Improved Transmission of Constant-Differential Circuit

The improved transmission characteristic of the constant-differential circuit is compared to that of the original direct-nozzle circuit in Fig. 6. It will be noted that for the normal transmitted pressure range of 3 to 18 psig, the change in nozzle clearance has been reduced from 0.00209 in. to 0.00171 in. Even more important is the improvement in linearity; the deviation from a straight line has been reduced from 0.00052 in. to 0.00009 in.

The ideal nozzle-clearance characteristic of the constant-differential circuit is calculated from the expression

$$x = \frac{K_1}{K_2}\sqrt{\frac{(P_s - P_n)P_n}{(P_n - P_t)P_t}} \qquad [4]$$

where P_n is the upstream pressure at the nozzle. When the

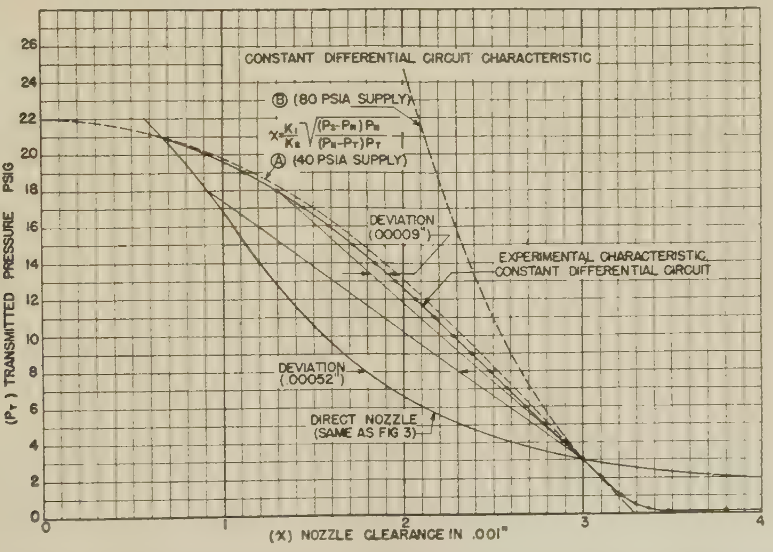

Fig. 6 Nozzle Clearance Versus Transmitted-Pressure Constant-Differential Circuit

values of supply pressure P_s, and nozzle differential $(P_n - P_t)$, used in the experimental work are substituted in the equation, the dotted curve *A* results. The differences between the experimental data and the calculated curve, in the region below the normal transmission range, may be attributed largely to the failure of the booster pilot to maintain a constant differential pressure across the nozzle at very low values of the transmitted pressure. Within the normal transmission range it will be noted, that the experimental curve more nearly approaches a straight line than does the calculated curve. The difference between the two curves arises from the fact that the air-supply orifice in Fig. 5 is a tubular restriction (0.012 in. diam × $^1/_2$ in. long), instead of a thin plate. The flow in this restriction does not follow the simple square-root law assumed for Equation [4]. If the supply restriction is intermediate between a capillary tube and a thin-plate orifice, the nozzle-clearance characteristic can be made to approximate a straight line even more closely.

In maintaining a practically constant pressure drop across the transmitter nozzle by the addition of the booster pilot described, we have greatly reduced the variation in one of the three factors responsible for changes in the nozzle clearance. This has considerably improved the linearity of the transmission characteristic. The system is not null balance in a true sense, however, because a distinctly different nozzle clearance is required for each value of transmitted pressure. Whenever it is desired to transmit pressures in an exactly 1:1 ratio, this system will be satisfactory only when the over-all spring rate of the transmitter is kept very low. For example, with a spring rate of 100 psi per in., a change in nozzle clearance of 0.00171 in. causes the transmitted pressure range to be 0.171 psi less than the measured range. This is an error of over 1 per cent based upon a 15-psi range. In still other applications of the force-balance transmitter, the force is supplied by a source incapable of appreciable deflection without greatly decreasing the accuracy of measurement. In one instance, the permissible deflection of the force-applying member was held to 0.0001 in., obviously an impossibility with the system just described, unless elaborate and cumbersome lever mechanisms were used.

The problem that remains then is to eliminate the remaining two variables affecting nozzle clearance, so that a truly null-balance system will result. One of these variables, the effect of changes in the differential across the air-supply orifice, has been removed in curve *B*, Fig. 6. Values for this curve were calculated on the basis that the air-supply pressure was high enough, so that a critical flow condition always existed across the fixed supply orifice. The performance could be easily attained in practice, with the circuit in Fig. 5, by using a supply pressure of approximately 80 psia.

There are two important objections to using such a high supply pressure, namely (1) possible damage to the receiving equipment from excessive pressure in the event of transmitter failure; and (2) the small size required for the fixed orifice. The method for obtaining curve *B*, therefore, cannot be considered as a practical improvement, and furthermore, it cannot compensate at all for the change in density of gas at the nozzle.

Of the three variables contributing to changes in nozzle clearance, one has been substantially reduced, in a practical manner, by the use of a constant differential across the transmitter nozzle. The two remaining variables are changes in flow caused by variation in the differential across the supply orifice, and the changes in the density of the air at the nozzle, resulting from changes in the transmitted pressure. Both of these variables could be removed if the flow of balancing air were controlled so as to increase in proportion to the square root of the absolute transmitted pressure. This condition has been very nearly accomplished in the circuit shown in Fig. 7. The circuit illustrated is similar to Fig. 5 in that a booster pilot is used to maintain a constant pressu drop across the transmitter nozzle. The only difference is tha the supply of air to the balancing circuit is regulated by an automatic flow controller instead of an orifice.

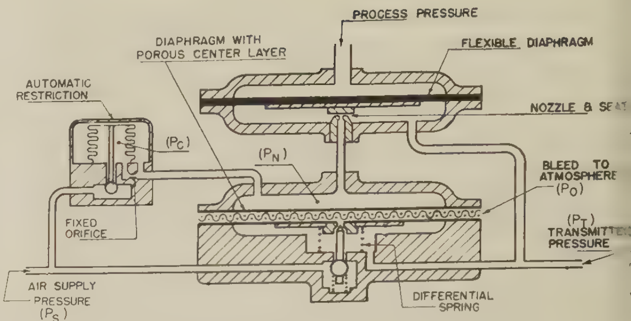
PROCESS PRESSURE
DIAPHRAGM WITH POROUS CENTER LAYER
FLEXIBLE DIAPHRAGM
AUTOMATIC RESTRICTION
NOZZLE & SE
(P_C)
(P_N)
BLEED TO ATMOSPHERE (P_O)
FIXED ORIFICE
(P_T) TRANSMITT PRESSURE
AIR SUPPLY PRESSURE (P_S)
DIFFERENTIAL SPRING

Fig. 7 Transmitter Using Compensated Flow With Consta Differential

Automatic Flow Controller Regulates Air Supply T Balancing Circuit

In this flow controller the differential across a fixed self-contained orifice is applied across a flexible bellows. The bellow controls the position of a valve to maintain the differential at constant value. Since the fixed orifice in the flow controller subject to substantially the same absolute pressure as the nozz in the transmitter, the flow will be very nearly compensated fo the variations in density of the gas at the nozzle. Since this ci cuit also maintains a constant differential across the nozzle, it ha eliminated almost completely the causes for variation of nozz clearance as a function of transmitted pressure.

An experimental curve run with this circuit is shown in Fig. along with the constant-differential characteristic by way of comparison. The calculated ideal curve is also shown. The deviati of the experimental curve from the ideal curve can be attribu almost entirely to two factors: (1) the inability of the flow co troller to function as the supply pressure is approached; and (to the inability of the booster pilot to maintain a constant d ferential at low values of the transmitted pressure. It will noted that even the ideal curve is not an absolutely verti line. The difference occurs because the absolute pressure at t flow-controller orifice differs from that at the transmitter no by a finite value, which is required to maintain flow in the c cuit.

A comparison of the nozzle clearance curve of the final circ with that of the constant-differential circuit shows a number important improvements. The deviation from linearity has b reduced from 0.00009 in. to 0.00001 in. This reduction will r sult in a corresponding improvement in the linearity of the tran mission system. It is also noted that with the improved circu the total variation in nozzle clearance over the normal tran mission range of 3 to 18 psig has been reduced from 0.00171 i to 0.00011 in. With a transmitter spring rate of 100 psi p in., the error in range of a 1:1 transmitter will thereby be reduc from 0.171 psi (1.1 per cent) to 0.011 psi (0.07 per cent).

Variations in Manufacture of Transmitters

It can be appreciated that in the manufacture of pneuma transmitters there will be some variation in these values. T range of a specific pressure-transmitter will therefore va slightly when it is used with different auxiliary circuit comp nents, even from the same production lot. Since the total redu tion in range is much less with the improved circuit, using co pensated flow with constant differential, it follows that the var tion in range will also be less. For example, assume that

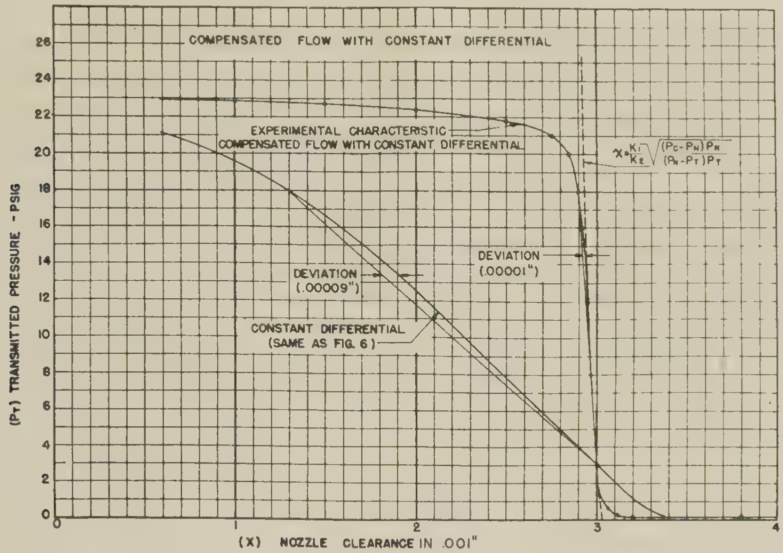

Fig. 8 Nozzle Clearance Versus Transmitted Pressure; Compensated Flow With Constant Differential

ransmitter having a spring rate of 100 psi per in. were set up the circuit in Fig. 7, with auxiliary components which exactly eproduced the curve in Fig. 8. Also assume another trans-itter with another set of components which, because of variation manufacture, produced a variation in nozzle clearance of twice at amount. A reduction in transmitted range in the first case ould be 0.011 psi; in the second case it would be 0.022 psi. he difference in range between the two systems is only 0.07 per ent, a value small enough so that the systems could be considered ompletely interchangeable for industrial use. For the constant-ifferential circuit, the corresponding variation caused by inter-anging circuit auxiliaries would be 1.1 per cent. In many ases this would require recalibration to provide sufficient ac-racy.

With the improved circuit, the nozzle clearance is consider-ly greater than that of either the original direct-nozzle circuit the intermediate constant-differential circuit within the trans-ission range, particularly at the higher transmitted pressures. he desirability of this condition arises from the fact that with eater nozzle clearance the transmitting circuit is inherently ore stable; also, the greater nozzle clearance permits more ariation in the parallelism of the mating surfaces involved. rom the standpoint of instrument manufacture these are both ery important gains.

Comparison of Pneumatic Circuits

Comparing the pneumatic circuits in Fig. 1 and Fig. 7, we find that both use orifices for controlling the flow of balancing air Because of the low differential pressure used in the improved circuit, however, its orifice may have several times the area of that in the original circuit (0.024 in. diam compared to 0.012 in. diam). The greater area makes the improved circuit less subject to the effects of normal impurities in the air supply.

In both the circuits of Fig. 1 and Fig. 5 the flow of air through the nozzle becomes greater with an increase of supply pressure. The nozzle clearance and hence the transmitted pressure, will be affected. In the improved circuit, the flow is substantially independent of the supply pressure because it is governed by an automatic flow controller. The importance of this characteristic to instrument users is demonstrated by the results of a practical test of the supply-pressure effect on the various circuits operating at mid-scale. A supply-pressure increase of 5 psi produced a corresponding increase in the transmitted pressure of 0.12 psi for the system in Fig. 1, and 0.21 psi for the system in Fig. 5. On the other hand, a change of 25 psi resulted in only 0.01-psi change in the transmitted pressure of the improved system using compensated flow.

The various auxiliary-circuit components in Fig. 7 have been combined in a single relay which is shown in cross section in Fig. 9. The lower section of this relay comprises a booster pilot whose action is identical with that previously described. The upper section is a modification of the automatic flow controller illustrated in Fig 7. Pilot air passes from the supply connection to the nozzle in the flow-controller unit, then continues through

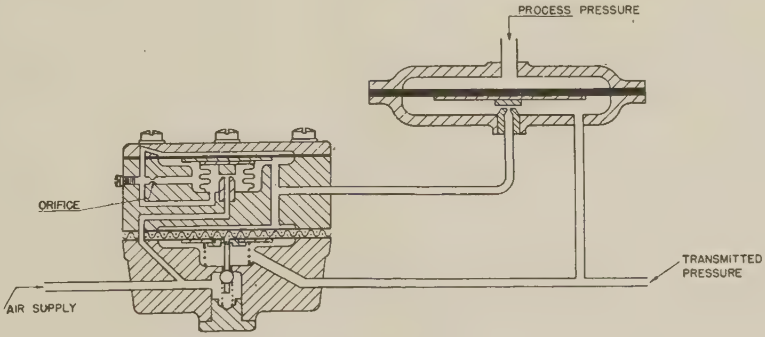

Fig. 9 Schematic Diagram of Pressure Transmitter, Using Pilot Which Incorporates Compensated-Flow and Constant-Differential Principles

the metering orifice and is conducted by external piping to the transmitter nozzle. Note that the pressure drop through the metering orifice is effective on the major portion of the upper diaphragm, so that any tendency of the flow to depart from a fixed value results in corrective throttling action by the nozzle seat.

In the design of this relay the factors causing changes in clearance of the transmitter nozzle have been reduced so far as consistency with practical methods of manufacture will allow. For example, reference to Fig. 7 shows that the supply pressure must exceed the maximum transmitted pressure at least by the sum of the differential pressures across the orifice of the flow controller and across the nozzle of the transmitter. Therefore the values of these differentials have been made as low as possible, (1 psi and 2 psi, respectively), so as to maintain the same transmission-range and supply-pressure values as are used with t earlier circuits.

The differential pressure across the transmitter nozzle should low for an additional reason. It has been pointed out th changes in nozzle clearance result, even in the calculated id curve, because of the finite value of this differential. It wou appear desirable, therefore, to reduce this differential to a ve low value; but if this were done, either the flow of balancing would necessarily be reduced, resulting in a slower-acting rela or the diameter of the transmitter nozzle would have to be great increased. Furthermore, manufacturing variations and the r sults of aging would have a proportionately greater effect on t value of the differential. Therefore the differential must be bas upon practical considerations at a slight sacrifice of theoretic perfection.

Some Properties and Mechanical Applications of Compar

By J. J. HITOV,[1] BELLEVILLE, N. J.

Some of the properties and applications of a relatively ittle-known synthetic material, "compar," are preiented. A modified polyvinyl-alcohol resin, it is manu'actured as tubing in the extruded state and is molded in nany forms, over a wide range of formulations. The lata contained in the paper have not previously been dislosed, so the author hopes that they may help in the soluion of particular problems for which better-known maerials may not have proved suitable.

COMPAR is the generic name, coined by the author's company, for compounded modified polyvinyl-alcohol resins to distinguish them from the raw polymer polyvinyl lcohol. Since the monomer, vinyl alcohol, is not isolable under iormal conditions, the polymer is made, indirectly, from polyinyl acetate. Polyvinyl alcohol is a white powder and is manuactured in several grades of varying degrees of polymerization nd hydrolysis.

The raw polymers do not exhibit thermoplastic properties. 'hey do not soften under heat and pressure but instead, form ard horny masses. When plasticized and modified, however, hey do exhibit some thermoplastic properties. Thus they often under heat and pressure and can, with proper precautions, e remolded and re-extruded.

Extrusion of compar is at present limited to tubing of various zes. Both in the extruded and in the molded states, the comars are elastic, have a wide range of tensile strengths, excellent olvent and abrasion resistance, and a range of high- and lowmperature resistance. Some formulations differ from other ynthetic resins in that they are soluble in cold water. Others, owever, are available which do not dissolve in water even at 30 F. They are either transparent, translucent, or opaque, deending upon the formulation and thickness. They also have an nlimited range of color possibilities.

CHARACTERISTICS OF COMPAR

Solvent Resistance. Most compars are almost completely unfected by all nonwater-soluble organic solvents. Table 1 shows e per cent swell of a typical compar in various solvents. These gures show that aliphatic and aromatic hydrocarbons, chloriited hydrocarbons, esters, and petroleum oils have a negligible fect upon these modified polyvinyl-alcohol products.

Table 2 shows the effect of carbon tetrachloride on the swell id durometer characteristics of alkyl polysulphides, butadienerylonitrile copolymers[2] and compar. These figures illustrate early the superiority of the compars to the synthetic rubbers in is respect. The effect of solvents on the tensile strength of bbers, natural and synthetic, is well known. The tensile strength of the compars is not changed by room-temperature immersions in these solvents. Table 3 shows the tensile strength of one compar after immersion in several solvents. These figures indicate that the tensile strength is not decreased by immersion in these solvents. They are representative of the effect on many of the compars and hold true for all of the water-insoluble organic liquids.

TABLE 1 SOLVENT RESISTANCE OF COMPAR;[a] TYPE 0

Liquid	Per cent change in volume 48 hr	1 week	1 month	3 months
Di-isobutylene	−0.8	−0.6	−0.5	−0.9
SAE No. 30 oil	−0.3	0.4	0.4	0.2
Xylol	0.3	0.7	1.3	0.8
Perchloroethylene	−1.4	−1.3	−0.6	−0.5
Butyl acetate	−4.3	−6.0	−4.8	−3.8

[a] Room-temperature immersions.

TABLE 2 COMPARATIVE RESISTANCE OF ALKYL POLYSULPHIDES, BUTADIENE-ACRYLONITRILE COPOLYMERS,[2] AND COMPAR TO CARBON TETRACHLORIDE[a]

	Butadiene-acrylonitrile copolymers No. I	No. II	Alkyl polysulphides	Compar
Volume increase, per cent	29	56	16.8	0.3
Per cent change in durometer (Shore-type A)	−21	−20	−18	0

[a] 48 hr at room temperature.

TABLE 3 TENSILE STRENGTH OF TYPE 00 COMPAR BEFORE AND AFTER IMMERSION IN ORGANIC LIQUIDS[a]

	Psi
Original	2880
After 3 months in:	
Xylol	2990
Alcohol	3020
SAE No. 30 oil	2920

[a] Room temperature.

TABLE 4 PHYSICAL PROPERTIES OF MOLDED COMPARS

Type	00	0	1	2	3
Tensile strength, psi	4000–5000	3000–4000	2500–3500	1400–1800	800–1200
Ultimate elongation, per cent	450–550	450–550	450–550	400–500	450–550
Hardness (Shore durometer Type A)	95	85–95	75–85	65–75	50–60

Tensile Strength, Hardness, and Elongation Characteristics. The compars are available in a wide range of tensile strengths and hardnesses. Both are functions of the amount and type of plasticizer and grade of polyvinyl alcohol used. The ultimate elongation characteristics do not vary widely and are in the range of about 500 per cent. Table 4 presents these properties for five standard molded compars. The stress-strain relationships of these compounds are shown in Fig. 1. The last point in each curve represents the breaking point. The relationship is also shown for one GR-S tread compound.

When the compars are extended up to 100 per cent and released immediately, the permanent set incurred varies from zero for the softest compound to about 6 per cent for the higher-durometer compounds. When thus extended and held for 10 min before release, the permanent set varies from 3 to 6 per cent. At 300

---

[1] Molding Engineer, Resistoflex Corporation.

[2] Synthetic Rubber Data—Acadia Synthetic Products.

Contributed by the Rubber and Plastics Division and presented the Semi-Annual Meeting, Chicago, Ill., June 16–19, 1947, of e AMERICAN SOCIETY OF MECHANICAL ENGINEERS.

NOTE: Statements and opinions advanced in papers are to be derstood as individual expressions of their authors and not those the Society.

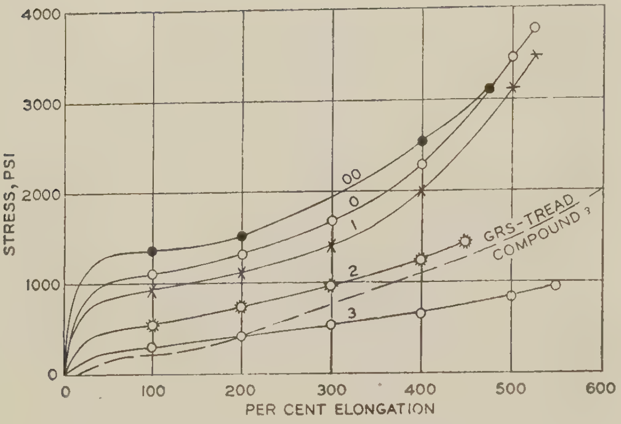

FIG. 1 STRESS-STRAIN DIAGRAM

(Determined in accordance with ASTM Specification D412-41.)

per cent elongation for 10 min, the softest compounds suffer a 50 per cent permanent set, the hardest about 125 per cent.

Abrasion Resistance. Complete comparisons of the abrasion-resistance characteristics of compars and synthetic rubbers are not available. Test data are available for two synthetic rubbers and compar, which show the latter to be superior in this respect. Table 5 presents these data.

Water Sensitivity. The compars are not recommended for use with water or water solutions. The extremely water-sensitive types will dissolve in water at room temperature. The water-resistant types will not dissolve. For example, the compar shown in Table 3 with a tensile strength of 2880 psi has a residual tensile strength after immersion in water (room temperature) for 3 months, of 900 psi. After the same period of time in water at 140 F its tensile strength is 500 psi. It undergoes a volume increase of 55 per cent and 152 per cent under the same conditions, respectively. Extrusion compounds are available which swell only 15 and 25 per cent when immersed in water for 24 hr at room temperature and 140 F, respectively.

Permeability. The compars are practically impermeable to nonwater-soluble organic vapors and gases. Permeability data are available for normal and isobutane, and normal and isobutylene.[4] Table 6 shows the permeability of these gases through tubing of natural and synthetic rubbers, and compar. The permeability of hydrogen of compar and a host of rubber and plastic films is shown in Table 7. This table shows that the permeability coefficient of the second best film is 296 times as great as that of polyvinyl alcohol.

AGING CHARACTERISTICS

The properties of the compars reach certain fixed values after aging, which are different from the values for freshly processed products. The properties thus affected are shrinkage, tensile strength, hardness, and low-temperature flexibility.

Shrinkage. The compars undergo a shrinkage of from 0 per cent for some compounds to 5 per cent for others, after processing. Under room conditions they will then remain fairly stable and no additional shrinkage will occur. This condition is illustrated in Table 8.

TABLE 5 ABRASION RESISTANCE—ASTM D-394-37T

	Polychloroprene		Poly-sulphide	Compar	
	Filled	Unfilled	Unfilled	Extruded	Molded
Volume loss per sq in. of material per 100 revolutions of abrading wheel, cu in.	0.0153	0.0371	0.0539	0.0045	0.0053
Abrasion loss as compared to polychloroprene, filled, per cent	100	248	353	29.5	34.2

TABLE 6 PERMEABILITY OF HYDROCARBON GASES THROUG FLEXIBLE TUBING[4]

(Cubic centimeter per square centimeter of internal area per millime thickness of wall per minute for pressure difference of 1 atmosphere.)

	$P \times 10^3$			
Tubing	i-butylene	n-butylene	i-butane	n-butan
Natural rubber, amber	1.06	1.66	0.37	1.09
Pure gum amber	1.02	2.05	0.21	1.50
Red rubber, cloth finish	0.69	0.66	0.26	0.70
Synthetic rubber, oil-proof	0.024	0.061	0.004	0.017
Cloth finish, black	0.102	0.317	0.029	0.111
Compar	...	0.00037 first 10 days 0.00016 two weeks on		

TABLE 7 PERMEABILITY OF HYDROGEN OF RUBBER AN PLASTIC FILMS[a]

Polymer	Permeability coefficient $P \times 10^8$
Natural rubber (pale crepe)	30.08
Polybutadiene	34.06
Gutta-percha	9.31
Polychloroprene	7.15
Butadiene-styrene copolymer	23.67
Butadiene-acrylonitrile copolymer	8.91
Polythene	3.91
Polyisobutylene	5.02
Polystyrene	11.30
Polyvinyl acetate	7.47
Polyvinyl chloride	1.48
Polyvinyl alcohol	0.005

[a] "Gas Permeability and the Microstructure of Polymers," by S. Reitlinger, *Rubber Chemistry and Technology,* vol. 19, April, 1946, pp. 38 391.

NOTE: *P* expressed in cubic centimeters of hydrogen per square cen meters per second for a thickness of 1 cm and a pressure difference of 1 at

TABLE 8 EFFECT OF AGING, UNDER ROOM CONDITIONS, O SHRINKAGE

	Per cent decrease in dimensions		
Time after molding	Type 0	Type 2	Typ 3
1 week	3.7	3.0	0
2 weeks	3.9	3.0	...
1 month	4.5	3.6	0.3
3 months	4.2	3.6	0

TABLE 9 EFFECT OF AGING, UNDER ROOM CONDITIONS, O TENSILE STRENGTH

	0	2	
Original tensile strength, psi	2100	590	
After 1 month	3500	1600	1
After 3 months	3500	1600	1

Tensile Strength. The tensile strength increases to a certa maximum with aging. Table 9 shows the original tensile strengt of freshly molded compars and the values attained after 2 wee and 3 months, respectively. After approximately 1 mont these values reach a maximum. The attainment of these max mum values may be hastened by aging for short periods of tim at elevated temperatures.

Hardness. The durometers of the freshly molded compa are lower than the values shown in Table 4. It is only aft aging that they attain those equilibrium values. These da are presented in Table 10. Here, again, it is seen that maximu values are attained after about 1 month under room conditions.

Low-Temperature Flexibility. The low-temperature flexibili of compars depends upon the formulation and the time and ter perature to which exposed prior to cold-testing. A tubing co position is available which is flexible at —76 F and lower, prior high-temperature aging. After aging for 1 week at 160 F it

---

[3] "Effect of Milling on Properties of Hevea and Buna Rubbers," by W. B. Wiegand and H. A. Braendle, *Industrial and Engineering Chemistry,* vol. 36, 1944, pp. 699–702.

[4] "Permeation of Hydrocarbon Gases Through Rubber Tubing," by M. J. Stross, J. R. Riley, and H. M. Eby, *Journal of the Institute of Petroleum,* Birmingham, England, vol. 30, June, 1944, pp. 153–166.

ABLE 10 EFFECT OF AGING AT ROOM CONDITIONS ON DUROMETER[a] OF COMPARS

Compound	0	2	3
Original	69	61	47
1 week	81	62	46
2 weeks	82	62	46
1 month	85	65	50
3 months	84	65	48

[a] Shore type A.

ABLE 11 EFFECT OF AGING ON LOW-TEMPERATURE FLEXIBILITY OF COMPARS

	Temp. at which flexible, deg F		
ompound	Fresh	3 months old	4 months old
0	—58	—40	—40
1	—58	—40	—40
2	—58	—40	—40
3	—76	—58	—58

till flexible at —40 F. If exposed to the atmosphere for several ours it will regain many of its original low-temperature charcteristics. The compars are more flexible when freshly molded han they are after aging. Here again, given equilibrium values re attained as shown in Table 11.

Applications

Hose. The properties described indicate the type of applicaion for which compar is suited. It is most widely used where olvent- and oil-resistance properties are required. Thus flexible ompar hose is used in automotive applications for gasoline and il lines, and for Diesel fuel lines in trucks and tractors. Hose ssemblies and gaskets are also used in dry-cleaning equipment. ne of the important advantages of the compar tube in this pplication is that it does not discolor the solvents. An interestng application is shown in Fig. 2. The compar lines are conucting cooling oil for the x-ray machine shown. In this aplication it was found that the dielectric of the oil was changed by contact with synthetic-rubber lines. This property is completely unaffected by compar. Another exacting application is in the hot-doping process for finishing fabric-covered surfaces in airplanes. Fig. 3 shows such an application, in which the hose must withstand the action of solvent at 175 F, and the erosive action of the dope.

The low permeability property of compar has found application in industrial refrigeration and in industrial and domestic air-conditioning units. Resistance and impermeability to the freons and methyl chloride are essential in these applications. Fig. 4 shows a portable air-conditioning unit using long flexible compar hose. This property also decided the use of compar for propane- and butane-gas lines.

Compar hose is also used for chloropicrin and DDT spray hose, hydraulic oil, and high-pressure lubrication systems.

Molded Products. Molded compar is used as wipers in wire, cable, and hose-lacquering applications. Fig. 5 shows such an application. Abrasion resistance is also important in this application.

Some additional applications are as squeegees in the silk-screening and other processes, as a base for lenses in grinding with xylol, gaskets for paint cans, fire extinguishers, greenhouse fumigation equipment, watch-cleaning apparatus and in perfume-industry equipment.

Compar sheets have found applications as a base cover in sandblasting equipment. In one application this material replaced $1^1/_2$-in. boiler plate, which lasted only several hours. The compar sheets have been used for days without serious damage. Fig. 6 shows a sandblasting operation using compar as the base. However, compar is not recommended for indiscriminate use in such operations. The particle size of the grit and the angle at which it hits the sheet are important considerations. In some

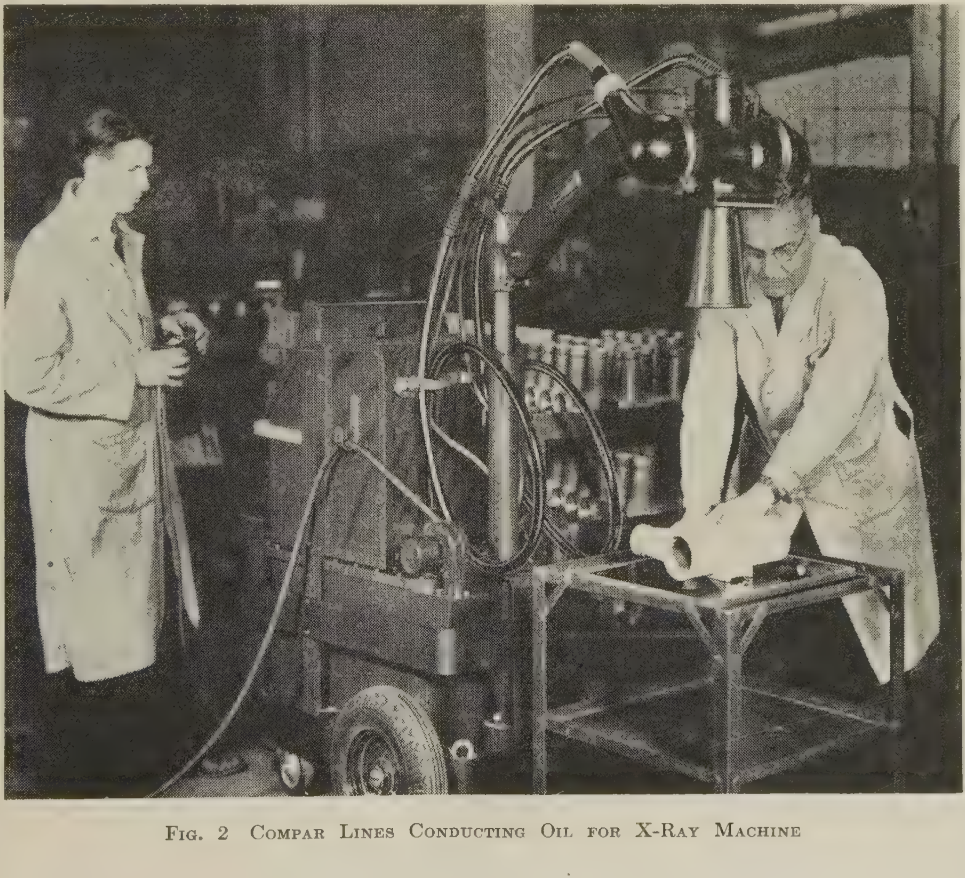

Fig. 2 Compar Lines Conducting Oil for X-Ray Machine

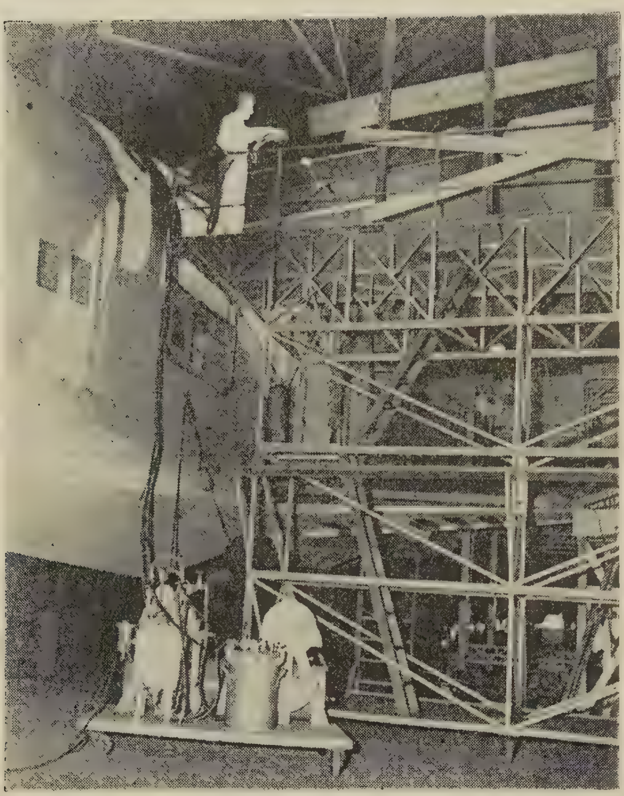

Fig. 3 Hot "Dope" Application With Compar Lines

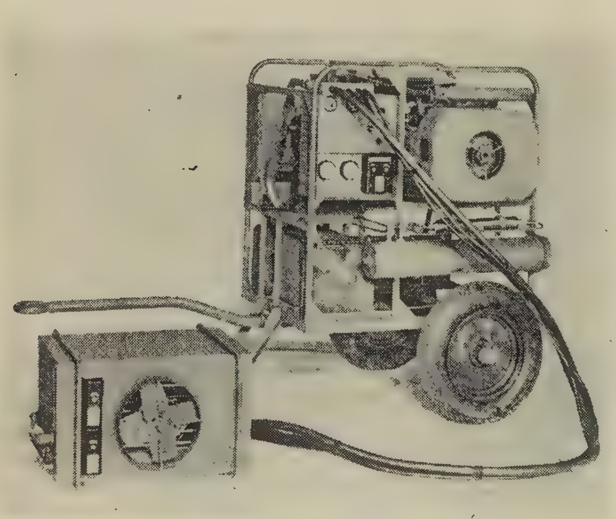

Fig. 4 Portable Air-Conditioning Unit Using Compar Lines

combinations of these factors, the compars have proved unsatisfactory.

A second abrasion-resistant application is that of friction rollers in the paper and can industries. Fig. 7 illustrates this application. In the paper industry an important feature is the fact that the paper is not discolored by the compar rollers.

The molded compar has also found use as a cushioning belt in file-straightening equipment.

With the development of aromatic solvent inks, there is an increasing demand for compar in the printing field. The use of compar printing plates has been delayed because of the limitations of the molding facilities available to the industry. In the molding operation, compar must be cooled under pressur Since the printing industry has been using rubber plates th molding presses are not equipped with cooling systems. It likely that the new inks will make the use of compar mandator

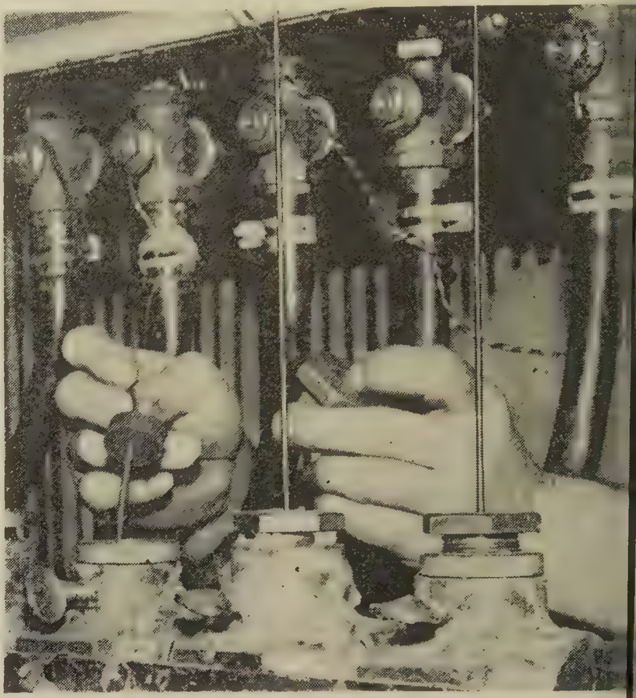

Fig. 5 Compar Wipers in Lacquering-Tower Applicati

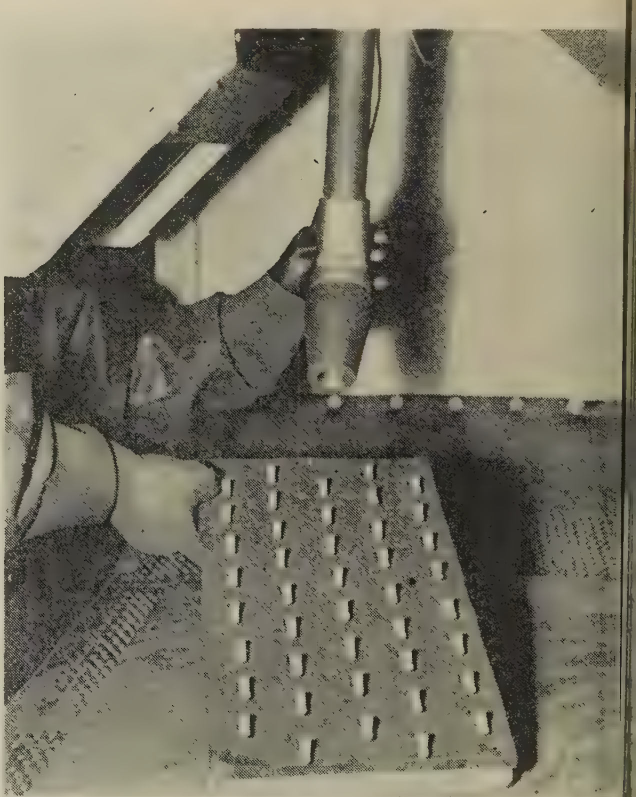

Fig. 6 Molded Compar Sheet Being Used as Base in Sa
Blasting Operation

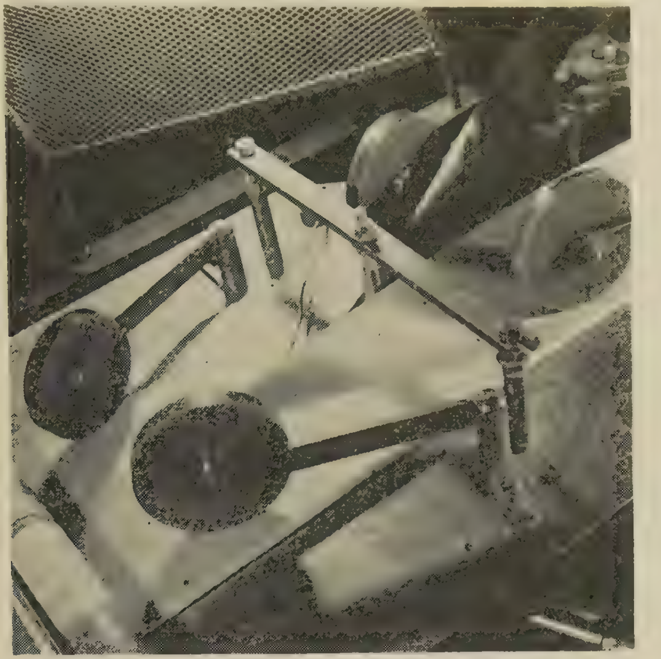

Fig. 7 Compar Friction Rollers in Folding Paper

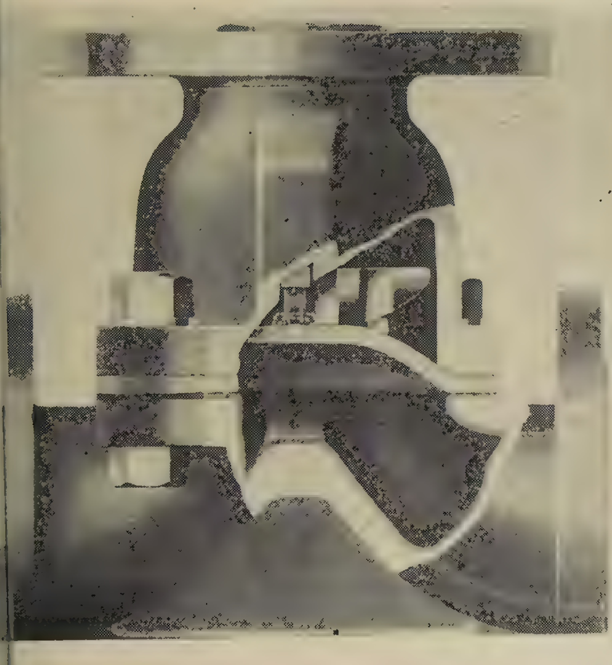

Fig. 8 Valve Using Compar Diaphragm[5]
(Open position.)

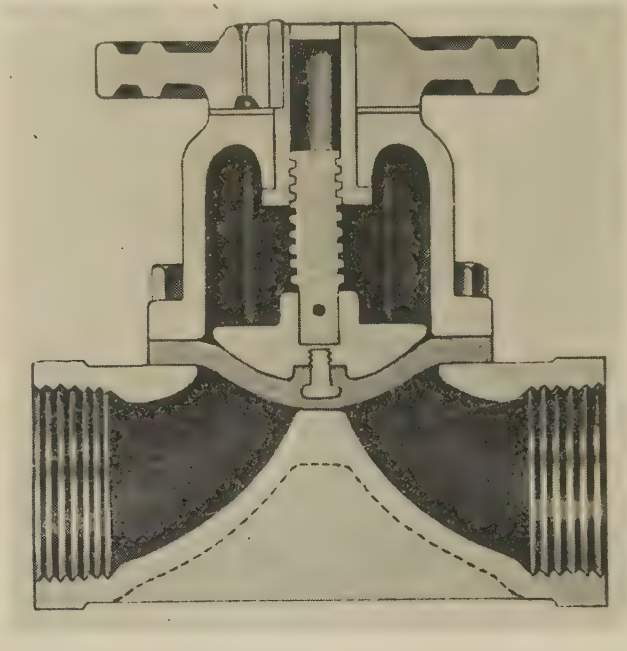

Fig. 9 Valve Using Compar Diaphragm[6]
(Closed position.)

nilar considerations have served to increase the interest in
mpar printing rolls.

Recent tests indicate that compar far outlasts sucker and
ter rubbers in can-industry applications. A specially com-
unded compar has found an important application as a valve
phragm.[5] Figs. 8 and 9 show these valves with diaphragm in-
lled in both open and closed positions. These compar dia-
ms have proved their value in handling the chlorinated and
matic hydrocarbons.

Some of the properties and applications of a relatively little-known synthetic material have been presented. It is hoped that this information, much of which has heretofore remained undisclosed, may solve some particular problems for which the better-known materials may not be suitable, thus perhaps advancing industrial technology another millimeter in the miles it must yet travel.

---

[5] The Hills-McCanna Saunders patent valve.

[6] Figs. 8 and 9 are shown through the courtesy of the Hills-McCanna Co.

Cross-Laminated Oak

By E. GEORGE STERN,[1] BLACKSBURG, VA.

Three-ply cross-laminated oak panels with oak or yellow-poplar core of $^{25}/_{32}$ or $1^1/_4$ in. total thickness, and 7 × 7 in., or 12 × 12 in. in area, were subjected to exposure tests of repetitive and/or alternating drying at slightly below 100 C, and/or soaking at laboratory temperature for 48 hr, in order to determine the influence of internal stresses due to exposure on the dimensional stability and durability of such panels. The test results indicate that these panels can be cross-laminated satisfactorily to withstand extreme exposure conditions such as may occur in service, if their cross sections are properly balanced and their plies are properly assembled. The Tennessee Valley Authority designed and built a continuous-press pilot plant for the production of these 12-in-wide panels of any desirable length.

General

CONTINUOUS three-ply cross-laminated oak boards with tongued and grooved edges, approximately $^{25}/_{32}$ × 12 in. in net cross section, are manufactured by cross-laminating three layers of 3-in-wide oak slats of 0.27 ± 0.003 in. thickness and of random lengths into endless boards. This is accomplished under a continuous manufacturing procedure with a special press set up in the Knoxville pilot plant of the Regional Products Research Division of the Tennessee Valley Authority.[2]

Boards and panels of other total thicknesses can be manufactured according to the same procedure. The thicknesses of surface and core layers of slats need not be the same. Thus the $^{25}/_{32}$-in. cross section may be made up by utilizing slats, e.g., $^3/_{16}$ in. thick for top and bottom layers and $^{13}/_{32}$ in. thick for the core. Depending upon the use intended for the prefabricated board, a variety of wood species may be used for its manufacture, with the individual layers of slats built of the same or different hardwood or softwood species. The top-surface layer may be of selected material, the bottom layer of somewhat less desirable, and the core of low-grade material. The selection of slats for the top-surface layer may be restricted to include only close-grained, edge-grained (or quarter-grained) slats within a certain color range and structure, free of knots, deficiencies, and defects. The core slats may consist of soft hardwood, such as yellow poplar or other relatively resilient wood. This may result in a greater dampening capacity for such boards, than for those of solid oak or other dense hardwoods. Thus the laminated or cross-laminated prefabricated and mass-produced boards and panels may be designed in structure and composition and manufactured accordingly for the particular purpose they are to serve.

If the 12-in-wide boards or planks are cross-laminated, they should show better dimensional stability and warp and cup less than a solid piece of wood of the same dimensions during change in moisture content, both during manufacture and while in use. Since a thermosetting phenol-resorcinol-formaldehyde-resin glue can be used for their manufacture, delamination of the boards or planks will not occur as a result of moisture absorption by the fully polymerized waterproof glue.

When the moisture content of the wood is changed with great rapidity and in a wide range because of fluctuations in the relative humidity of the air, or because of direct contact of the boards and planks with moisture and/or exposure to heat, extreme conditions exist. Under those conditions delamination may take place as a result of excessive internal stresses set up by the variation in change in dimensions of the outer and inner layers of cross-laminated slats. While with change in moisture content wood does not change its longitudinal dimensions appreciably, the dimensional stability perpendicular to its fibers may be even less than one tenth of the one parallel to its fibers. In cross-laminated panels, this change in dimension perpendicular to the fibers is at least partly restricted by the glue lines firmly connecting adjacent cross-laminated fibers. This may result in relatively large internal stresses. Since glue lines can be made stronger than the wood they connect, these stresses may be resisted by the glue lines but are limited by the shear resistance along the grain of the wood used for the adjacent layers.

Internal stresses resulting from exposure to extremes in relative humidity of the surrounding air, or from direct moisture contact by the panels, may be minimized to a certain extent by proper selection of the thickness ratios for surface and cross-layers. Because of differences in dimensional stability of different wood species, proper selection of wood-species combinations for surface and core layers may result in reduced internal stresses, although in many cases, from the manufacturing viewpoint, such species combinations may not be considered economically feasible or otherwise practical. Internal stresses due to change in moisture content can be reduced by preventing rapid changes in moisture content, by retarding such changes by means of application of coatings or sealers to the wood surfaces, and/or by impregnating part or all of the wood.

Data have been established on the influence of (1) various thickness combinations for the outer and inner layers of slats, (2) various wood-species combinations for the outer and inner layers of slats, (3) impregnation of surface slats, on dimensional stability and durability of cross-laminated boards and panels as indicated in Figs. 1 to 6. To determine these influences on an accelerated basis, the test panels were exposed to extreme conditions, i.e., to repetitive and/or alternating drying at slightly below 100 C, and/or soaking at laboratory temperature for 48 hours.

The tests were limited to a study of panels of 7 × 7 in. cross-laminated with urea-formaldehyde-resin glue and of 12 × 12 in. cross-laminated with phenol-resorcinol-resin glue, with total panel thicknesses of $^{25}/_{32}$ and $1^1/_4$ in. The wood species investigated were red, white, and chestnut oak, with the addition of yellow poplar for core slats. Most of the wood was clear matched material. In interpreting the test results, these limitations should not be overlooked.

---

[1] Director, Wood Research Laboratory, Associate Research Professor, Department of Wood Construction, Virginia Polytechnic Institute.

[2] "Manufacturing Laminated Lumber, Development of Processes and Machines for Production System," by R. B. Taylor, *Mechanical Engineering*, vol. 68, 1946, pp. 539–542.

This paper was prepared in collaboration with the Tennessee Valley Authority and presented at the Wood Industries Division Meeting, Madison, Wis., June 12–13, 1947, of THE AMERICAN SOCIETY OF MECHANICAL ENGINEERS. For further details, see Virginia Polytechnic Institute Engineering Experiment Station Bulletin No. 47, "Limitations in Cross-Laminating of Oak Under Extreme Service Conditions," 1947.

NOTE: Statements and opinions advanced in papers are to be understood as individual expressions of their authors and not those of the Society.

The study was performed in the VPI Wood Research Laboratory, under auspices of the VPI Research Foundation, Inc., and under sponsorship of the Regional Products Research Division of the Commerce Department of the Tennessee Valley Authority.

Influence of Exposure Conditions

The estimated average moisture content of the principal interior woodwork in dwellings may vary from 4 per cent in Salt Lake City, Utah, to 13.5 per cent in New Orleans, La.[3] At severely exposed locations, such as directly above a noninsulated heating unit, the moisture content may decrease to as little as 1 to 2 per cent and, for example, in humid basements, may increase to 18 per cent and more. When the wood is exposed to direct contact with water for a relatively long period, the moisture content may increase to 30 per cent and more. To determine the influence of exposure extremes on cross-laminated oak flooring, test panels were exposed 48 hr to drying or soaking, to repetitive 48 hr of drying or soaking, and to repetitive 48 hr of drying or soaking followed by single or repetitive soaking or drying, respectively, as indicated in Fig. 1. These exposures influenced in various degrees the resulting moisture content, causing internal stresses of direct influence on durability (see Fig. 2), dimensional stability (see Fig. 3), warpage and cupping (see Fig. 4), and the strength of the glue lines (see Fig. 5).

The durability and resistance to shear of the glue lines of 7 × 7-in. and 12 × 12-in. laboratory-assembled panels, as correlated to their exposure conditions, is summarized in Tables 1 and 2, with ultimate shear-test stresses upon exposure given for the moisture content at test and adjusted for 12 per cent moisture content.

The influence of exposure on the glue-line shear resistance of control and of variously exposed 12 × 12-in. oak panels is shown in Fig. 6. The data for individual panels are somewhat erratic, and adjustments for the influence of moisture content and of the angle of annual growth rings to direction of applied shear load on the shear resistance of the glue lines might have been justified. The general trend, however, of decrease in glue-line shear resistance with increase in exposure cycles can be observed.

For panels conditioned to 9 per cent moisture content, exposure to 48 hr soaking was more severe than exposure to 48 hr drying, because of larger internal stresses within the panels during soaking, as evidenced by a larger number of failures of soaked than of oven-dried panels. Soaking, however, caused softening of the oak which allowed a larger amount of creep within the soaked than within the oven-dried plies, thus resulting in smaller internal stresses in the glue lines and consequently in less decrease in strength of the glue lines of soaked panels than of those of oven-dried panels. The first exposure cycle of as many as nine caused extremely large internal stresses and major adjustments within the panels, resulting in a large percentage of decrease in shear resistance of the glue lines. Initial and local failures called for certain releases of internal stresses. Hence during exposure after initial and local failure, overstressing and further deterioration of the glue lines of test panels were only small. One or two complete exposure cycles of 48-hr drying or soaking were satisfactorily resisted by almost all test panels.

A limited number of repetitive or reversed exposures were withstood by the glue lines and by the wood of the majority of properly balanced $1^1/_4$ or $^{25}/_{32}$-in. oak and yellow-poplar-core panels. However, repetitive or reversed soaking cycles caused excessive internal stresses even in several of the properly balanced yellow-poplar-core and veneered panels. Hence the test-exposure conditions, with the exception of repetitively reversed exposure cycles, were not too extreme for properly balanced an well cross-laminated oak panels with phenol-resorcinol-resi glue lines. Consequently these panels should be satisfactor for use even under extreme service conditions.

Influence of Type of Glue and Size of Panel

Urea-formaldehyde-resin glue lines deteriorate faster durin exposure to oven-drying and soaking than phenol-resorcinol-resin glue lines. The strength of urea-formaldehyde-resin glu lines, however, may be sufficient to withstand internal stresse due to exposure, provided the stresses are not excessive. T determine the extent of these internal stresses and the resistanc offered to them by urea-formaldehyde-resin glue lines, a series o tests were performed on three-ply cross-laminated 7 × 7-in. oak panels with Uformite CB-552 glue lines. Internal stresses resulting from exposure of these panels were of course smalle than those in 12 × 12-in. panels cross-laminated with phenol-resorcinol-resin glue. Thus the conclusion cannot be drawn that 12 × 12-in. panels withstand the same exposure as simila 7 × 7-in. panels were found to withstand.

Urea-formaldehyde-resin glue lines withstood single exposures and single-exposure reversals and internal stresses due to these exposures in most of the $^{25}/_{32}$-in-thick panels with $^1/_4$ or $^3/_{16}$-in-thick faces, and in all $^{25}/_{32}$-in-thick panels with $^1/_{20}$ or $^1/_{16}$-in-thick face veneers, but in none of the $1^1/_4$-in-thick test panels. A comparison of these data with those for 12 × 12-in. panel cross-laminated with phenol-resorcinol glue indicates that the latter glue lines were fully satisfactory even for additional repetitions of exposure of the larger $1^1/_4$ and $^{25}/_{32}$-in-thick tes panels. A comparison of the strength of the glue lines show that the urea-formaldehyde glue lines and the phenol-resorcino glue lines in the 7 × 7-in. and 12 × 12-in. panels, respectivel were found to be approximately equally strong upon similar te exposures.

The relatively high shear resistance upon exposure, and th durability of most of the 7 × 7-in. panels with $^1/_4$ and $^3/_{16}$-in faces and especially with $^1/_{20}$ and $^1/_{16}$-in-thick face veneers, le to the conclusion that the urea-formaldehyde glue lines of panel with thin faces were not overstressed during exposure, and there fore may be entirely satisfactory for three-ply cross-laminate 7 × 7-in. panels with relatively thin faces, but not for cros laminated lumber with thick face plies if to be used under e treme service conditions.

Influence of Total Thickness of Panel

Cross-laminated panels may be built up to any desirable thic ness and used under extreme service conditions provided th internal stresses due to exposure are not excessive for the glu lines used. The internal stresses in thicker panels are neces sarily larger than those in thinner panels of otherwise identica construction. By balancing properly the thickness of the ind vidual plies, these internal stresses may be held within satis factory limits. Desirable thickness for flooring without sub flooring has been $1^1/_4$ in. and standard thickness for flooring o subflooring has been $^{25}/_{32}$ in. Since the principal market fo 12-in-wide three-ply cross-laminated panels should be fo flooring to be laid without or with subflooring, the study of th influence of total thickness of the three-ply cross-laminated oa panels on the resistance to exposure under extreme service co ditions was limited to $1^1/_4$ and $^{25}/_{32}$ in. thicknesses.

The resistance of phenol-resorcinol-resin glue lines to seve exposure allowed the construction of both $1^1/_4$ and $^{25}/_{32}$-in-thic three-ply 12 × 12-in. cross-laminated oak panels which wit stood the internal stresses caused by extreme exposure cond tions. A comparison of $1^1/_4$ and $^{25}/_{32}$-in-thick oak test pane indicates that panels of both thicknesses resisted equally we

---

[3] "Moisture Content of Wood in Dwellings," by Edward C. Peck, U. S. Department of Agriculture Circular No. 239, Table 2, 1932.

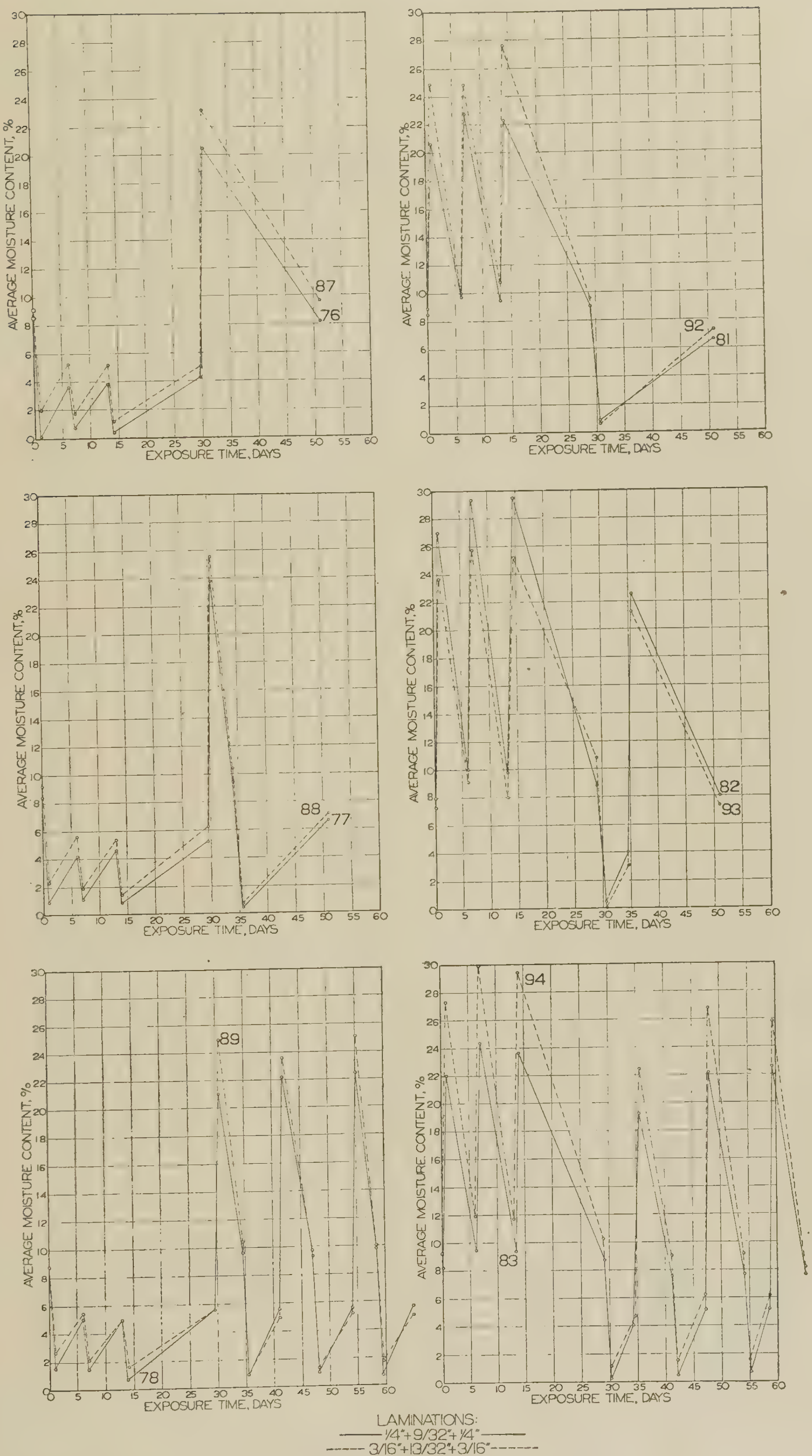

FIG. 1 TYPICAL EXPOSURE SCHEDULES AND RESULTING AVERAGE MOISTURE CONTENT FOR $^{25}/_{32}$ × 12 × 12-IN. PANELS

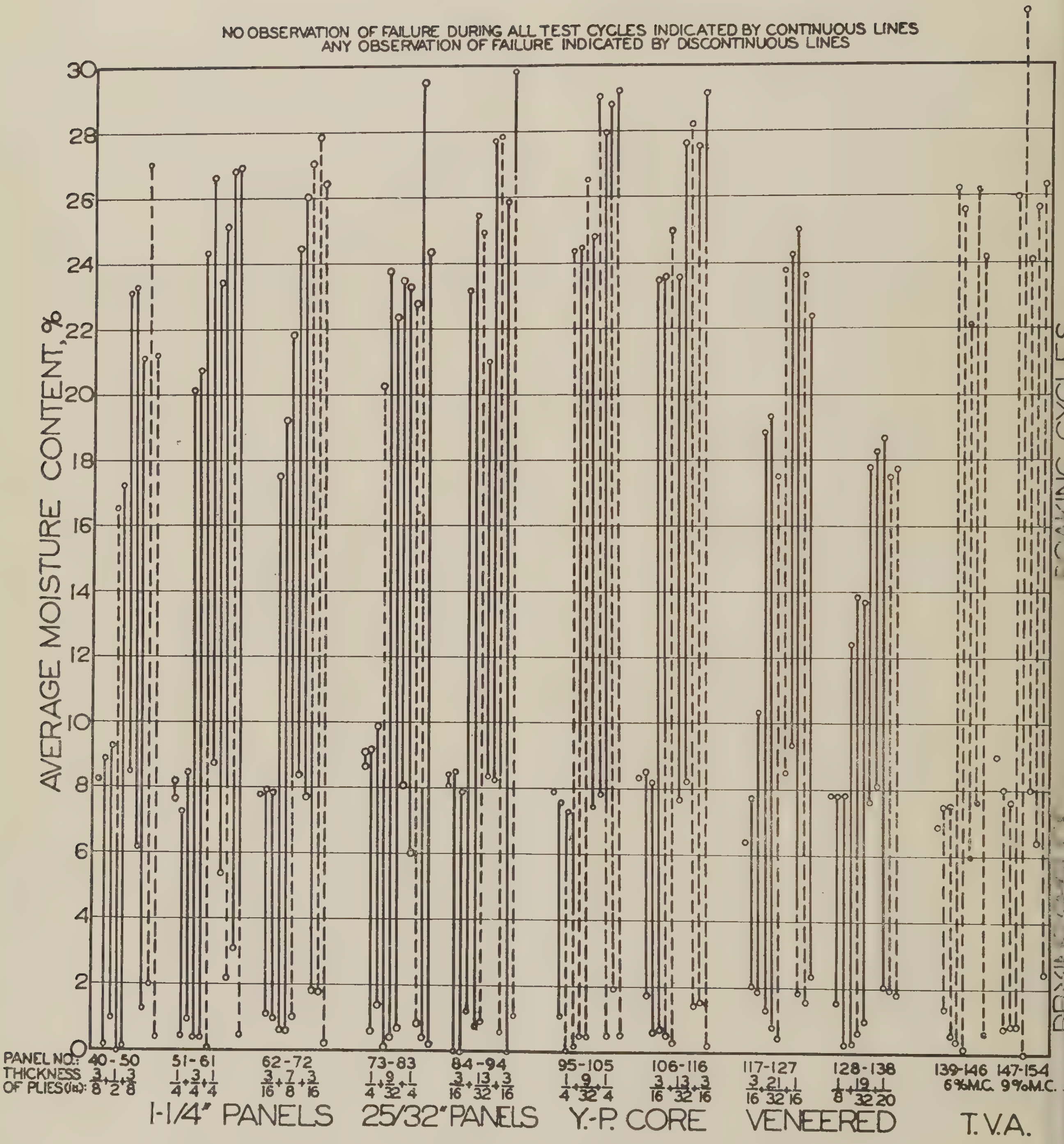

Fig. 2 Diagrammatic Summary for Durability of 12 × 12-In. Panels

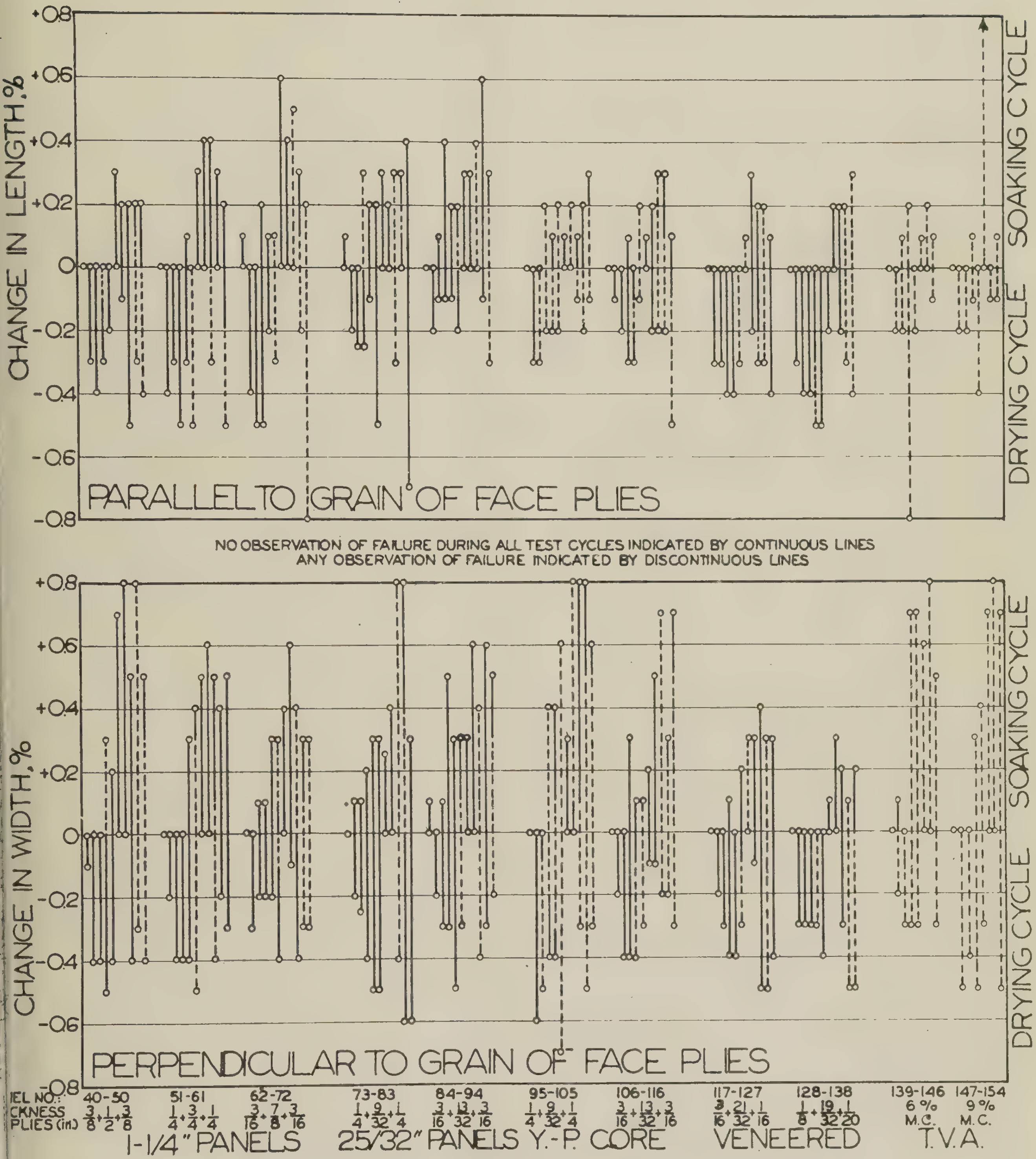

Fig. 3 Diagrammatic Summary for Dimensional Stability of 12 × 12-In. Panels

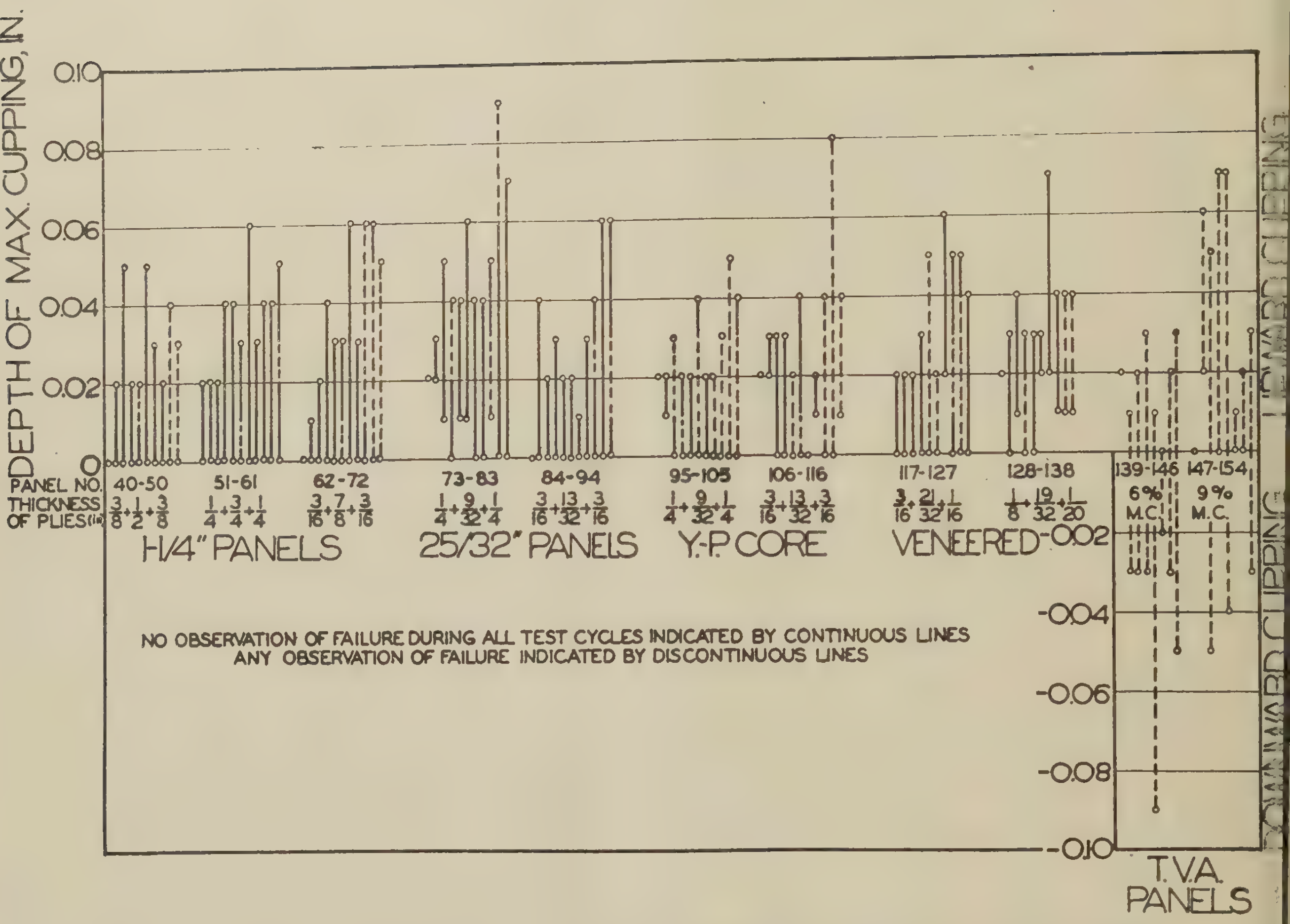

Fig. 4 Diagrammatic Summary for Maximum Over-All Warpage and Cupping of 12 × 12-In. Panels

exposure to repetitive oven-drying and subsequent soaking and oven-drying, while triple drying cycles, followed by triple soaking and drying cycles were resisted only by $^{25}/_{32}$-in-thick panels with $^{1}/_{4}$-in-thick faces. Exposure to repetitive soaking and repetitive soaking followed by single or repetitive drying and soaking cycles was resisted better by the $^{25}/_{32}$-in-thick panels.

Influence of Thickness Combination of Individual Laminae

Thin face veneers have been glued to thick cores to make three-ply cross-laminated panels for furniture and other structures which can be exposed to extreme service conditions without showing excessive warpage or delamination. "Theoretically, a three-ply cross-laminated panel should have a core of a thickness equal to 80 per cent of the thickness of the total panel."[4] According to this theory, $1^{1}/_{4}$-in-thick three-ply cross-laminated panels should have a core thickness of 1 in. and a face-veneer thickness of $^{1}/_{8}$ in., while $^{25}/_{32}$-in-thick panels should consist of a $^{5}/_{8}$-in-thick core and $^{5}/_{64}$-in-thick faces. These thin faces would not be satisfactory for three-ply flooring panels if not impregnated or otherwise treated to withstand wear. To determine how thick the faces of three-ply cross-laminated panels can be without introducing excessive internal stresses due to exposure to extreme service conditions, and to obtain data on the optimum thickness combinations for $1^{1}/_{4}$ and $^{25}/_{32}$-in-thick panels, exposure tests were performed on such panels with thicknesses of face plies ranging from $^{1}/_{2}$ to $^{3}/_{16}$ in. for $1^{1}/_{4}$-in-thick panels, and from $^{5}/_{16}$ to $^{1}/_{20}$ in. for $^{25}/_{32}$-in-thick panels.

Internal stresses in $1^{1}/_{4}$ × 7 × 7-in. panels with $^{1}/_{2}$, $^{7}/_{16}$, $^{5}/_{16}$, $^{1}/_{4}$, and $^{3}/_{16}$-in-thick faces were excessive for the ure formaldehyde-resin glue lines used. Panels of this thickness a sembled with this glue and thinner faces were not tested. Phen resorcinol-resin glue lines, however, resisted internal stresses i many of the $1^{1}/_{4}$ × 12 × 12-in. panels with $^{3}/_{8}$, $^{1}/_{4}$, and $^{3}/_{16}$- thick faces, despite the larger size of these panels. All of th panels showed satisfactory resistance to single and repetiti drying cycles. The construction of $1^{1}/_{4}$-in-thick panels wi $^{1}/_{4}$-in-thick faces and a $^{3}/_{4}$-in-thick core, however, appears to the most satisfactory one of the three thickness combinatio tested.

The smaller internal stresses due to exposure in $^{25}/_{32}$-in-thic panels, as compared with those in $1^{1}/_{4}$-in-thick panels, were r sisted by the urea-formaldehyde-resin glue lines of many of th exposed $^{25}/_{32}$ × 7 × 7-in-thick panels. Stresses in panels wi $^{5}/_{16}$-in-thick faces were excessive. But stresses in most of th panels with $^{1}/_{4}$ or $^{3}/_{16}$-in-thick faces and in all panels with or $^{1}/_{20}$-in-thick faces were fully resisted. Most of the $^{25}/_{32}$ 12 × 12-in. panels with phenol-resorcinol-resin glue lines resiste internal stresses due to exposure, the panels with $^{1}/_{4}$-in-thi faces being somewhat more satisfactory.

Influence of Hardwood and Softwood Species for Core

Internal stresses in cross-laminated panels, resulting fro differences in the dimensional instability of the laminae paral and perpendicular to their fibers, may be reduced by using f the cross-ply those wood species which have a relatively l

---

[4] *Wood Products*, vol. 50, July, 1945, p. 12.

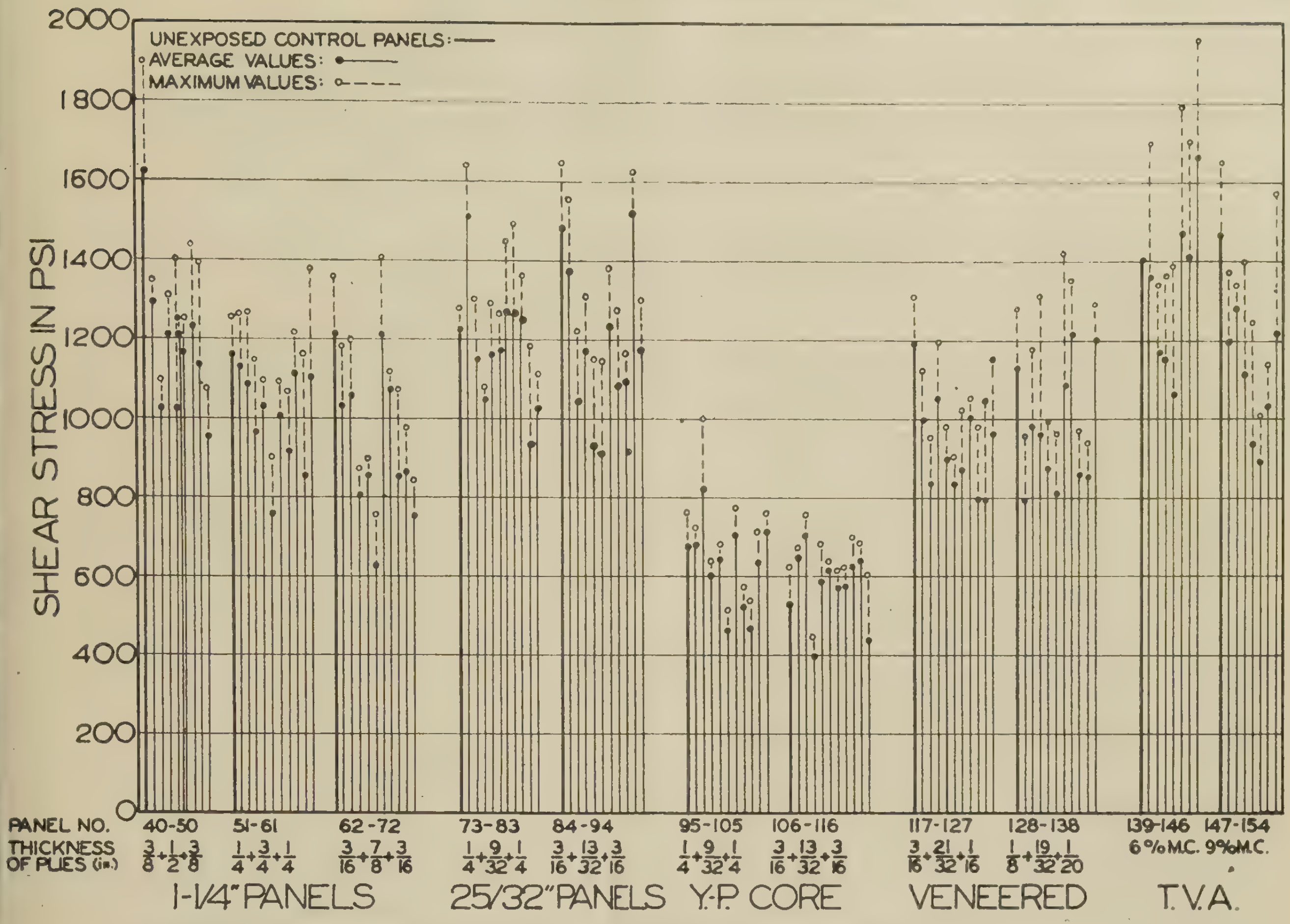

Fig. 5 Diagrammatic Summary for Average and Maximum Shear Resistance of Glue Lines of 12 × 12-In. Panels

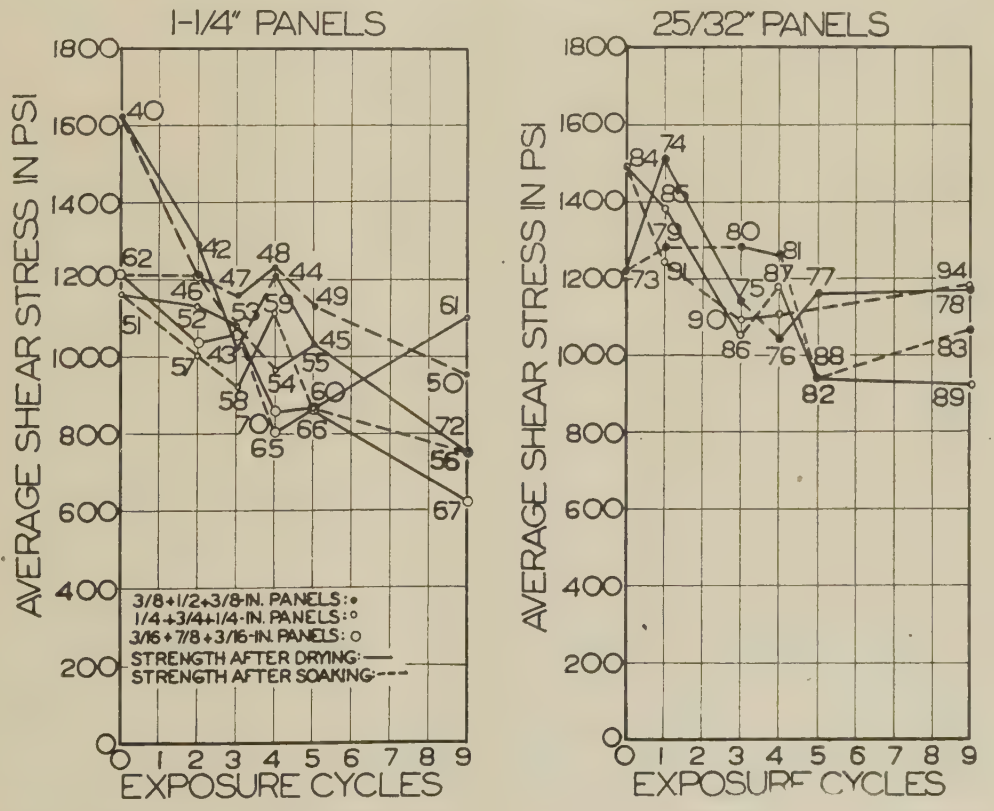

Fig. 6 Average Shear Resistance of Glue Lines of 12 × 12-In. Panels as Influenced by Exposure and Test Variables

TABLE 1(*a*) DURABILITY OF 7 × 7-IN. PANELS

Test Panel	Plies		Control Panel	Exposure					
	Faces in.	Core in.		D	DS	DS Cycles	S	SD	SD Cycles
25/32" Oak	5/16	5/32	-	000	-	-	X	0	-
	1/4	9/32	X	0XX	XX	XX	X	0	-
	3/16	13/32	-	0XX	X	X0	XX	X	0X
	1/20	21/32	-	X	X	X	X	X	X
	1/16	21/32	-	X	X	X	X	X	X

TABLE 1(*b*) DURABILITY OF 12 × 12-IN. PANELS

Test Panel	Plies		Control Panel	Exposure Cycles					Exposure Cycles				
	Faces in.	Core in.		D or DD	DDD	DDDS	DDDSD	DDDSD +SDSD	S or SS	SSS	SSSD	SSSDS	SSSDS +DSDS
1-1/4" Oak	3/8	1/2	X	XXXX	XXX	0X	X	-	XXXXX	XX0X	X0X	0X	0
	1/4	3/4	X	XXXXX	XXXX	XXX	XX	0	XXXXX	XXXX	0XX	0X	0
	3/16	7/8	X	XXXXX	XXXX	XXX	XX	0	XX0X0	X000	000	00	0
25/32" Oak	1/4	9/32	X	XXXXX	XXXX	0XX	XX	X	XXXXX	X0XX	0XX	0X	X
	3/16	13/32	X	XXXXX	XXXX	XXX	XX	0	XXXXX	X0XX	0XX	XX	0
Y.P. Core	1/4	9/32	X	XXXXX	00X0	0X0	00	0	XXXXX	0XXX	000	00	0
	3/16	13/32	X	XXXXX	XXXX	XXX	00	0	XXXXX	X0XX	00X	00	0
Ve-neered	3/16	21/32	X	XXXXX	XXXX	XXX	X0	-	0XXXX	XX0X	00X	0X	X
	1/8	19/32	X	XXXXX	XXXX	XXX	0X	-	XXXXX	XX00	X00	00	0

Key: D = Drying
S = Soaking
X = No observation of failure upon exposure
O = Observation of failure upon exposure

modulus of elasticity in shear parallel to the fibers. In the case of 3-ply laminated or cross-laminated balanced flooring, the damping capacity of the flooring can also be increased by using material with high damping capacity for the core of the panel. By yielding slightly, spruce or fir in the center ply of laminated lumber relieves some of the internal stresses, thus reducing the tendency to rupture in or along the glue lines. Virginia pine, soft maple, yellow poplar, cottonwood, buckeye, and other softwood species have been recommended for this purpose. Ready availability of these species in the same general vicinity of the over-all logging operations for the oak to be used for the face plies is of course a necessity from the economic viewpoint.

The possible advantages of the use of a soft core wood led to the performance of a series of tests to determine their value as core material in 3-ply cross-laminated flooring. Experiments were performed on $^{25}/_{32}$-in. cross-laminated panels with $^{9}/_{32}$ and $^{13}/_{32}$-in-thick yellow-poplar cross-laminated cores between $^{1}/_{4}$ and $^{3}/_{16}$-in-thick oak faces, respectively.

During the 48-hr test period, these panels were dried out approximately just as much as the other all-oak panels under investigation, while the water absorption of yellow-poplar-core panels was only slightly, if any, larger than that for all-oak panels.

The durability of the yellow-poplar-core panels was limited by the shear resistance of the yellow-poplar to the internal stresses caused by exposure, as fully satisfactory glue lines between yellow-poplar core and oak faces could be obtained, evidenced by 100 per cent yellow-poplar shear failure in shear tests, and by consistent yellow-poplar shear failure, if any, for the test panels. The FPL shear-parallel-to-grain strengths (corrected for 12 per cent moisture content) of 1100 and 2000 psi, respectively,[5] for yellow poplar and white oak compare with corrected shear-strength data of 575 and 1190 psi for cross-laminated test specimens sawed from $^{25}/_{32}$-in. oak-faced panels with yellow-popl and oak cores, respectively. Thus the shear-parallel-to-gra strength of yellow poplar is 55 per cent of that of white oak, an the strength of the yellow poplar cross-laminated to oak is 48 p cent of that of oak cross-laminated to oak. The shear-streng values for cross-laminated yellow-poplar-core and all-oak pane are 48 and 40 per cent smaller than for the respective woo species.

None of the yellow-poplar-core panels exposed to either a sing drying or soaking cycle showed any wood or glue failure. T more balanced panels with $^{13}/_{32}$-in. cores also withstood repe tive drying and soaking, and even single reversals of exposu from drying to soaking, while some of the less balanced pane with $^{9}/_{32}$-in. cores showed incipient failures during their repetiti exposures. All yellow-poplar-core panels failed, however, up repetitive soaking or repetitive drying followed by single or petitive soaking.

The dimensional stability of cross-laminated yellow-popla core panels, parallel to the grain direction of the oak faces, wa found to be somewhat greater than for the corresponding al oak. On the other hand, the dimensional stability of thes panels perpendicular to the grain direction of the oak faces wa somewhat smaller than for the corresponding all-oak panels.

The over-all warpage and cupping of the yellow-poplar-cor panels were the minimum to be expected for the exposure extreme to which the panels were subjected and were smaller than for th corresponding all-oak panels. This relation held even upon ob servation of initial local shear failures which resulted in limite release of restraint to warpage and cupping. Hence $^{25}/_{32}$-in thick oak panels with a cross-laminated core of clear yellow pop lar can be considered to remain flat under normal exposure con ditions and satisfactorily flat even under the more extrem conditions which do not call for advanced shear failure of th core.

The test observations led to the following conclusions: (1

---

[5] "Strength and Related Properties of Woods Grown in the United States," by L. J. Markwardt and T. R. C. Wilson, U. S. Department of Agriculture Technical Bulletin No. 479, Table 1, 1935.

TABLE 2(*a*) SHEAR RESISTANCE OF GLUE LINES OF 7 × 7-IN. PANELS IN PSI

Test Panel	Plies Faces in.	Plies Core in.	Control Panel	Exposure Cycles DS	Exposure Cycles SD	Control Panel	Exposure Cycles DS	Exposure Cycles SD
			For Moisture Content at Test			Adjusted for 12 Pct. Moisture Content		
25/32" Oak	1/4	9/32	1040	1080	—	890	910	—
	3/16	13/32	—	1140	1230	—	1050	940
	1/20	21/32	—	1510	1590	—	1310	1200
	1/16	21/32	—	1520	1270	—	1275	990

TABLE 2(*b*) SHEAR RESISTANCE OF GLUE LINES OF 12 × 12-IN. PANELS IN PSI

Test Panel	Plies Faces in.	Plies Core in.		Control Panel	Exposure Cycles D or DD	DDD	DDDS	DDDSD	DDDSD +SDSD	Exposure Cycles S or SS	SSS	SSSD	SSSDS	SSSDS +DSDS
1-1/4" Oak	3/8	1/2	For M.C. at Test	1620	1290	1020	1210	1020	—	1210	1160	1230	1130	950
	1/4	3/4		1160	1130	1080	960	1030	750	1000	910	1110	850	1100
	3/16	7/8		1210	1030	1050	800	850	620	1210	1070	[illegible]	860	750
25/32" Oak	1/4	9/32		1220	1510	1145	1040	1160	1170	1230	1280	1260	940	1030
	3/16	13/32		1490	1380	1050	1150	940	920	1240	1090	1100	1530	1180
Y.P. Core	1/4	9/32		680	690	630	610	650	470	710	520	470	640	720
	3/16	13/32		630	650	710	400	520	620	570	500	630	650	440
Veneered	3/16	21/32		1200	1000	840	1060	900;940	--	880	1010	800	800	970
	1/8	19/32		1140	800	990	970	800;820	--	1060	1220	870	860	1210
1-1/4" Oak	3/8	1/2	Adjusted for 12 Pct. M.C.	1400	1000	970	980	600	—	1090	1050	965	990	820
	1/4	3/4		1000	890	860	830	800	560	930	760	890	750	800
	3/16	7/8		1030	820	830	670	660	470	1080	970	690	750	630
25/32" Oak	1/4	9/32		1090	1230	960	900	940	910	1130	1060	1020	800	870
	3/16	13/32		1290	1100	840	1080	780	700	1110	990	920	1280	1010
Y.P. Core	1/4	9/32		590	575	650	525	520	360	640	490	320	550	580
	3/16	13/32		560	540	560	350	470	470	510	520	520	560	405
Veneered	3/16	21/32		960	750	650	870	640;580	—	770	910	590	670	820
	1/8	19/32		970	600	700	740	615;600	--	890	1060	650	710	1000

Key: D = Drying
S = Soaking
Underlined values for panels showing test failures

$^5/_{32}$-in. cross-laminated panels with a $^{13}/_{32}$-in. yellow-poplar core withstand more extreme exposure conditions than those with a $^9/_{32}$-in. yellow-poplar core; (2) panels with a core of either thickness withstand extreme exposures satisfactorily, provided these exposures are not repetitive; and (3) panels with $^{13}/_{32}$-in. core withstand even extreme repetitive exposures, provided they are not repetitively reversed from one extreme to the other. The observed failures, however, indicate that the shear resistance parallel to the grain of cross-laminated yellow poplar is insufficient to withstand the most extreme exposure conditions which may occur in service. Therefore it appears that soft hardwood species similar in their characteristics to yellow poplar can be used satisfactorily as core material in cross-laminated panels, provided (1) the core is not too thick, (2) the thicknesses of the two surface plies are well balanced, and (3) the finished product is not exposed to too extreme conditions.

INFLUENCE OF TREATMENT OF FACES

In the preliminary tests on the 7 × 7-in. cross-laminated panels, it was determined that a minimum of internal stresses caused by exposure, to the test extremes, hence maximum resistance to failure, could be assured if the faces consist of thin laminae. In the case of flooring, the top face must be planed and sanded, and must be thick enough to withstand considerable wear and possible resanding after use and abuse. If thin veneers are to be used for the top face of 3-ply cross-laminated flooring, they should be treated to increase their resistance to wear. Such treatment would also somewhat stabilize the dimensions of the faces and provide a moisture sealer, a feature desirable for retarding fluctuations in moisture content of the panels and, consequently, for decreasing sudden temporary extremes in internal stresses due to exposure. Simultaneously, such treatment may allow final finishing of the flooring during the assembly bonding, by polymerizing the impregnating material with the pressure and heat required for setting of the glue lines. Veneers can be sawed smoothly enough to allow satisfactory bonding without sanding. Hence $^1/_8$ and $^3/_{16}$-in-thick sawed veneer, sanded only on the one side exposed to view upon cross-laminating, were selected for the tests. These veneers were impregnated with Du Pont's "Arboneeld." However, other possibly more satisfactory materials might have been used, particularly since more complete penetration and better wear resistance of the surface would have been desirable and since a very high pressure must be applied to Arboneeld-impregnated wood to obtain the desirable glossy surface finish. Many of the tapelessly spliced joints of the veneers failed during drying after impregnation because of unequal shrinkage of the veneer strips. Hence many of the faces consisted of two individual veneer strips, not of a single veneer.

Cross-laminated oak panels with impregnated face veneers revealed satisfactory resistance to the single, repetitive, and reversed exposures of 48-hr drying and soaking. Many of the panels withstood the internal stresses due to exposures and did not show any failures. Most of the exceptions were panels with spliced faces with thicknesses of adjacent veneers varying too much to allow a satisfactory bond along the edges of adjacent veneers. Sanding of the veneers after instead of before impregnation would have resulted in a more uniform thickness and probably would have eliminated local glue-line failures along face joints during exposure. The impregnated face veneers did not show any checks, while the relatively thick untreated core of some of the panels checked considerably during repetitive exposures. Drying and moisture absorption of the panels during exposure were considerably retarded, if compared with those for panels with nonimpregnated faces. While, for instance, the moisture content of the latter panels upon repetitive 48-hr soaking reached values as high as 30 per cent, the moisture content of the panels with impregnated faces of $^1/_8$ and $^3/_{16}$ in. thicknesses rose to no more than 19 and 25 per cent, respectively.

Shrinkage and swelling of panels with impregnated face veneers was reduced some, but did not differ greatly from other all-oak panels withstanding the extreme exposure cycles. However, no such extreme shrinkage and swelling could be observed for the former panels as was found for some of the latter panels. Better stabilization might have been obtained with more complete impregnation of the faces. Because of the uniformity in change in dimensions without any extremes, even the observed degree of stabilization can be considered advantageous.

The observed warpage and cupping during exposure of panels with impregnated and nonimpregnated faces were very similar.

The average shear resistance of the glue lines between impregnated oak veneers and the nonimpregnated oak core of two nonexposed $^{25}/_{32}$-in. cross-laminated panels was 1170 psi and, corrected for 12 per cent moisture content of the wood, was 970 psi. These values compared with 1355 and 1190 psi, respectively, for $^{25}/_{32}$-in. cross-laminated oak panels, and with 655 and 575 psi, respectively, for $^{25}/_{32}$-in. cross-laminated yellow-poplar-core panels. The average shear resistance for 20 exposed panels was 940 psi and, corrected for 12 per cent moisture content, was 740 psi. Thus the resistance was respectively 20 and 26 per cent smaller than for the nonexposed panels, and compared with 1170 and 980 psi, respectively, for the all-oak panels, and with 605 and 520 psi for the yellow-poplar-core panels.

The increased difference in dimensional stability between impregnated faces parallel to their grain and the nonimpregnated core perpendicular to its grain, as compared with the difference in panels with untreated faces, resulted in large internal stresses due to exposure and may be the reason for the large (20 and 26 per cent) decreases in average strength of the exposed glue lines. These values compare with the reported 14 and 18 per cent decreases for the all-oak panels, and the 7 and 10 per cent decreases for the yellow-poplar-core panels. Since many of the panels with impregnated faces withstood the extreme exposure conditions, the limited shear resistance of the glue lines must have been sufficient to offset the internal stresses due to exposure.

The information obtained for the 3-ply cross-laminated test panels with impregnated face veneers indicates that such panels, even if subjected to extreme service conditions, should satisfactorily resist any internal stresses resulting from exposure, provided these panels were properly assembled.

Influence of Manufacturing Conditions

To obtain comparative data for laboratory-assembled and TVA-manufactured 3-ply cross-laminated all-oak flooring, $^{25}/_{32}$ × 12 × 12-in. panels with 3 plies of uniform thickness and hot-glued in the continuous TVA press were subjected to exposure simultaneously with similar panels cold-glued in the laboratory. Preliminary test data indicated that entirely satisfactory glue lines can be obtained with the phenol-resorcinol glue if used either hot or cold, provided proper gluing procedures are followed. Thus a direct comparison can be made between the laboratory- and TVA-assembled panels, although the oak used for the two panel series was not matched. The VPI panels were made from oak having a moisture content of approximately 9 per cent. The TVA panels were assembled with conditioned slats having a moisture content of approximately 6 or 9 per cent, in order to determine the benefit, if any, of lower or higher moisture content of the oak during its assembly.

The testing of the panels produced in the TVA pilot plant revealed that there was some discontinuity of glue lines, some appreciable variation in slat thickness between adjacent slats, and some use of oak of insufficient strength for the core material. These deficiencies became apparent in localized failures during the exposure tests. Plans are being made at the plant for correcting these deficiencies. Stress concentrations due to exposure along the glue lines adjacent to the localized glue-line deficiencies resulted in glue-line failures, defective panels, relatively large dimensional instability, and excessive warpage and cupping. The use of rubber glue-spreader rolls, the installation of restraining rollers of decreased width in the feeding mechanism of the TVA press, closer control of slat thickness, and elimination of decayed and low-strength slats for core material should alleviate the deficiencies found in the TVA panels and make them suitable for use under conditions in which even abnormal exposures are expected.

The glue lines of the unexposed panel assembled with slats having 9 per cent moisture content were 14 per cent stronger than those of the unexposed panel assembled with slats having 6 per cent moisture content. On the other hand, glue lines of the exposed panels assembled with slats having 9 per cent moisture content were 17 per cent weaker than those of the exposed panels assembled with slats having 6 per cent moisture content. A comparison of the glue-line strength of unexposed and exposed panels indicates decreases in strength of 7 and 33 per cent for panels assembled with slats having 6 per cent and 9 per cent moisture content, respectively. These data compare with a decrease in strength of 12 per cent due to exposure for the corresponding laboratory-assembled panels. A comparison of the glue-line strength data for TVA hot-glued and VPI cold-glued panels indicates that the unexposed TVA panels assembled with slats having 6 and 9 per cent moisture content were 6 per cent and 21 per cent, respectively, stronger than the VPI panel, while the exposed panels were, respectively, 12.5 per cent stronger and 6 per cent weaker than the VPI panels.

It is doubtful whether valid comparisons can be made of the foregoing data on the strength of the glue lines, because of the variation in thickness and discontinuity of the glue lines, and particularly because of stress concentrations due to discontinuity both during exposure and testing. Although the glue lines of hot-assembled panels were expected to be approximately 9 per cent stronger than those for cold-assembled panels, according to preliminary test data, and although the glue lines for the TVA panels were not continuous throughout the width of the panels and test specimens, the data indicate the completely satisfactory polymerization of the glue lines in the continuous press and during subsequent storage conditioning. Even for the locally strong bond, however, the glue-line stress concentrations during exposure were excessive because of the discontinuity of the glue lines. Thus more or fully continuous glue lines for the TVA assembled panels should fully eliminate the occurrence of any glue-line failures on exposure to extreme service and laboratory conditions.

CONCLUSIONS

Exposure conditions which may occur in service were found to be a limiting factor for the cross-laminating of oak. Exposure to 48-hr soaking of panels previously conditioned to 9 per cent moisture content was more severe than exposure to 48-hr oven-drying at 97 C. One or two complete exposure cycles of 48-hr drying or soaking were withstood by almost all properly balanced and assembled $1^{1}/_{4}$ and $^{25}/_{32}$-in-thick panels cross-laminated with phenol-resorcinol-resin glue, while a limited number of repetitive or reversed exposures were withstood by the majority of those panels. Hence such panels should be satisfactory even under extreme service conditions.

Phenol-resorcinol-resin glue proved to be more desirable than urea-formaldehyde-resin glue for cross-laminating panels subjected to extreme exposure conditions. For panels with a minimum of internal stresses due to extremes in exposure, such as thin cross-laminated panels with thin face plies, urea-formaldehyde-resin glue can be used satisfactorily.

The thickness of the cross-laminated panels influenced the resistance to exposure. Thus $1^{1}/_{4}$-in-thick panels, assembled with urea-formaldehyde glue, failed upon exposure, while many of the $^{25}/_{32}$-in-thick panels, assembled with this glue, proved to be satisfactory. Better resistance to exposure also was found for $^{25}/_{32}$-in-thick panels cross-laminated with phenol-resorcinol-resin glue than for $1^{1}/_{4}$-in-thick panels, assembled with this glue.

Thin face veneers proved to be exceedingly satisfactory for 3-ply cross-laminated panels exposed to extreme conditions. However, if in order to provide greater surface-wear life, thicker faces are a requirement, for $1^{1}/_{4}$-in-thick panels, the combination of $^{1}/_{4}$-in-thick façes and a $^{3}/_{4}$-in-thick core may be the most satisfactory one of those tested; and for $^{25}/_{32}$-in-thick panels, the combination of $^{1}/_{4}$-in-thick faces and a $^{9}/_{32}$-in-thick core might be preferable to the one with $^{3}/_{16}$-in-thick faces and a $^{13}/_{32}$-in-thick core.

Yellow-poplar-core panels with oak faces could be assembled and withstood exposure satisfactorily, provided the core was not too thick, the thicknesses of the two surface plies were well balanced, and exposure was not too extreme. Thus the combination of a soft hardwood core and oak faces was found entirely feasible for 3-ply cross-laminated panels with an over-all thickness of $^{25}/_{32}$ in.

Impregnation of thin face plies can be advantageous as regards resistance to exposure of the cross-laminated panel.

Laboratory-assembled panels proved to be more satisfactory than those glued up in the continuous press of the Tennessee Valley Authority because of certain deficiencies in the assembly of the latter panels. Since these deficiencies can be eliminated easily, and consequently fully satisfactory glue lines can be obtained, panels properly manufactured with the continuous press should withstand such exposure as may occur even under extreme service conditions.

Stress Notch Sensitivity With Eccentric Holes

By L. SCHAPIRO,[1] and R. H. ESLING,[1] SANTA MONICA, CALIF.

The tension strength of several cross sections containing holes of several diameters in several positions of eccentricity have been determined experimentally for aluminum alloys 24S-T, 75S-T, and 14S-T. A mathematical expression is suggested for the relationship between strength, hole size, and eccentricity of hole. The relative stress notch sensitivity of the three aluminum alloys is found to be the same with eccentric holes as had been reported for central holes or external notches.

Nomenclature

The following nomenclature is used in the paper:

E = eccentricity, dimensionless
x = fraction of cross-sectional area removed by a hole, dimensionless
s = distance from axis of hole to original center of the section, in.
c = width of the section parallel to s, in.
S_u = ultimate strength of material without holes, psi
S_n = ultimate strength of a specimen containing a hole, psi
$y = \dfrac{(1-x)S_n}{S_u}$ (gross area efficiency), dimensionless
y_0 = y value of a central holed specimen, dimensionless
m = constant
n = constant
e = base of natural logarithms
$A = \log_{10} \mathrm{e}$
p = constant
u = constant
v = constant

General

Spar caps containing large bolt holes are becoming more common in aircraft wing construction. A knowledge of the static strength of a section containing an eccentric hole and a comparison of spar cap materials in this condition are quite desirable. Moseley[2] has studied this problem and has indicated a need for further investigation. He also has indicated the presence of a "size effect" in his test results.

Further studies of this problem are now reported, seeking to clarify the following points:

1 Can the "size effect" be evaluated?

2 Can the effect of hole eccentricity be mathematically evaluated in a manner similar to the evaluation of "notch strength" advanced by one of the authors?[3]

3 Is the evaluation of notch strength thus advanced[3] invalid for central holes, as reported by Stevenson?[4]

Materials and Specimens

Aluminum alloys 14S-T, 75S-T, and 24S-T were studied. A complete test series was conducted for 24S-T alloy only, since previous tests rated it the most stress-notch-sensitive of the three alloys. By "stress notch sensitivity" the authors refer to a parameter that indicates the effect of a notch, or any section discontinuity, upon the static ultimate stress of the material. The relationships disclosed for this alloy were spot-checked with the other two materials.

The complete test series comprised six different cross sections from $^1/_{20}$ sq in. (0.10 × 0.50 in.) to 4.5 sq in. (1.50 × 3.00 in.), three hole sizes of 10, 20, 30 per cent removed area, and two positions of eccentricity in addition to central holes. Each specimen geometry, evaluated for each alloy, was tested in duplicate.

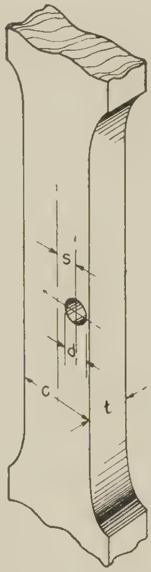

Fig. 1 General Shape of Tension Specimen With Eccentrically Positioned Hole

The complete test series for the 24S-T alloy was not obtainable from one lot of material. The two lots used were of somewhat different properties. For one lot, mean ultimate strength (of eight tests) was 69,250 psi with mean 2-in. elongation 14.7 per cent; for the other lot, mean ultimate strength was 69,800 psi with mean elongation 17.3 per cent. The variation in ductility of the two lots of material is believed to affect the stress notch sensitivity, and test results are co-ordinated with material batch.

Test specimens were of the customary shoulder type with the parallel-sided portion 2 in. or longer. Fig. 1 illustrates a specimen with an eccentric hole.

Methods of Test

Loading. Static tension loading to rupture was performed in either of two Baldwin-Southwark hydraulic testing machines (capacities 60 kips and 400 kips, respectively) equipped with Tate-Emery weighing systems. Specimens were held in the test machine by means of wedge grips. Special care was used in aligning a specimen visually during gripping to obtain axial loading. Specimens were loaded hydraulically at a rate in the elastic range (an autographic 2-in. nonaveraging extensometer was attached to each specimen) of 1 per cent strain per min, and in the plastic range of 30 per cent strain per min.

Load Measurement. Maximum load was read from the Tate-Emery recorder for all specimens which fractured instantaneously across the entire section. Some specimens with eccentric holes, especially at the larger eccentricity values, first fractured across the smaller section only. At this first fracture the load dropped automatically (with redistribution of strain), and then increased until the remaining section fractured. In some cases

---

[1] Douglas Aircraft Company, Inc.

[2] "Notch Effects in High-Strength Aluminum Alloy Spar Caps," by D. L. Moseley, *Journal of the Aeronautical Sciences*, vol. 13, 1946, p. 397.

[3] "Notch Sensitivity of High Strength Aluminum Alloys—Theoretical Aspects," by L. Schapiro and H. E. North, *Journal of the Aeronautical Sciences*, vol. 13, 1946, p. 391.

Presented at the Aviation Division Meeting, Los Angeles, Calif., May 26–29, 1947, of The American Society of Mechanical Engineers.

Note: Statements and opinions advanced in papers are to be understood as individual expressions of their authors and not those of the Society.

[4] "The Effects of Open Holes on the Tensile Strength of Some Aluminum Alloys," by C. H. Stevenson, *Journal of the Aeronautical Sciences*, vol. 13, 1946, p. 395.

the load at second fracture was higher and in some cases lower than the load at first fracture. For such specimens, first fracture load was used for the ultimate strength value.

Computations. Ultimate strength is computed in all cases as maximum load divided by initial area. For specimens containing holes, initial area is considered as cross-sectional area calculated from outer dimensions less area of hole. For specimens with holes, the ultimate strength so calculated is termed notched strength.

No standard method of expressing eccentricity is extant. Moseley's eccentricity expression is convenient and quite suitable.[3] Eccentricity is expressed as the ratio of the shift of the center of gravity of a cross section (due to the presence of a hole) to the original width (measured parallel to the direction of the shift of the center of gravity). It can be shown that this definition can be expressed as

$$E = \frac{x}{1 - x} \cdot \frac{s}{c} \qquad [1]$$

With this manner of expressing eccentricity, its largest value would occur when the edge of a hole is at the edge of a specimen. For this maximum eccentricity, the numerical value decreases from 0.5 as the hole diameter decreases. Fig. 2 illustrates this eccentricity parameter and could be used by other interested investigators. By way of example, a specimen having a hole diameter that is 0.2 of the specimen width with the hole eccentrically positioned so that its center is displaced from the specimen axis by 0.2 of the specimen width would be assigned an eccentricity of 0.05.

Plots are made of notch-strength ratio versus eccentricity for constant removed areas, and a three-dimensional plot relating notch-strength ratio, removed area, and eccentricity is constructed. An equation is derived for the three-dimensional surface of relationship, and a physical significance of the constants in the equation is suggested. The stress notch sensitivity of the three test materials is compared on the basis of the constants of their respective equations of relationship. Notch-strength ratio, $[(1 - x)S_n]/S_u$, is plotted instead of notched strength as a more definite relationship with the other factors is established thereby.

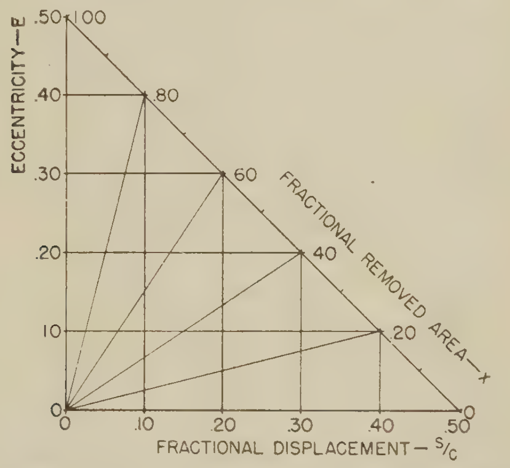

Fig. 2 Relationship of Eccentricity E With Hole Size x and Hole Displacement s/c Given by Equation $E = \frac{x}{1 - x} \cdot \frac{s}{c}$

Results and Discussion

Central Holes. Test data for central holes in 24S-T material are plotted in Fig. 3 to reveal size effect of cross section. F each hole size (i.e., constant fraction of removed area), the notch strength ratio, $[(1 - x)S_n]/S_u$, appears to decrease with i creasing area of cross section (dotted lines in Fig. 3). When however, the test data are considered in terms of the two di tinct lots of test material (as previously described), a constanc of notch-strength ratio seems evident without a size effect (soli lines in Fig. 3). This interpretation of the test data, to rule ou size effect, appears to be substantiated also by the results of th eccentric-hole tests. Replotting the data of Fig. 3, without si effect, further emphasizes the difference between the two lots o test material, Fig. 4. The relationship between notch strengt and notch depth for these two lots is approximated by the equa tions

$$y_0(\text{24S-T}) = 0.912e^{-0.480Ax} \text{ (Lot No. 1)}$$

$$y_0(\text{24S-T}) = 0.862e^{-0.492Ax} \text{ (Lot No. 2)}$$

which are of the form

$$\frac{(1 - x)S_n}{S_u} = me^{-nAx} \qquad [2$$

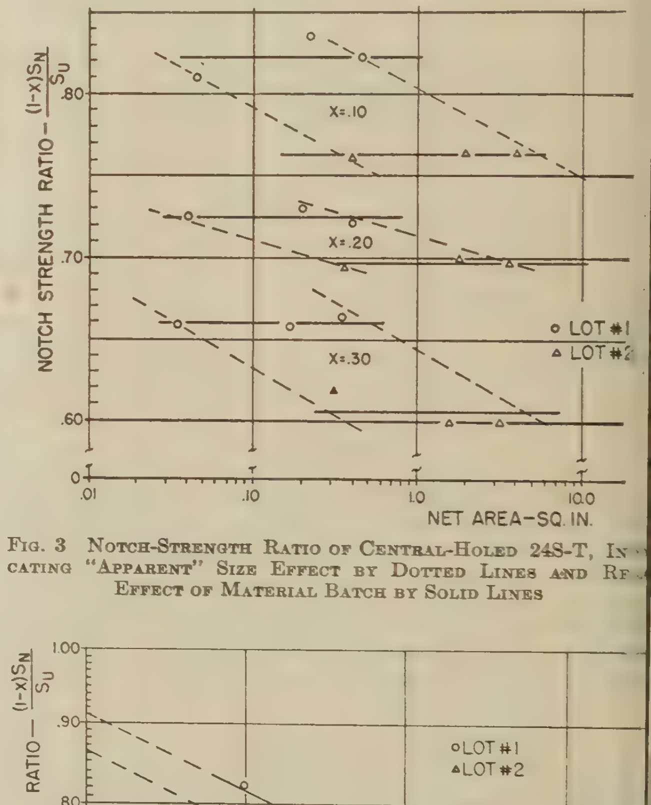

Fig. 3 Notch-Strength Ratio of Central-Holed 24S-T, In cating "Apparent" Size Effect by Dotted Lines and R Effect of Material Batch by Solid Lines

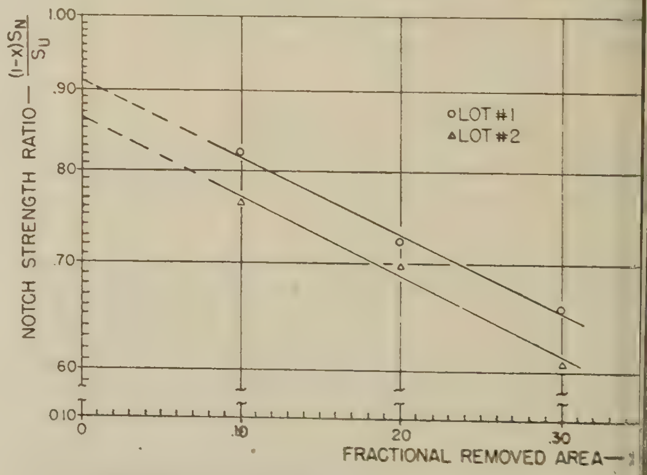

Fig. 4 Notch-Strength Ratio of Central-Holed 24S-T, Re plotted From Fig. 3, Without Effect of Size

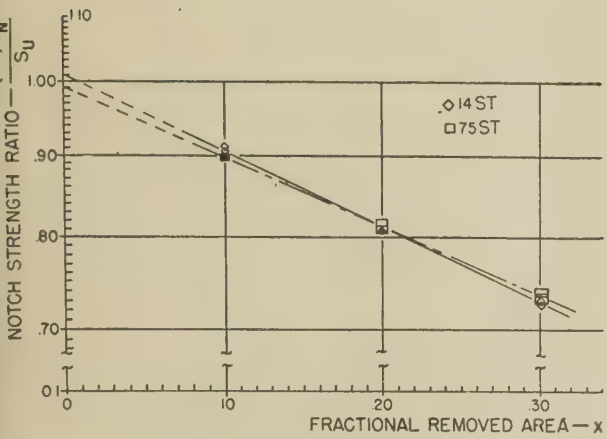

FIG. 5 NOTCH-STRENGTH RATIO OF CENTRAL-HOLED 14S-T AND 75S-T

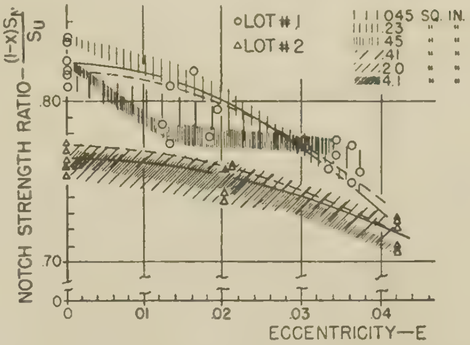

FIG. 6 NOTCH-STRENGTH RATIO OF ECCENTRIC-HOLED 24S-T WITH HOLE SIZE $x = 0.10$

(Solid curves are best fits to data; dotted curves are plotted from Equation [5]. Solid points are two coincident test results.)

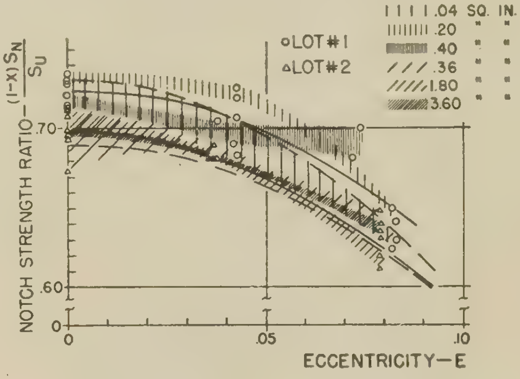

FIG. 7 SAME AS FIG. 6 FOR $x = 0.20$

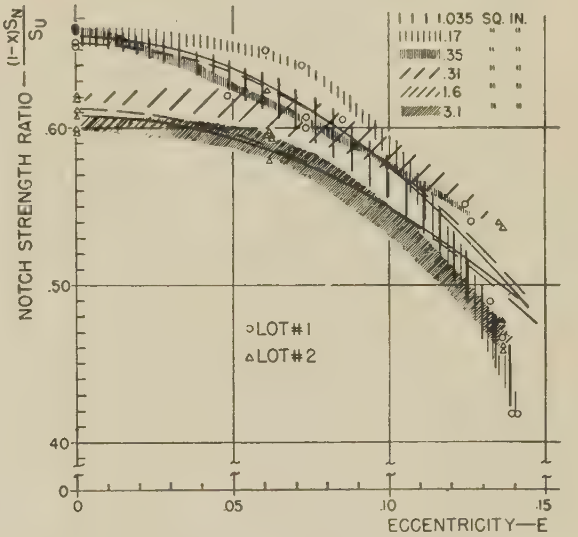

FIG. 8 SAME AS FIG. 6 FOR $x = 0.30$

It should be noted that for central holes the value of m is not unity, as one of the authors had previously indicated.[3] Fig. 4 corroborates the data reported by Stevenson.[4] Spot-check data for 14S-T and 75S-T, with one cross section only, are presented in Fig. 5 and are approximated by the respective equations

$$y_0(\text{14S-T}) = 1.01e^{-0.486Ax}$$

$$y_0(\text{75S-T}) = 1.00e^{-0.445Ax}$$

The constants m and n of Equation [2] both serve as an index of stress notch sensitivity and may be physically interpreted in the following manner: m is an index of the stress notch sensitivity of a material "to the presence of an infinitely small" central hole; n is an index of the stress notch sensitivity of a central holed material "to increasing hole size." It would thus appear that the strength of alloys 14S-T and 75S-T is not sensitive to a central hole (m is approximately unity for both) but that alloy 24S-T is markedly sensitive to a central hole (average m 0.887). All three alloys are of nearly equal sensitivity to increasing hole size of a central hole.

It may also be said that the effect of the presence of a central hole is greater than the effect of hole size on the strength of these alloys (the variations of m are greater than the variations of n).

Eccentric Holes. Test results with eccentric-holed specimens are presented in Figs. 6 to 8, inclusive, for the two lots of 24S-T, and in Figs. 9 and 10 for the spot-check tests with 14S-T and 75S-T. The 24S-T results indicate no size effect but a definite difference between the two lots of material.

Parabolic curves of the form

$$E^2 = -4p\,(y - y_0) \quad [3]$$

are fitted to the test data, and the relationship between p and x for each material is determined graphically. The relationship is indicated in Fig. 11 for all test materials and is of the form

$$p = u\,x + v \quad [4]$$

The combination of Equations [1], [2], [3], and [4] expresses the total relationship between notch strength, hole size, and eccentricity of hole, and is given by

$$y = me^{-nAx} - \frac{1}{4}\left(\frac{x}{1-x}\right)^2 \frac{(s/c)^2}{ux + v} \quad [5]$$

The three-dimensional relationship represented by Equation [5] is illustrated in Fig. 12 for the 24S-T material (lot No. 1). The constants m, n, u, and v of Equation [5] are all material constants with some physical significance. The constants m and n are the same ones discussed for central holes and retain the same physical significance with eccentric holes. The additional material constants u and v may be physically interpreted in the following manner: v is an index of the stress notch sensitivity of an infinitesimally holed material to increasing eccentricity; u is an index of the effect of hole size on v.

A tabulation of the Equation [5] material constants for 24S-T, 14S-T, and 75S-T aluminum alloys is presented in Table 1. From

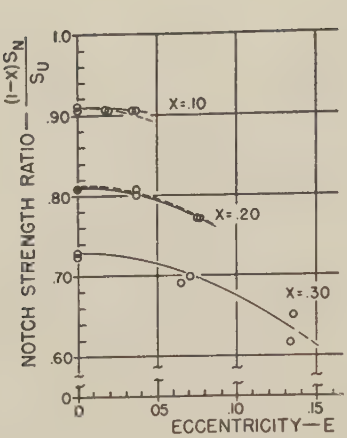

Fig. 9 Notch-Strength Ratio of Eccentric-Holed 14S-T
(All notations as per Fig. 6.)

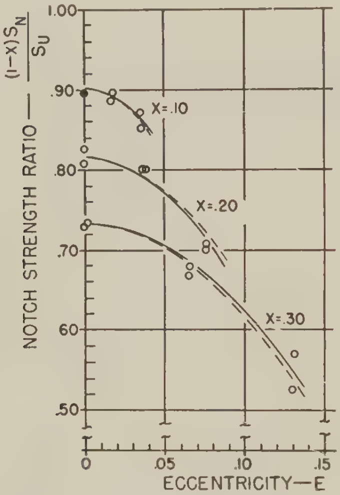

Fig. 10 Notch-Strength Ratio of Eccentric-Holed 75S-T
(All notations as per Fig. 6.)

these constants it may be concluded that alloy 24S-T is more stress-notch-sensitive than alloys 14S-T and 75S-T in respect to a central hole or an eccentric hole. Alloys 14S-T and 75S-T are of nearly equal stress notch sensitivities in respect to a central hole but alloy 75S-T is somewhat more sensitive to an eccentric hole.

Conclusion

The authors' attempt at approximating notch-strength data by a mathematical formula and using the constants of such a formula for comparing materials has been performed in the hop that other investigators may seek to apply the formula to othe metals and thereby make a small step forward in basic knowl edge. A mathematical valuation of stress notch sensitivit may relate to a corresponding valuation for "brittleness" an "triaxiality."

TABLE 1 STRESS NOTCH SENSITIVITY MATERIAL CONSTANTS

Constants	14S-T	75S-T	24S-T[a]
m, index for central hole.....	1.01	1.00	0.887
n, index for increasing hole size of central hole......	0.486	0.445	0.486
v, index for eccentricity......	0.026	0.0005	—0.007
u, index of hole size effect on *v*.....................	0.062	0.075	0.14

[a] Mean value for Lots Nos. 1 and 2.

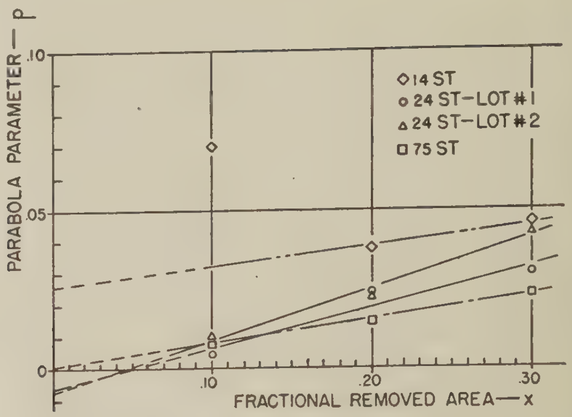

Fig. 11 Graphical Solution of Equation [4]

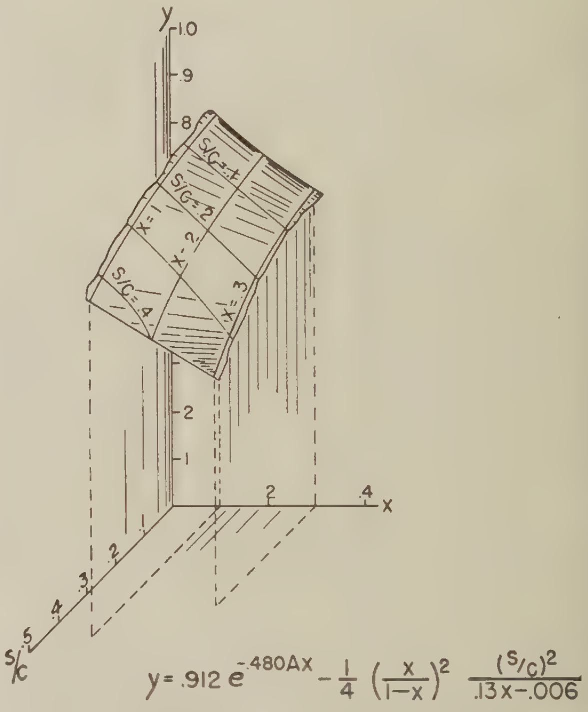

Fig. 12 Three-Dimensional Relationship Between Notc Strength Ratio, Hole Size, and Hole Displacement for 24S- Lot No. 1

Discussion

Some Effects of Pressure Loss on the Open-Cycle Gas-Turbine Power Plant[1]

J. K. **Salisbury.**[2] The writer was interested to compare the esults obtained by Messrs. Yellott and Lype with those obained by methods which he presented in a discussion of a paper ;iven before The Society of Naval Architects and Marine Engiieers.[3] When corrected for the slightly different viewpoint aken by the authors, the agreement between the two results is xcellent. The authors have found, for certain conditions, a derease in thermal efficiency of 9.5 per cent, which corresponds to .n increase in fuel rate of 10.50 per cent, while the writer's method indicates a loss of 10.54 per cent. The curves from the original discussion are reproduced herewith, in the thought that they may be of general interest, together with an outline of their derivation.

A few differences in viewpoint exist between the authors' method of approach to the problem, and that used by the writer in the curves shown in Fig. 1 of this discussion. For example, the authors regard the pressure ratio across the compressor to be the constant one, and they conceive that pressure drops across any restriction between the compressor and turbine reduce the turbine pressure ratio. The writer has considered that the turbine pressure ratio is fixed, and that pressure drops between compressor and turbine cause an increase in the compressor pressure ratio. In actual fact, the authors have changed both the turbine and the compressor pressure ratios when pressure drop is introduced into the cycle, in order that under both conditions the cycle pressure ratio is at its optimum value. This fact, however, does not affect the check between the authors' result and the writer's result to any appreciable extent, because of the flatness of the efficiency or fuel-consumption curve in the vicinity of the opti-

---

[1] By J. I. Yellott and E. F. Lype, published in the November, 947, issue of Trans. ASME, vol. 69, pp. 903–911.

[2] General Engineering and Consulting Laboratory, General Elecric Company, Schenectady, N. Y. Mem. ASME.

[3] "A Marine Gas Turbine Plant," by C. R. Soderberg, R. B. Smith, nd A. T. Scott, Trans. The Society of Naval Architects and Marine ngineers, vol. 53, 1945, pp. 249–289.

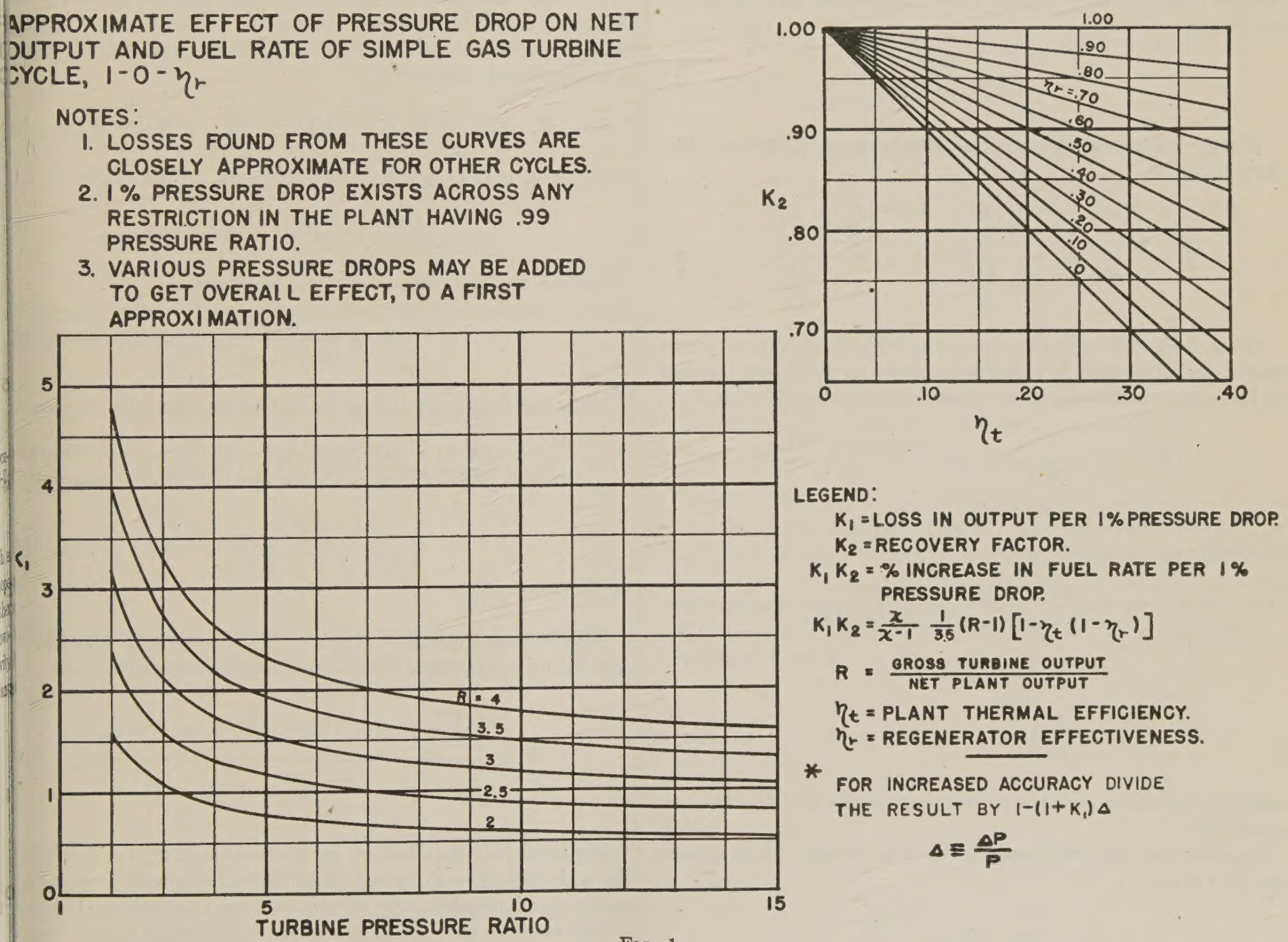

Fig. 1

mum pressure ratio; it is this fact which enables the excellence of check between the two results.

There is some question as to whether the authors' implication that pressure-drop loss is the difference in performance at the respective optimum pressure ratios is a desirable definition. It certainly is correct, and for one who is choosing design conditions, it is probably the proper one. However, another equally reasonable, and somewhat simpler, viewpoint is to consider it as the loss caused by introducing pressure drop in the system at essentially constant cycle pressure ratio, as the writer prefers to do. A restriction may be introduced into the duct between turbine and axial-flow compressor with no change in turbine pressure ratio (justifying the viewpoint of constant turbine pressure ratio, as opposed to constant compressor pressure ratio, because no physical change in the machines is required), and one result is an increase in fuel consumption. This increase in fuel consumption is the loss due to pressure drop. It is not only easily defined, but is easily checked by test, and frequently is the one in which users of gas turbines will have greatest interest.

The writer's originally published data claimed only that the results were approximate, that is, they were based upon the slope of the loss curve at zero pressure drop, having been obtained by differentiation, whereas there is an appreciable increase in the rate of loss at the higher pressures, which is not covered by this method. The following outline of the derivation provides an exact method, from which the approximate method easily may be derived; the nomenclature is apparent from the context, and all values are for a flow of 1 lb per sec of air. The fuel rate of a gas-turbine power plant is equal to the fuel burned divided by the net power

$$f = \frac{F}{W} \ldots\ldots\ldots\ldots\ldots\ldots [1]$$

A general expression for the fractional change in fuel rate may then be found

$$\frac{\Delta f}{f} = \frac{f' - f}{f} = \frac{1 + \dfrac{\Delta F}{F}}{1 + \dfrac{\Delta W}{W}} - 1 = \frac{\dfrac{\Delta F}{F} - \dfrac{\Delta W}{W}}{1 + \dfrac{\Delta W}{W}} \ldots\ldots [2]$$

If we designate by R the ratio of turbine gross output to net power, then the ratio of compressor power to net power is equal to $(R - 1)$. It may easily be shown that this is given by

$$(R - 1) = \frac{1}{\dfrac{t\eta_c\eta_t}{x} - 1} \equiv \frac{\text{compressor power}}{W} \ldots\ldots [3]$$

in which

$$t = \frac{\text{turbine inlet temperature}}{\text{compressor inlet temperature}}, \text{ (both in degrees F, absolute)}$$

$$x = \left(\frac{P_2}{P_1}\right)^{\frac{k-1}{k}}, \quad \text{where } P_2 > P_1$$

and the efficiencies are those of the compressor and turbine, respectively.

Consider now the fractional change in net power. It is apparent that since

$$W = W_t - W_c = \frac{W_c}{R - 1}$$

$$\frac{\Delta W}{W} = \frac{-\Delta W_c}{W_c}(R - 1) \ldots\ldots\ldots\ldots [4$$

and also that

$$\frac{\Delta W_c}{W_c} = \frac{\Delta x}{x - 1} \text{ (neglecting } \Delta\eta_c) \ldots\ldots\ldots [5$$

It may easily be shown that for any increase in compressor pressure ratio, caused by restrictions between turbine and compressor

$$\frac{\Delta x}{x - 1} = \frac{x}{x - 1}(y - 1) = \frac{\Delta W_c}{W_c} \ldots\ldots\ldots [6$$

in which

$$y = \left(\frac{P_2'}{P_2}\right)^{\frac{k-1}{k}}$$

where P_2' is the higher compressor discharge pressure (with pressure drop), and P_2 is the original compressor discharge pressure (without pressure drop).

Thus from Equations [4] and [6]

$$\frac{\Delta W}{W} = -\left(\frac{x}{x - 1}\right)(y - 1)(R - 1) \ldots\ldots\ldots [7$$

Consider the total fuel burned, which may be given by the following equation, in which the specific heat and other proportionality constants are omitted for brevity, and the W values are expressed in degrees F:

$$F = [T_t - (T_0 + W_c)] - \eta_R[(T_t - W_t) - (T_0 + W_c)] \ldots [8$$

in which η_R is the regenerator effectiveness. From which

$$\Delta F = -\Delta W_c(1 - \eta_R) \ldots\ldots\ldots\ldots [9$$

However, by the definition of thermal efficiency

$$F = \frac{W_c}{(R - 1)\eta_{th}} \ldots\ldots\ldots\ldots [10$$

Thus the fractional change in fuel burned may be written

$$\frac{\Delta F}{F} = -\frac{\Delta W_c}{W_c}(R - 1)\eta_{th}(1 - \eta_R)$$

$$= -\frac{x}{x - 1}(y - 1)(R - 1)\eta_{th}(1 - \eta_R) \ldots [11$$

by Equation [6]

Substituting Equations [11] and [7] in Equation [2], we obtain the final expression for the fractional change in fuel rate

$$\frac{\Delta f}{f} = \frac{\dfrac{x}{x - 1}(y - 1)(R - 1)[1 - \eta_{th}(1 - \eta_R)]}{1 - \dfrac{x}{x - 1}(y - 1)(R - 1)} \ldots [12$$

Equation [12] involves no approximations but, by expanding the quantity $(y - 1)$, using the binominal theorem, a useful approximate expression may be obtained for the fractional change in fuel rate per per cent pressure rise due to restriction. This is found to be

$$\frac{\frac{\Delta f}{f}}{\frac{\Delta P_2}{P_2}} = \frac{\left(\frac{x}{x-1}\right)(R-1)\left(\frac{k-1}{k}\right)\left(1-\frac{1}{2k}\frac{\Delta P_2}{P_2}+\ldots\ldots\right)\left[1-\eta_{th}(1-\eta_R)\right]}{1-\frac{\Delta P_2}{P_2}\left(\frac{x}{x-1}\right)(R-1)\left(\frac{k-1}{k}\right)\left(1-\frac{1}{2k}\frac{\Delta P_2}{P_2}+\ldots\right)} \quad ..[13]$$

Or, in the nomenclature of the previously published material

$$\frac{\frac{\Delta f}{f}}{\frac{\Delta P_2}{P_2}} = \frac{K_1\left(1-\frac{1}{2k}\frac{\Delta P_2}{P_2}+\ldots\right)}{1-K_1\left(\frac{\Delta P_2}{P_2}\right)\left(1-\frac{1}{2k}\frac{\Delta P_2}{P_2}+\ldots\right)}[K_2]\ldots.[14]$$

Since no rmally we think in terms of pressure drop (referred to the higher pressure) instead of pressure rise (referred to the lower pressure) Equation [14] is converted to this basis by remembering that

$$\frac{\Delta P_2}{P_2} = \frac{\frac{\Delta P_2}{P_2'}}{1-\frac{\Delta P_2}{P_2'}} \equiv \frac{\Delta}{1-\Delta}\ldots\ldots\ldots\ldots.[15]$$

where P_2' is the higher and P_2 the lower pressure, and Δ signifies the fractional pressure drop, referred to the higher pressure. Using this relationship in Equation [14], and approximating the denominator series by unity

$$\frac{\Delta f}{f} = \frac{\left(\frac{\Delta}{1-\Delta}\right)\left(1-\frac{\Delta}{2k(1-\Delta)}\right)}{1-K_1\left(\frac{\Delta}{1-\Delta}\right)}K_1K_2$$

$$= \Delta\frac{\left(1-\frac{\Delta}{2k(1-\Delta)}\right)}{1-\Delta(1+K_1)}K_1K_2$$

$$\frac{\Delta f}{f} = \Delta\left[\frac{1-0.357\frac{\Delta}{1-\Delta}}{1-(1+K_1)\Delta}\right]K_1K_2\ldots\ldots\ldots.[16]$$

For small pressure drops the numerator of the bracketed expression becomes nearly equal to unity, so that

$$\frac{\Delta f}{f} = \Delta\frac{K_1K_2}{1-(1+K_1)\Delta}\ldots\ldots\ldots\ldots.[17]$$

Finally, by considering the denominator of Equation [17] as unity, we arrive at the original expression used by the writer

$$\lim_{\Delta\to 0}\left(\frac{\frac{\Delta f}{f}}{\Delta}\right) = K_1K_2\ldots\ldots\ldots\ldots\ldots\ldots[18]$$

Thus successively more accurate approximations are obtained by using Equations [18], [17], [16], and [12], the last being exact. Using Equation [18] to check the authors example, we may obtain a first approximation of the loss. Calculation reveals that $x = 1.532$ and $(R - 1) = 1.544$, for a turbine pressure ratio of 4.45/1.

From Fig. 1 of this discussion, or by calculation, $K_1 = 1.270$ and $K_2 = 0.8776$. For 8 per cent pressure drop;

$$\frac{\Delta f}{f} = 0.08 \times 1.270 \times 0.8776$$

$$= 8.92 \text{ per cent}$$

which differs by a considerable amount from the true value because of the rather large magnitude of the pressure drop.

This discrepancy is greatly reduced with little extra effort by using Equation [17]

$$\frac{\Delta f}{f} = 0.08\frac{1.270 \times 0.8776}{1-(2.270)0.08}$$

$$\doteq 10.90 \text{ per cent}$$

A still further improvement results from using Equation [16]

$$\frac{\Delta f}{f} = 0.08\left(\frac{1-0.357\frac{0.08}{0.92}}{1-2.270 \times 0.08}\right)1.270 \times 0.8776$$

$$= 10.63 \text{ per cent}$$

And, finally using the exact method, Equation [12]

$$\frac{\Delta f}{f} = \frac{\left(\frac{1.532}{0.532}\right)(0.0241)(1.544)[1-0.306(1-0.60)]}{1-\frac{1.532}{0.532}(0.0241)(1.544)}$$

$$= 10.54 \text{ per cent}$$

which agrees with the authors' value of 10.50 per cent.

The writer believes Equation [17] to be the most practicable, and sufficiently accurate for most purposes.

AUTHORS' CLOSURE

The authors' reply to Mr. Salisbury's discussion is already provided by the discusser himself. The authors were primarily interested in establishing the optimum design conditions, while the discusser was interested in showing the effect of pressure loss under fixed operating conditions. Inasmuch as both methods are correct, the results obtained are, of course, identical.